Bettis Atomic Power Laboratory
P.O. Box 79
West Mifflin, PA 15122-0079

Bechtel Bettis, Inc.

B-MT(SRME)-51

FEB 2 1 2006

Manager, Pittsburgh Naval Reactors Office
U. S. Department of Energy
Post Office Box 109
West Mifflin, Pennsylvania 15122-0109

Subject: Processing of Refractory Metal Alloys for JOYO Irradiations

Dear Sir:

Attached is a summary of the refractory metal processing experienced by candidate Prometheus materials as they were fabricated into specimens destined for testing within the JOYO test reactor, ex-reactor testing at Oak Ridge National Laboratory (ORNL), or testing within the NRPCT. The processing is described for each alloy from the point of inception to the point where processing was terminated due to the cancellation of Naval Reactor's involvement in the Prometheus Project. The alloys included three tantalum-base alloys (T-111, Ta-10W, and ASTAR-811C), a niobium-base alloy, (FS-85), and two molybdenum-rhenium alloys, one containing 44.5 w/o rhenium, and the other 47.5 w/o rhenium. Each of these alloys was either a primary candidate or back-up candidate for cladding and structural applications within the space reactor. Their production was intended to serve as a forerunner for large scale production ingots that were to be procured from commercial refractory metal vendors such as Wah Chang.

INTRODUCTION:

Refractory metal alloys under consideration for cladding and core applications within the Prometheus Project included tantalum-base, niobium-base and molybdenum-base alloys. Candidate tantalum-base alloys included T-111, Ta-10W, and ASTAR811C; niobium –base candidates included only FS-85; and the molybdenum base candidates included molybdenum-high rhenium alloys with rhenium contents ranging from 41-47.5 weight percent (w/o).

Each of these alloy classes displays different strengths and weaknesses. The tantalum and niobium-base alloys readily can be formed into complex shapes and welded with little difficulty. The Ductile-to Brittle-Transition-Temperature (DBTT) of wrought and welded components fabricated from these alloys remains well below room temperature, an important attribute during fabrication and system start-ups. However, a major concern with both niobium and tantalum-base alloys is their propensity to become contaminated by oxygen, nitrogen, and other interstitials. Contamination can occur during processing operations, including vacuum annealing and welding. It could also occur during space reactor operations as a result of contact with oxide or nitride–based fuels, or as a result of contact with an impure gas coolant. If contamination is severe enough, the alloys can become significantly embrittled.

Molybdenum alloys exhibit a significantly lesser tendency to become contaminated. However, fabricability of molybdenum and most of its alloys is appreciably poorer than that of niobium and tantalum-base alloys. Weldments made within pure molybdenum and most of its alloys exhibit DBTTs that are well above room temperature. Simple forming operations are also more problematic for molybdenum compared to niobium and tantalum alloys. These fabrication concerns can be partially overcome by the inclusion of rhenium as an alloying constituent. Additions of this element to molybdenum at levels approaching 50 w/o result in significant improvement in the ductility of molybdenum with respect to both forming and welding operations. These high rhenium levels, however, can result in the formation of rhenium-rich phases during processing or thermal exposures. Furthermore, in-reactor exposures cause additional rhenium-rich precipitates to form. As a consequence, microstructural phase instability is a major concern for the Mo-Re alloys. Decreases in rhenium content should reduce the propensity to form rhenium-rich precipitates during processing or in-reactor exposure, but this reduction comes at the expense of fabricability. The optimum rhenium level needed to maintain good fabricability while minimizing formation of rhenium-rich precipitates is not certain and indeed was under active investigation at the time of Prometheus Project restructuring.

The uncertain impact of irradiation on molybdenum-rhenium behavior is a concern that applies to all of the refractory metal alloys. The high melting point of these alloys, usually denoted as an advantage, can lead to irradiation damage below 1000 K. This damage can lead to irradiation creep rates during irradiation that can rival thermal creep rates observed at much higher exposure temperatures. The low temperature damage can also lead to irradiation embrittlement, an issue during post irradiation or transient conditions. Irradiation testing of these alloys has been limited. The testing that has occurred usually has been conducted at temperatures or fluence values that were significantly different from those considered for Prometheus.

Testing within JOYO-1 was intended to eliminate these uncertainties in irradiation behavior. Specimen types were to include biaxial creep specimens, tensile specimens, and tensile and density and conductivity discs. From these specimens, information would have been gained on irradiation creep properties, strength, micro-structural stability, swelling, and thermal conductivity.

Except for Ta-10W and powder metallurgical versions of several molybdenum-rhenium alloys, none of these alloys are available commercially. As a point of reference, the last time ASTAR-811C was melted by a commercial vendor was more than 30 years ago. FS-85 was melted ~ 10 years ago. The lack of recent experience, combined with the long lead times required for procurement of large ingots, made it necessary to melt most JOYO refractory metal candidates on a laboratory scale if insertion dates were to be met. Consequently, most of the candidate alloys were melted as small laboratory ingots at Pittsburgh Materials Technology Inc. (Large, PA), a local vendor with extensive experience in melting and processing of these alloys. The production of these laboratory scale ingots was intended to serve as a forerunner for large production ingots that were to be procured from commercial refractory metal vendors such as Wah Chang (Albany, OR). Melting and processing of these large ingots were believed to be necessary steps in re-establishing the commercial infrastructure for these alloys.

Space limitations within JOYO-1 made it necessary to limit in-reactor testing to one alloy from each of the three classes. ASTAR-811C was chosen to represent the tantalum-base alloys primarily because of its exceptional strength and creep behavior. The presence of 250 ppm carbide resulting in the formation of small carbide precipitates is the primary reason for this strength. The T-111 and Ta-10W alloys remained as back-ups. Ta-10W, as noted, is the only commercially available tantalum

candidate alloy. Both are simpler alloys than ASTAR-811C and derive their increased strength relative to pure tantalum from solid solution strengthening by their major alloying constituents.

FS-85 was selected to represent the niobium-base alloys. Previous efforts during SP-100 [Reference (1)] focused on the Nb-1Zr alloy with PWC-11 (Nb-1Zr + 1000 ppm carbon) as a back-up. However, NRPCT evaluations of SP-100 efforts concluded that the strength of Nb-1Zr was too low to merit consideration for JOYO-1. Furthermore, it appeared that the alloy lacked reproducibility because there was a wide variation in creep behavior generated from various Nb-1Zr ingots melted either during or before the SP-100 era. This difference in creep behavior occurred despite similar chemistry levels among ingots. A subsequent NRPCT review of niobium alloys developed during the last 30 years concluded that the FS-85 solid solution strengthened alloy was the best choice to represent the niobium alloys for JOYO-1 testing. The alloy provided the best blend of fabricability and high-temperature strength.

For the final class of materials, the molybdenum alloys, the molybdenum-47.5 rhenium alloy was selected. This level of rhenium will cause the greatest amount of rhenium-bearing precipitates to form during fabrication or in-reactor exposures. However, the level also ensures the highest level of ductility in wrought product and ensures that as-welded components will exhibit a DBTT well below room temperature. The lower rhenium (molybdenum-44.5 rhenium) alloy was chosen as the back-up.

DISCUSSION:

All of the alloys, with the exception of the molybdenum-44.5 rhenium alloy, were double consumable arc melted as 3-inch diameter ingots at Pittsburgh Materials Technology Inc. The Mo-44.5Re alloy was obtained from Rhenium Alloys (Cleveland, OH) in the form of a 3-inch diameter billet manufactured via powder metallurgical (PM) methods. All of the alloys were intended to be processed through a series of fabrication steps that began with extrusion into either flats or rounds, and were then to be processed further by swaging, rolling, tube drawing, or machining.

Several of the alloys were processed into final sheet product. From this material, small sub-size tensile and creep specimens were machined. Others were processed into thin-walled tubing and biaxial creep components that were welded into small biaxial creep specimens at the Pacific Northwest National Laboratory (PNNL) located in Hanford, WA. The welding of these specimens was an abbreviated qualification effort that originally had been intended to supply small pressurized biaxial creep specimens for testing within the JOYO test reactor in O-arai, Japan. A summary of the processing for each alloy is provided in flow sheets 1, 2, and 3.

The enclosed report contains details on the processing of these refractory metal alloys. The report is divided into three sections. Section I describes the major processing steps experienced by these materials. Section II expands upon the detail and rationale for many of the individual process steps. The final section (III) discusses the proper processing approaches for these unique materials. The report is intended to: 1) allow future engineers to complete the processing of archived materials that were stopped in mid-process, and 2) allow future engineers to test final processed specimens and remain confident about the individual specimen's pedigree. Equally as important, all of the sections are written from the perspective of a processing engineer. Sufficient details are provided that will enable future metallurgists to understand how to properly process these high potential materials and avoid many of the common processing pitfalls.

This report is provided to satisfy TACOM 2996155.

Very truly yours,

R. F. Luther, Advisory Engineer
Space Reactor Materials Engineering
MT- Advanced Materials Technology

M. E. Petrichek, Associate Engineer
Space Reactor Materials Engineering
MT- Advanced Materials Technology

Approved by:

R. Baranwal, Acting Manager
Space Reactor Materials Engineering
Materials Technology

Reference: (1) Peter Ring, "SP-100 Materials and Fabrication Technology Lessons Learned," SP-100 Program Information Release #1199, March 1994.

Enclosure: Basic Processing Methods of T-111, Ta-10W, FS-85, Mo-47.5 Re and ASTAR-811C Sample Production

Basic Processing Methods of T-111, Ta-10W, FS-85, Mo-47.5Re, and ASTAR-811C Sample Production

R. F. Luther
M. Petrichek

ABSTRACT:

Documented herein is a description of refractory metal processing of specimens destined for testing within the JOYO test reactor, ex-reactor testing at Oak Ridge National Laboratory (ORNL), or testing at other facilities within the NRPCT. The processing is described for each alloy from the point of inception to the point where processing was terminated due to the cancellation of Naval Reactor's involvement in the Prometheus Project. The alloys included three tantalum–base alloys T-111, Ta-10W, and ASTAR-811C, a niobium-base alloy, FS-85, and two molybdenum-rhenium alloys, one containing 44.5 w/o rhenium, and the other 47.5 w/o rhenium. Nominal compositions are listed in Table 1.

Table 1: Prometheus Project- Nominal Refractory Metal Compositions

Weight Percent	T-111	ASTAR-811C	FS-85	Ta-10W	Mo-47.5Re	Moly-44.5 Re
Ta	90	Balance	27.5	90	-	-
Mo	-	-	-	-	52.5	55.5
Nb	-	-	Balance	-	-	
Re	-	1	-	-	47.5	44.5
W	8	8	10	10	-	-
Hf	2	0.7	-	-	-	-
C	-	0.025	-	-	-	-
Zr	-	-	0.85	-	-	-

Each of these alloys was either a primary candidate or back-up material for cladding and structural applications within the space reactor. The majority of the processing occurred at Pittsburgh Materials Technology (PMTI), a small vendor with extensive experience in processing of refractory metals. Other vendors included Wright Patterson Air Force base, Rhenium Alloys, True Tube, and numerous local machining vendors. Final product configurations include as-melted final ingots, sheet-bar and round extrusions, swaged solid rod stock, thin as-rolled sheets, 0.250-inch diameter tubing, biaxial creep components, as well as sub-size tensile specimens. Final inventory of the reactor specimens and in-process material can be seen in Table 2.

The production of these alloys was also intended to serve as a forerunner for large scale production ingots that were to be procured from commercial refractory metal vendors such as Wah Chang (TWCA) of Albany, OR.

INTRODUCTION:

This document describes in detail the processing of each alloy listed in Table 1 prior to the termination of the Prometheus project. All of the alloys, with the exception of the molybdenum-44.5 w/o rhenium alloy, were melted as laboratory size ingots at Pittsburgh Materials Technology, Inc. (PMTI). The

Table 2: Inventory of Materials

Material	ID	Location	Application	Last Processing Step & corresponding location in Flowcharts 1-3	Description
ASTAR-811C	X0410LR	PMTI	Biaxial creep sample tubes	Swaged	Diameter: 0.4635 in
				5T	Length: 9 5/8 in
					Rod
T-111	X0410MI	PMTI	Biaxial creep sample end caps	Swaged	Diameter: 0.2675 in
				8E	Length: 8 in
					Rod
T-111	X0410MI	PMTI	Biaxial creep sample end caps	Swaged	Diameter: 0.2655 in
				8E	Length: 3.75 in
					Rod
ASTAR-811C	X0410LR	PMTI	Biaxial creep sample end caps	Swaged	Diameter: 0.2825 in
				8E	Length: 18 in
					Rod
ASTAR-811C	X0410LR	PMTI	Biaxial creep sample end caps	Swaged	Diameter: 0.2825 in
				8E	Length: 8.25 in
					Rod
T-111	X0465	PMTI	Biaxial creep samples	Extruded	Diameter: 1.17 in
				2T	Length: 5.3 in
					Extruded Round Bar
ASTAR-811C	14077	PMTI	Biaxial creep samples	Extruded	Diameter: 1.15 in
				2T	Length: 4.63 in
					Extruded Round Bar
ASTAR-811C	X0465	PMTI	Melt sample for metallography	Melted	Diameter: 2.45 in
				1	Length: 0.1880 in
					Melt sample
ASTAR-811C	X0465	PMTI	Melt sample for metallography	Melted	Diameter: 2.45 in
				1	Length: 0.1880 in
					Melt sample
FS-85	X0563	PMTI	Tensile Samples	Rolled	Length: 7.5 in
				11F	Thickness: 0.040 in

Table 2: Inventory of Materials					
Material	**ID**	**Location**	**Application**	**Last Processing Step & corresponding location in Flowcharts 1-3**	**Description**
FS-85	X0563	PMTI	Tensile Samples	Rolled	Length: 18 in
				11F	Thickness: 0.040 in
FS-85	X0563	PMTI	Tensile Samples	Rolled	Length: 18 in
				11F	Thickness: 0.040 in
FS-85	X0563	PMTI	Tensile Samples	Rolled	Length: 7.75 in
				11F	Thickness: 0.040 in
FS-85	X0563	PMTI	Tensile Samples	Rolled	Length: 7.75 in
				11F	Thickness: 0.040 in
FS-85	X0563	PMTI	Tensile Samples	Rolled	Length: 6 in
				11F	Thickness: 0.040 in
FS-85	X0563	PMTI	Tensile Samples	Rolled	Length: 7.5 in
				11F	Thickness: 0.040 in
FS-85	X0563	PMTI	Tensile Samples	Rolled	Length: 6.5 in
				11F	Thickness: 0.040 in
FS-85	X0563	PMTI	Tensile Samples	Rolled	Length: 8.25 in
				11F	Thickness: 0.040 in
FS-85	X0410MJ	PMTI	Biaxial creep samples end caps	Swaged	Diameter: 0.27 in
				8E	Length: 11.25 in
FS-85	X0410MJ	PMTI	Biaxial creep samples end caps	Swaged	Diameter: 0.27 in
				8E	Length: 10 in
FS-85	X0410MJ	PMTI	Biaxial creep samples	Swaged	Diameter: 0.45 in
				5T	Length: 33 in
Ta-10W	X0410MJ	PMTI	Biaxial creep samples	Swaged	Diameter: 0.50 in
				5T	Length: 10.25 in
Ta-10W	X0410MJ	PMTI	Biaxial creep samples	Swaged	Diameter: 0.50 in
				5T	Length: 34 in
Ta-10W	X0410MJ	PMTI	Biaxial creep samples	Swaged	Diameter: 0.50 in
				5T	Length: 34 in

Table 2: Inventory of Materials

Material	ID	Location	Application	Last Processing Step & corresponding location in Flowcharts 1-3	Description
Ta-10W	CVAM 1679	PMTI	Biaxial creep samples	Extrusion	Diameter: 1.18 in
				2T	Length: 10 in
Ta-10W	CVAM 1679	PMTI	Biaxial creep samples	Extrusion	Diameter: 1.18 in
				2T	Length: 3.5 in
T-111	N/A	Bettis	Biaxial creep specimen end caps	Machined to final dimensions	Diameter: 0.25 in
				11E	34 Top End Caps
					34 Bottom End Caps
FS-85	N/A	Bettis	Biaxial creep specimen end caps	Machined to final dimensions	Diameter: 0.25 in
				11E	70 Top End Caps
					70 Bottom End Caps
ASTAR-811C	N/A	PMTI	Biaxial creep specimen tubes	Tube Drawing	OD: 0.25 in, ID: 0.225 in
				13T	Length: 1.25 in
					42 tubes
T-111	N/A	PMTI	Biaxial creep specimen tubes	Tube Drawing	OD: 0.25 in, ID: 0.225 in
				13T	Length: 1.25 in
					54 tubes
FS-85	N/A	PMTI	Biaxial creep specimen tubes	Tube Drawing	OD: 0.25 in, ID: 0.225 in
				13T	Length: 1.25 in
					46 tubes
T-111	N/A	PMTI	Biaxial creep specimen tubes	Tube Drawing	OD: 0.25 in, ID: 0.225 in
				13T	Length: 26 in
T-111	N/A	PMTI	Biaxial creep specimen tubes	Tube Drawing	OD: 0.25 in, ID: 0.225 in
				13T	Length: 27.5 in
ASTAR	N/A	PMTI	Biaxial creep specimen tubes	Tube Drawing	OD: 0.25 in, ID: 0.225 in
				13T	Length: 12 in
ASTAR	N/A	PMTI	Biaxial creep specimen tubes	Tube Drawing	OD: 0.25 in, ID: 0.225 in
				13T	Length: 27 in

Table 2: Inventory of Materials					
Material	**ID**	**Location**	**Application**	**Last Processing Step & corresponding location in Flowcharts 1-3**	**Description**
Ta-10W	X0410MJ	PMTI	Tensile Samples	Extruded	Thickness: 1.12 in
				1F	Length: 28 in
T-111	T-111-75	Bettis	Tensile Samples	Machined to final dimensions	Thickness: 0.040 in
				12F	Length: 1 in
					50 pieces
T-111	T-111-30	Bettis	Tensile Samples	Machined to final dimensions	Thickness: 0.040 in
				12F	Length: 1 in
					30 pieces
Mo-47Re	MoRe-C	Bettis	Tensile Samples	Machined to final dimensions	Thickness: 0.040 in
				6R	Length: 1 in
					70 pieces
Mo-47Re	MoRe-H	Bettis	Tensile Samples	Machined to final dimensions	Thickness: 0.040 in
				7M	Length: 1 in
					40 pieces
Mo-47Re	MoRe-C	Bettis	Tensile Samples	Machined to final dimensions	Thickness: 0.040 in
				6R	Length: 1 in
					6 pieces
Mo-47Re	MoRe-H	Bettis	Tensile Samples	Machined to final dimensions	Thickness: 0.040 in
				7M	Length: 1 in
					6 pieces
FS-85	FS-85-30	Bettis	Tensile Samples	Machined to final dimensions	Thickness: 0.040 in
				12F	Length: 1 in
					6 pieces
FS-85	FS-85-75	Bettis	Tensile Samples	Machined to final dimensions	Thickness: 0.040 in
				12F	Length: 1 in
					6 pieces
ASTAR-811C	ASTAR-811C-30	Bettis	Tensile Samples	Machined to final dimensions	Thickness: 0.040 in
				12F	Length: 1 in
					40 pieces

Table 2: Inventory of Materials					
Material	**ID**	**Location**	**Application**	**Last Processing Step & corresponding location in Flowcharts 1-3**	**Description**
ASTAR-811C	ASTAR-811C-75	Bettis	Tensile Samples	Machined to final dimensions	Thickness: 0.040 in
				12F	Length: 1 in
					6 pieces
Mo-44.5 Re Powdered Metal	N/A	PMTI	Tensile Samples	Extrusion Third Processing Step	2-inches x 0.8-inches x 30-inches

molybdenum-44.5 rhenium alloy was obtained from Rhenium Alloys, Inc. in the form of a 3-inch diameter billet manufactured via powder metallurgical (PM) methods. Rhenium Alloys is the major supplier of both pure rhenium and molybdenum-rhenium alloys in the U.S. The five melted alloys and the single PM alloy were intended to be processed through a series of fabrication steps that began with extrusion into either flat or rounds, and were to be further processed by swaging, rolling, tube drawing, or machining.

Several alloys were processed into final sheet product. From this material small sub-size tensile and creep specimens were machined. Others were processed into thin walled tubing and biaxial creep components that were welded into small biaxial creep specimens at the Pacific Northwest National Laboratory (PNNL) located in Hanford, WA. This welding trial was an abbreviated qualification effort that had been intended to supply small pressurized biaxial creep specimens for testing within the Japanese JOYO test reactor. A complete listing of materials fabricated for this effort is provided in Table 2. The table specifies both the material configuration and metallurgical condition of each piece. The vendors used for major fabrication and processing steps are listed in Table 3.

Fabrication Step	Vendor
Electrode Fabrication	Pittsburgh Materials Technology Incorporated (PMTI), Large, PA
Ingot Melting	Pittsburgh Materials Technology Incorporated (PMTI), Large, PA
Ingot conditioning and billet assembly	Pittsburgh Materials Technology Incorporated (PMTI), Large, PA
Extrusion	Wright-Patterson Air Force Base, Dayton, OH
De-cladding	Pittsburgh Materials Technology Incorporated (PMTI), Large, PA
Tube drawing of niobium and tantalum alloys	True Tube, Paso Robles, CA
Rolling/ Swaging	Pittsburgh Materials Technology Incorporated (PMTI), Large, PA
Machining of tensiles and biaxial creep end plugs	Kin-Tech, North Huntington, PA/ Vangura, Clairton, PA
Machining, pickling, and final annealing of biaxial creep components	Pittsburgh Materials Technology Incorporated (PMTI), Large, PA
Final assembly of biaxial creep specimens	PNNL, Hanford, WA

Table 3: List of Vendors used for Major Fabrication Steps

The report is divided into three separate sections. Section I provides a description of the major processing steps experienced by these materials. The section begins with the details of electrode construction that were used in melting and continues through fabrication of the respective alloys into their final configuration and metallurgical condition. A summary of the processing for each alloy is also provided in flow charts in Figures 1-3.

Also included in this section is a description of processing difficulties experienced during the fabrication effort as well as the status of product and material characterization. Section II expands upon the detail and rationale for many of the individual process steps. A discussion of the proper processing approaches for these unique materials is provided in Section III.

PROCESSING OF REFRACTORY ALLOYS FOR PROJECT PROMETHEUS

A. Electrode Fabrication and Melting

All of the alloys with the exception of the PM Mo-Re alloy were arc melted at PMTI as small laboratory size ingots using an alternating current (AC) Leybold-Heraeus melter. This is a unique melting method compared to the typical direct current (DC) melting method employed by most research facilities or commercial vendors. AC melting produces a more homogeneous ingot than DC melting. A further description of AC melting and the actual melting practices employed for these ingots are provided in Section II.

Flow Chart 1. Processing of MoRe Alloy

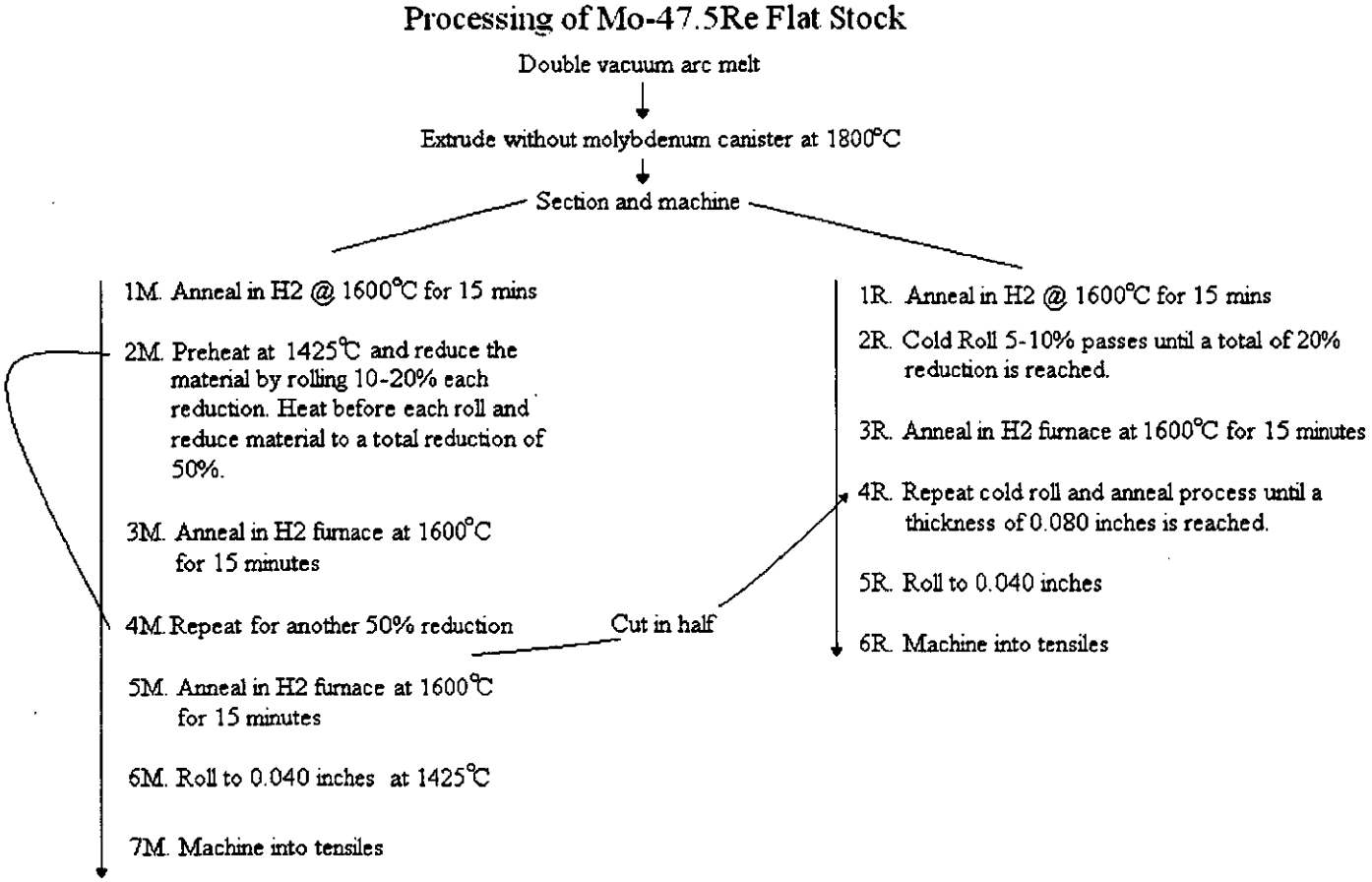

Figure 1: Flow Chart for Processing of Mo-Re alloys

Note-The PM Moly-44.5 Rhenium alloy was processed only through extrusion.

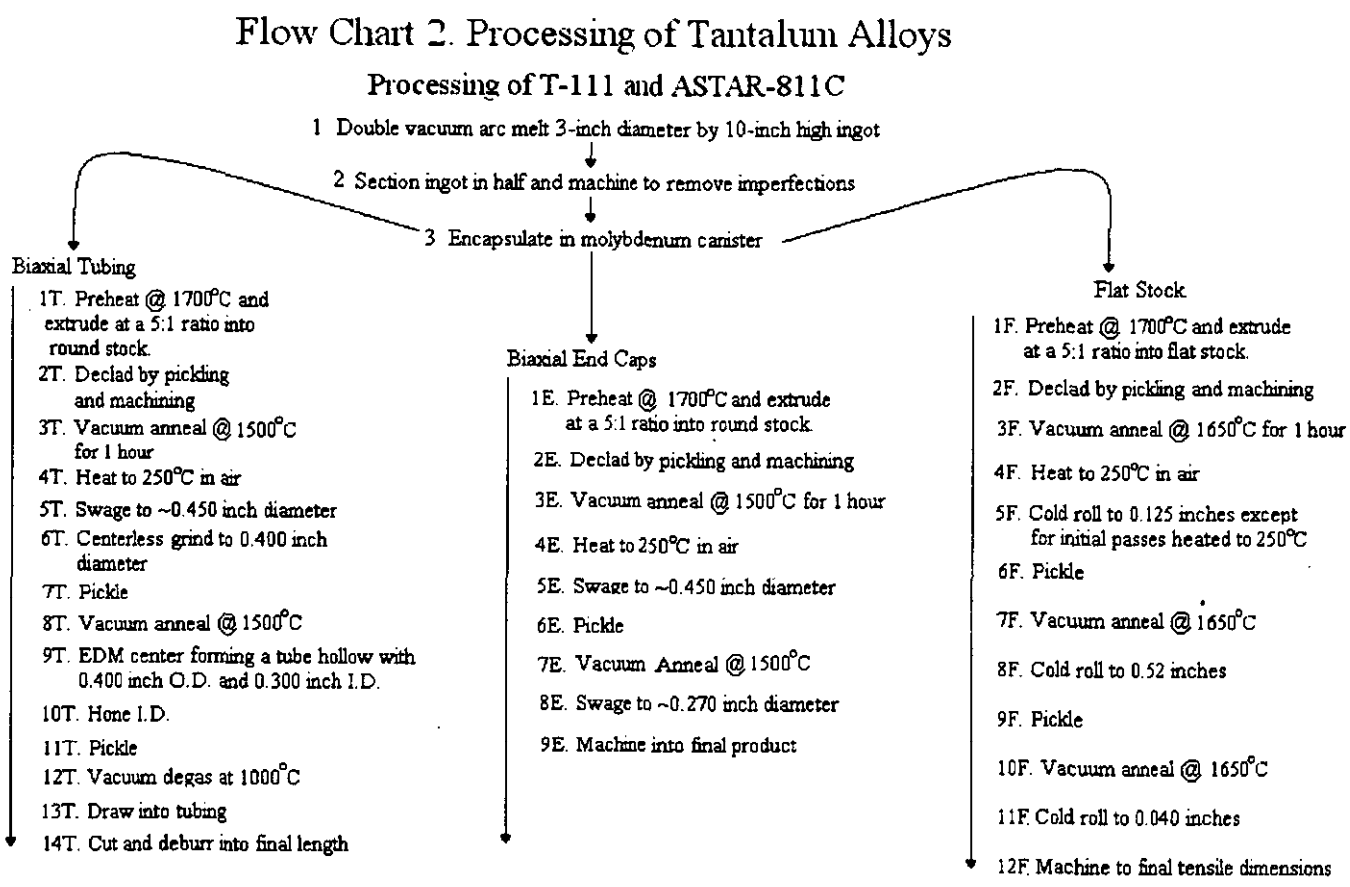

Figure 2: Flow Chart for Processing of Tantalum-base alloys T-111 and ASTAR-811C

Note- Ta-10W was extruded into both flats and rounds identical to T-111 and ASTAR-811C. The flat extrusion was left in the as-clad condition. A portion of the round extrusion was processed into 0.450-inch diameter rod and 0.275-inch rod and left in these conditions. Processing parameters to these process steps were identical to those used for T-111 and ASTAR-811C.

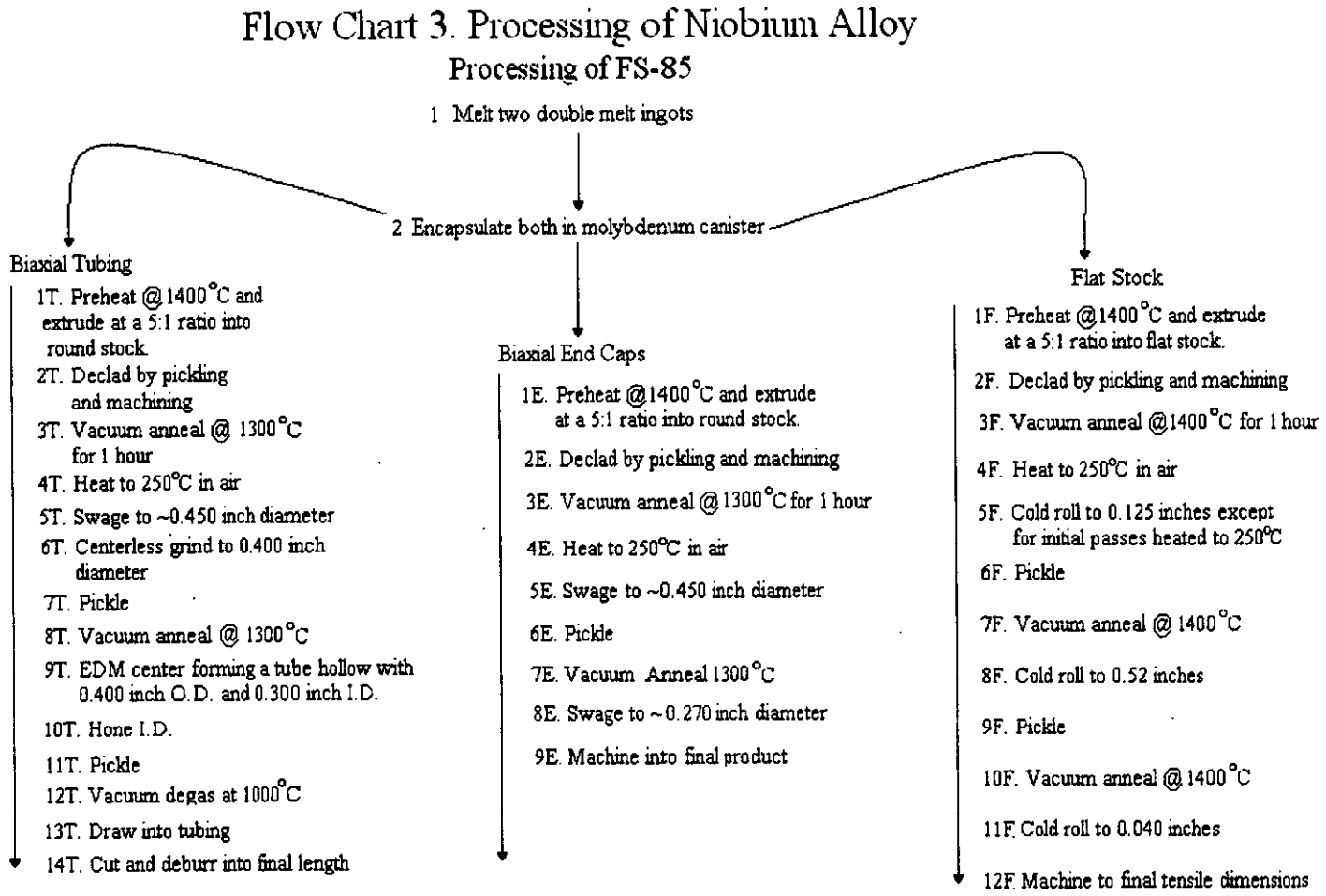

Figure 3: Flow Chart for Processing of the Niobium-base alloy, FS-85

Despite the employment of the AC furnace, all alloys were double consumable arc melted to ensure that they were homogeneous. The electrodes were assembled in a sandwich configuration, a method developed to improve alloying homogeneity within melted refractory-base ingots, Reference (1). The sandwich was comprised of the respective alloying ingredients in the form of either thin sheet or rod stock that were first clamped together and then welded. Simple tack welding is not adequate. Welding must produce an electrode that is both straight and robust enough to allow the electrode to be loaded into the furnace. However, most importantly welding must form an electrode that is capable of carrying a current of 3000-5000 amps over its entire length. The alloying constituents were evenly distributed along the entire length of the respective electrodes for each alloy. Electrode welding was performed in a high quality glove-box evacuated into the mid-10^{-5} torr range prior to backfilling with helium and subsequent GTAW welding. No filler metal was used during assembly. All metal components were pickled prior to electrode assembly and welding. Vendors that supplied the starting materials included the commercial refractory metal producers Wah Chang, Rhenium Alloys, and H.C. Starck, and are listed in Table 4 along with the metallurgical condition of each starting electrode component.

Carbon, if added, was inserted into the electrode as graphite string. Copies of the individual certifications for the starting metal raw materials stock are provided in Attachment B. The starting components for two ASTAR-811C electrodes are shown in Figure 4. The as-welded electrodes for both initial melts of T-111 are shown in Figure 5.

Table 4: List of Raw Materials Used In Electrode Fabrication for Initial Melts

Refractory Metals	Form	Vendor
Niobium	EB[(1)] melted & rolled sheet	Wah Chang, Albany, OR
Tantalum	EB[(1)] melted & rolled sheet	Wah Chang, Albany, OR
Molybdenum	5/8-inch dia. LCAC[(2)] Mo bar	H.C. Starck, Coldwater, MI
Hafnium	Melted & rolled sheet	Wah Chang, Albany,OR
Zirconium	Melted & rolled sheet	Wah Chang, Albany, OR
Rhenium	Sintered PM 0.5-inch dia. bar	Rhenium Alloys, Elyria, OH

(1)- EB= electron beam melted
(2)- LCAC= Low carbon arc cast pure molybdenum
(3)- PM = powder met

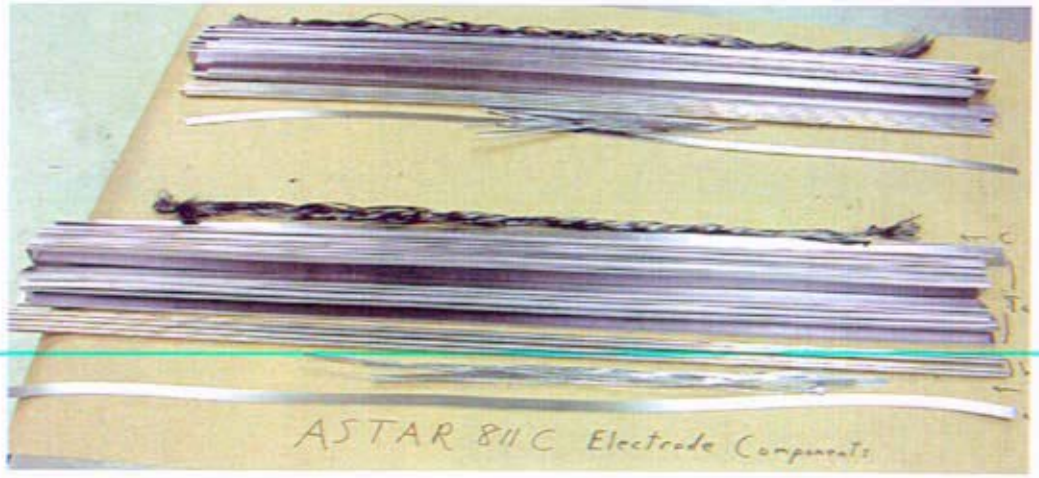

Figure 4: Sandwich electrode components for initial melts of ASTAR-811C (First melt electrodes). Each strip or rod represents individual pure elements (i.e., W, Hf, Re, or Ta). The carbon yarn used to add 250 ppm carbon is at the top of each set.

Figure 5: Two as-welded T-111 1st melt sandwich electrodes. A pure Ta threaded adapter is welded to the top (right) of each electrode. The adapter is used to attach the electrode to the furnace and then serves as the transmission path for the melt current to the electrode.

These electrodes were melted within a copper mold ~ 2 inches in diameter. For the majority of alloys, these two first melt ingots were then combined into a single electrode. This latter electrode was re-melted into a 2.85-inch diameter copper mold forming a single final melt ingot. For Ta-10W and FS-85, two separate final 2.85-inch diameter ingots were melted. The electrode configuration used for formation of the final melt ingots depended on the size of the copper crucible used for the first melt of the particular alloy. If the initial melts were conducted within a 2-inch mold, the two first melt ingots were simply faced off on the ingot top and bottom and then welded together. An adapter was also welded to the top of one of the ingots to form the second melt electrode. Minimal material was removed from the first melt ingot sidewalls except at locations where copper had rubbed-off during ingot removal from the copper crucible. A photograph of two final melt electrodes formed by this method is pictured in Figure 6. The majority of alloys in this program employed 2nd melt electrodes fabricated by this technique.

A different electrode configuration was used for the first melt ingots with diameters larger than 2-inches in order to maintain minimum clearances between the crucible and the electrode. A minimum gap of ~ ½ inch is necessary between the electrode and the crucible to minimize the possibility of arcing to the side of the crucible during melting. This gap would not be available if the > 2-inch diameter ingots were simply welded one on top of the other. In this case, the larger first melt ingot(s) were sectioned into quarters. After facing off the top and bottom of each quartered section, the sections were welded together alternating the top to bottom of each section to form a second melt electrode. Minimal material was removed from the ingot sidewalls prior to sectioning and GTAW re-welding.

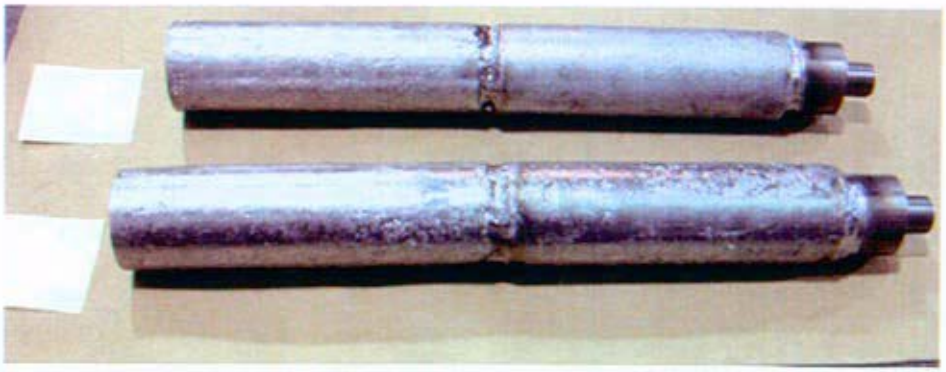

Figure 6: Two final melt electrodes formed from two first melt 2-inch diameter ingots

Both initial and final melts were conducted in vacuum for all of the tantalum-base and molybdenum-base alloys and in either argon or helium for the niobium-base alloy, FS-85. For Ta and Mo alloys, the melt chamber was evacuated into the mid 10^{-5} torr range or lower before the arc was struck. When melting FS-85, the chamber was first evacuated into the mid 10^{-5} torr range or better. Inert gas was then introduced into the chamber to a level of approximately 1/3 atmosphere before the arc was struck. Starting pads used for arc initiation for both initial and final melts always represented the base material (Ta, Nb, or Mo) and sometimes the actual alloy that was to be melted. Once the melt was completed, the starting pad was sectioned from the ingot bottom before further melting or processing. This would avoid alloy dilution along the ingot bottom or possible contamination. Complete melting parameters for the final melt ingots are provided in Table 5. A photograph of a typical final melted ingot is provided in Figure 7.

Table 5: PMTI Melting Parameters For Final Melt ~3.0-inch Diameter Ingots

Alloy	Ingot ID[3]	Avg.Voltage	Avg. amps	Melt time minutes	Melting Environment
T-111	CVAM 1600	24	4750	5.9	Vacuum 2×10^{-3} torr
ASTAR-811C	CVAM 1601	25	4500	6.1	Vacuum 5×10^{-3} torr
Ta-10W	CVAM 1619[2]	28	4600	3.3	Vacuum 5×10^{-4} torr
Ta-10W	CVAM 1621[1]	28	4500	3.3	Vacuum 5×10^{-4} torr
FS-85	CVAM 1602[1]	26	4500	3.3	1/3 atm helium
FS-85	CVAM 1603[2]	28	4500	3	1/3 atm helium
Mo-47.5Re	CVAM 1603	30	4700	3.3	Vacuum 1×10^{-4} torr

(1)- Extruded into round
(2)-Extruded into flat
(3)- Those alloys with a single CVAM number were sectioned in half and extruded into a flat and a round.

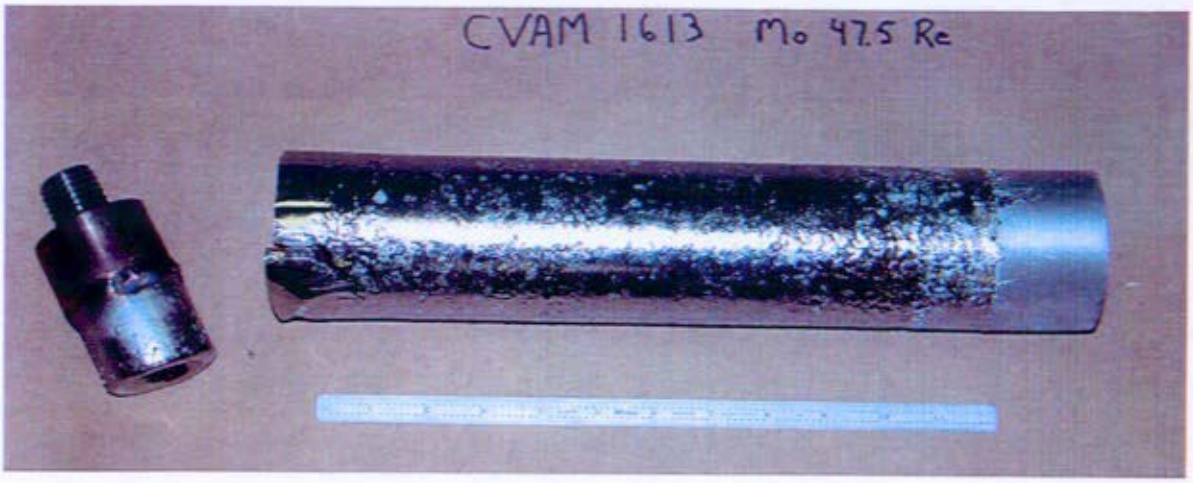

Figure 7: Final Melt 3-inch diameter Mo-47.5Re Ingot with starting pad still attached to the right. Remnant of the starting electrode is on the left.

B. Ingot Chemistry-Carbon concerns for ASTAR-811C; Oxygen & Rhenium Levels within Molybdenum-47.5Rhenium.

Following the second and final melt, the 2.85-inch diameter ingots were analyzed for the major alloying constituents as well as the interstitials carbon, oxygen, and nitrogen. In some cases the analysis was delayed to after ingot breakdown (i.e. extrusion). The results are listed in Table 6.

Table 6: Major Alloying Ingredients and Interstitials for the Inventoried Refractory Metal Alloys at Various Processing Steps

Alloy	Ingot I.D.	Form	Ta w/o	Nb w/o	Mo w/o	W w/o	Hf w/o	Zr w/o	Re w/o	C w/o or ppm	N w/o or ppm	O w/o or ppm
T-111 Target	N/A	N/A	90	-	-	8	2	-	-	0.01 max	0.005 max	0.010 max
	CVAM 1600	Ingot	90.4, 89.8	-	-	7.63, 8.16	1.87, 1.98	-	-	<0.005, <0.005	0.002, 0.0015	0.0026, 0.013
T-111	CVAM 1600	Extruded Round	90.1, 90.3	-	-	7.88, 7.75	1.87, 1.87	-	-	<0.005%, ,0.005%	0.002, 0.0017	0.0018, 0.0015
ASTAR-811C Target	N/A		90.15	-	-	8	0.85	-	1	0.025	0.005 max	0.010 max
ASTAR-811C	CVAM 1601	Ingot	89.5, 89.7	-	-	8.19, 8.09	0.96, 0.89	-	1.33, 1.29	0.0096, 0.02	0.0021, 0.0023	0.014, 0.0032
ASTAR-811C	CVAM 1601	Extruded Round	90.6, 90.5	-	-	7.42, 7.44	0.80, 0.81	-	1.15, 1.16	0.030, 0.029	0.0036, 0.0038	<0.001, 0.0012
ASTAR 811C	CVAM 1601	0.040-inch plate	90.1	-	-	7.95	0.80	-	1.09	0.0240	<10ppm	3 ppm
ASTAR 811C	CVAM 1601	0.040-inch plate	90.2	-	-	8.00	0.83	-	0.88	0.022	<10 ppm	6 ppm
Ta-10W	-	-	90	-	-	10	-	-	-	0.008	0.005	0.010

Table 6: Major Alloying Ingredients and Interstitials for the Inventoried Refractory Metal Alloys at Various Processing Steps

Alloy	Ingot I.D.	Form	Ta w/o	Nb w/o	Mo w/o	W w/o	Hf w/o	Zr w/o	Re w/o	C w/o or ppm	N w/o or ppm	O w/o or ppm
target												
Ta-10W	CVAM 1619	0.475-inch diameter rod	89.95			10.15				14 ppm	12 ppm	24 ppm
FS-85 Target	N/A	N/A	27.5	60.65	-	11	-	0.85	-	0.010	0.010	0.015
FS-85	CVAM 1602	Extruded Round	27.26, 28.23	60.7, 59.8	-	11.01, 11.00	-	0.96, 0.85	-	0.021, <0.005	0.0046, 0.005	0.0030, 0.0036
FS-85	CVAM 1602	In-process tubing	27.66	60.5	-	10.99	-	0.82	-	26ppm	<10ppm	1ppm
FS-85	CVAM 1602	Final tubing	27.79	60.2	-	11.12	-	0.82	-	68ppm	<0.10 ppm	4 ppm
FS-85	CVAM 1603	Extruded Flat	27.20, 27.33	61.4, 60.3	-	10.56, 11.46	-	0.83, 0.90	-	<0.005, 0.005	0.0047, 0.0034	0.0014, 0.0018
FS-85	CVAM 1603	0.040-inch							-	15.7ppm, 18.9ppm	15.4ppm, 12.8ppm	65.6ppm, 71.8ppm
Mo-Re Target			-	-	52.5	-	-	-	47.5	50ppm	-	<20ppm
Mo- Re	CVAM 1613	0.040-inch hot rolled							46.68	42.1ppm	4.2ppm	48.5ppm
Mo-Re	CVAM 1613	0040-inch cold rolled							46.17	38.2ppm	4.3ppm	52.2ppm
Mo-Re	CVAM 1613	Round Extrusion							46.67, 46.36	0.002, 0.011	0.001, 0.001	0.048, 0.017
Mo-Re	CVAM 1613	0.275-inch dia. rod								48.3 ppm	3.2 ppm	38.9 ppm

As a comparison, the acceptable alloying bands for large commercial ingots of several of the tantalum and niobium-base ingots are also listed in Table 7.

Table 7: Tentative Ingot/Billet Chemical Composition Requirements in Weight Percent for Large Commercial Ingots that were to be Procured from Wah Chang

ELEMENT	CLASS 1 Ta-10W MAX %/Min%	CLASS 2 ASTAR-811C MAX %/Min%	CLASS 3 FS-85 MAX%/Min%
Ta	Balance	Balance	29.0/26.0
W	9.00-10.15	8.500/7.500	11.0/9.00
Hf	-----	0.75/1.25	0.0200
Re	0.100	0.75/1.5	-
C	0.008	0.030/0.0200*	0.010
O	0.010	0.010	0.015
N	0.005	0.005	0.010
H	0.002	0.002	0.0015
Nb	0.100	0.100	Balance
Fe	0.005	0.005	0.005
Ti	0.020	0.020	0.020
Mo	0.020	0.020	0.010
Si	0.005	0.005	0.005
Co	0.005	0.005	0.005
Ni	0.005	0.005	0.005
Cu	0.005	0.005	0.005
Zr	0.020	0.020	1.5/0.75

* Carbon aim point for ASTAR-811C (not a requirement).
Values are maximum unless a range is specified

These latter levels had been tentatively agreed to by Wah Chang during negotiations, since terminated, for a contract to melt and fabricate commercial scale ingots of the Ta-10W, ASTAR-811C, and FS-85 alloys. For the most part, the alloying constituents fell within the tolerance bands that were to be employed for melting of the large ingots. There were several exceptions; each is discussed below:

- Carbon at one portion of the ASTAR-811C ingot was well below the 250 ppm aim point. However, the accuracy of an analysis taken from the outer skin portions of an ingot can be suspect and may not accurately represent the ingot interior. Later analysis for this ingot conducted after further processing indicated acceptable carbon levels.

- With respect to the interstitials of oxygen, nitrogen, and carbon for other alloys, the only major concern appears to be oxygen in the molybdenum-47.5 rhenium ingot. Analysis at the ingot stage as well as at later points in the process revealed oxygen levels of 40 ppm, a level well above the <20 ppm target. This will be further discussed in a later section.

- A final issue is the level of rhenium in the Mo-47.5 rhenium ingot. The target rhenium value was 47.5 w/o. The actual level measured at the ingot stage and at later stages in the process was slightly lower. The chemical analysis revealed rhenium contents ranging from 46.2-46.5. These marginally lower levels are not expected to be an issue. The level is high enough to ensure that sufficient ductility is present to ensure excellent weldability and processing characteristics similar to that provided by 47.5 w/o. At the same time, the rhenium level remains high enough to ensure that if tested in-reactor, the alloy would still provide a valid test of the concern that high levels of embrittling sigma and chi phases may be generated in Mo-Re alloys with high concentrations of rhenium.

C. Extrusion

Ingot breakdown for all alloys was conducted at Wright Patterson Air Force Base (WPAFB). Their facility employs a large 700 ton horizontal extrusion press for this process step. Each alloy was extruded into both a sheet bar extrusion and a round extrusion, with the exception of the PM molybdenum-44.5 rhenium alloy. This latter alloy was extruded only into sheet bar. Preparation for extrusion depended upon the final ingot height and the alloy composition. Melted ingots that had a final height of 9-10-inches were sectioned in half. Each half was machined either to fit into a molybdenum extrusion canister or machined to duplicate the shape of the extrusion canister. The ingots were always oriented and machined so that the top portion of the ingot would be extruded first. The rationale for this orientation is discussed in Section II. The two final melt ingots of Ta-10W and FS-85, both 4.5-5.5-inches in height, were machined to fit into canisters. All other tantalum-base alloys as well as the PM molybdenum-44.5 rhenium alloy were also encapsulated within molybdenum canisters. The arc cast molybdenum-47.5 rhenium alloy was not encapsulated and was machined to the same configuration and dimensions as the canister. Only a thin layer of commercial glass compound called Corning Glass 7052 was applied to the as-machined molybdenum-47.5 rhenium alloy prior to extrusion. It should be noted that minimal material was removed from the outer walls of this latter alloy when machining to shape. The result was that numerous pits were present on the outer walls prior to extrusion. This resulted in much rougher as-extruded surfaces for both extrusions of the molybdenum-47.5 rhenium alloy.

The molybdenum canister serves two functions during extrusion: 1) it protects the encapsulated refractory metal from interstitial contamination, and 2) it serves as a lubricant for the extrusion process. Encapsulation of the Mo-Re arc cast alloy was avoided because of the differing nature of

the molybdenum oxide formed during high temperature air exposure versus the behavior of the Group VB alloys (Nb & Ta) in a similar environment. When heated in air to a high temperature, a variety of oxides are formed on the surface of the Group VB alloys. Oxide formation is accompanied by a relatively rapid diffusion or penetration of oxygen and nitrogen into the underlying surface layers. Diffusion depth is a function of both temperature and time at temperature. This results in severe contamination for the Nb and Ta alloys. However, the oxide formed on heated molybdenum in air is extremely volatile and literally boils off as a visible cloud as soon as it forms. This phenomenon results in minimal penetration or contamination beyond the immediate surface. Based on these differences, it is critical that the Nb and Ta alloys are encapsulated within a canister as they undergo the extrusion process while it is not for the molybdenum-base alloys. As noted the molybdenum-47.5 rhenium arc cast alloy was not encapsulated whereas its sister alloy, the PM Mo-44.5 rhenium alloy, was encapsulated. The capsule provided additional protection for the PM alloy since it was uncertain if the alloy was fully dense when formed into the billet. Consequently, oxides could be entrapped with its interior even if they volatilized. A photograph of a molybdenum extrusion canister as well as the PM molybdenum-44.5 rhenium ingot machined to fit within the canister is displayed in Figure 8.

Figure 8: Right - Molybdenum canister approximately 6-inches high. Left - PM Molybdenum-44.5 rhenium alloy machined to fit within the canister.

Both encapsulated and bare ingots were pre-heated at WPAFB within an argon purged induction furnace to the temperatures specified in Table 8.

A thermocouple in contact with the bottom of the canister or ingot was used to monitor ingot temperature. Once at temperature, the ingots were immediately removed from the furnace and manually transferred to the extrusion press. Ingot removal from the furnace, transfer to the press, and loading into the press typically totaled less than 30 seconds. The ingots were then rammed through a round or rectangular shaped high strength die coated with ZrO_2. The reduction ratio for both types of extrusion typically ranged from approximately 5-6:1. The round extrusions were approximately 1- 3/8-inches in diameter whereas the rectangular sheet bars were approximately 8/10-inch thick and 1-7/8-inches wide. Extrusion lengths varied from 2 - 3-feet. A photograph of two molybdenum-47.5 rhenium extrusions and a FS-85 extrusion is provided in Figure 9. The extrusion parameters provided by WPAFB are listed in Table 8.

Table 8: WPAFB Extrusion Parameters

	T-111 (Round)	T-111 (Flat)	ASTAR-811C (round)	ASTAR-811C (Flat)	FS-85 (Round)	FS-85 (Flat)	Mo-47.5Re (Round)	Mo-47.5Re (Flat)
Billet Diameter (in)	2.896	2.905	2.89	2.921	2.92	2.95	2.845	2.855
Billet Length (in)	5.07	5.218	5.57	5.378	5.521	5.84	4.7	5.04
Billet Nose (in)	1	1	1	1	1	.5 x 45 degree	.5 x 45 degree	.5 x 45 degree
Billet Weight (lb)	16.3	16.88	17.78	16.86	12.72	14.04	13.4	14.35
Die Ratio (:1)	6	---	6	---	6	5.61	6.2	5.66
Die Type	60 Degree Conical	Rect. 90 degree	60 Degree Conical	Rect. 90 degree	60 Degree Conical	Rect. 90 degree	60 Degree Conical	Rect. 90 degree
Die Facing	ZrO2	ZrO2	ZrO2	ZrO2	ZrO2	ZrO2	ZrO2	ZrO2
Die Temp (F)	500	500	500	500	500	500	500	500
Container Temp (F)	500	500	500	500	500	500	500	500
Follow Block Carbon (in)	3	3	3	3	3	3	3	3
Container Size (in)	3.072	3.072	3.072	3.072	3.072	3.072	3.072	3.072
Follow Block Steel (in)	2.875	2.875	2.875	2.875	2.875	2.875	3	2.875
Billet Final Heat Temp (F)	3000	3000	3000	3000	2500	2500	3300	3300
Billet Final Heat by	Induction	Induction	Induction	Induction	Induction	Induction	Induction	Induction
Billet Final Heat Time (hrs)	0.983	0.7	0.833	0.833	0.717	---	---	---
Die Lube	Delatforge 144	Delatforge 144	Delatforge 144	Delatforge 144	Delatforge 144	Delatforge 144	Delatforge 144	Delatforge 144
Container Lube	TS 625	TS 625	TS 625	TS 625	TS 625	TS 625	TS 625	TS 625
Load Max (ton)	491.1	596.43	631.05	634.57	515.46	618.73	533.65	570.03
Ram Speed (ipm)	120	120	120	120	120	120	120	120
Accumulator (psi)	3400	3400	3400	3400	3400	3400	3400	3400
Extrusion Length (in)	22.75	26.25	26.5	31.25	26.5	28	24	23.2
Extrusion Diameter (in)	1.31	---	1.25	---	1.275	---	1.235	---
Extrusion Ratio	5.5	5.65	6.04	6.62	5.8	5.01	6.19	4.4
Comments	Air Cool	Air Cool	Air Cool	Air Cool	Air Cool	Slow Cool ext-234	ext-234	ext-234

Figure 9: Top - Two extrusions of the Mo-47.5 rhenium alloy. Both were extruded without a canister. Bottom - FS-85 alloy extruded with a canister.

Following extrusion, the outer surface of the molybdenum cladding covering the encapsulated ingots was relatively smooth for all alloys. Conversely both molybdenum-47.5 rhenium extrusions that were extruded without a canister exhibited much rougher surfaces. The pitted nature of the as-machined outer billet, noted above, caused much of the difference. However, the different nature of rhenium oxide as opposed to molybdenum oxide may have played a role.

D. De-Cladding for Niobium and Tantalum-Base Alloys

The extrusion process mechanically and metallurgically bonds the molybdenum canister to the extruded wrought product forming a thin molybdenum cladding entirely covering the extruded alloys. The cladding is removed by a combination of pickling and machining. The initial step consists of pickling in a bath of nitric acid (HNO_3). Nitric acid attacks only the molybdenum clad and leaves the underlying tantalum or niobium alloys intact. The cladding removal proceeds very slowly within the acid bath, typically taking 24-48 hours to complete. The technician monitoring the process must periodically refresh the acid bath as the chemical reaction slows. The surface (of the now revealed extruded alloy) after this initial pickle process is very dull in appearance and is combined with a rough bark-like surface. This surface is then exposed to a second pickle solution which attacks and removes approximately 0.002-0.003 inches of additional material. This second pickle ensures that all cladding remnants and potential contaminants have been removed. The composition of the second acid depends on the alloy composition. Typical compositions are provided in Table 9.

Table 9: Acid Compositions

Alloy	Pickling Acid Composition
ASTAR-811C	$45HF:45HNO_3:10H_2SO_4$
T-111	$45HF:45HNO_3:10H_2SO_4$
FS-85	1:1:1 ratio HNO_3, HF, H_2PO_4
Mo-47.5Re	$40HNO_3:40H_2O:20H_2SO_4$
Ta-10W	$45Hf:45HNO_3:10H_2SO_4$

Material removal during this second pickle is relatively rapid. When the acid is fresh the process can be completed in 5-10 seconds.

The PM molybdenum-44.5 rhenium alloy was processed only through extrusion and left with its clad intact. If the cladding had been removed, the identical procedure would have been used. However, for this alloy the final portion of the nitric acid pickle step would have to be closely monitored. The nitric acid pickle will not stop at the interface between the molybdenum cladding and the Mo-Re base material but will penetrate the interface and beyond, continuing to attack the underlying Mo-Re. However, the pure molybdenum cladding and the underlying Mo-Re exhibit subtle but distinctive differences in both texture and appearance. This makes it relatively easy for the technician to discern when the interface has been breached and the piece should be removed from the acid bath.

The two molybdenum-47.5 rhenium extrusions were extruded bare except for a thin layer of a Corning Glass compound so that removal of the clad was not an issue. However, as previously noted, the outer surfaces of both of these extrusions were relatively rough. These surfaces were machined and pickled to remove the majority of this roughness. However, many of the pits extended to depths that precluded their total removal. This may have played a role in the higher than specified oxygen levels noted earlier.

E. In-Process Anneals

In-process 1-hour vacuum anneals for the Nb and Ta alloys are typically performed after extrusion and at periodic points during secondary processing. The in-process vacuum anneals are intended to recrystallize and soften the material. This allows further reductions in thickness or diameter to be made without fear of cracking due to excessive work hardening. A secondary function is to remove any hydrogen that is absorbed during acid pickling, a step that is intended to clean the surface and remove any contamination. If the sole function of the vacuum anneal for the Nb and Ta alloys is to remove absorbed hydrogen, then the temperature of the vacuum anneal can be reduced to approximately 800 °C. In-process annealing temperatures employed for the Nb and Ta alloys are listed in Table 10.

Table 10: In-Process Vacuum Annealing Temperatures for Nb and Ta Alloys. Initial Annealing Temperature for the Molybdenum-47.5 Re Alloy is Also Listed.

Alloy	In-process Vacuum Annealing Temperature (°C)
T-111, Ta-10W, ASTAR-811C (all extrusions)	1500
FS-85 (flat extrusion)	1400
FS-85 (round extrusion)	1300
Mo-47.5Re round and flat (initial anneal only)	1600 (vacuum or H_2)

Two different temperatures were used for the in-process anneals of FS-85. The in-process anneals for the round extrusion were all conducted at 1300 °C whereas those used for the flat were conducted at 1400 °C. The round extrusion was processed first. The 1300 °C annealing temperature had been selected for FS-85 by the undersigned based on previous processing experience that indicated that 1300 °C should recrystallize this material during normal processing. However, following the processing of the round FS-85 extrusion into rod stock and tubing, it was determined that 1300 °C only partially recrystallized material from this particular FS-85 ingot. The reasons for this discrepancy in annealing response are not clear. Significant differences in the levels of either the major alloying elements or interstitial content were not apparent between the two ingots. Nevertheless, the in-process annealing temperature for the flat extrusion was increased to 1400 °C. The lower temperature may have played a role in the cracking observed during formation of FS-85 tubing, as will be discussed later in this document.

In-process annealing is also a necessary process step for the Mo-Re alloys. Similar to the Group VB alloys, annealing softens the material and allows further material reductions. However, there are two differences to note between the annealing practices for the Group VB and Group VIB alloys. These differences include: 1) annealing of molybdenum and other molybdenum alloys such as TZM and Mo-Re can be conducted either in a flowing hydrogen furnace or a vacuum furnace; the hydrogen atmosphere will actually reduce oxides present on the material surface, and 2) the tendency of the VIB alloys to adsorb hydrogen during the pickling process is much less than for the Nb and Ta alloys. A further discussion of the differences between the Group VB and VIB alloys is provided in the next section.

F. Swaging or Rolling

The mode of secondary breakdown was established by the configuration of the extruded product. The flat extrusions of all alloys except Ta-10W and PM molybdenum-44.5 rhenium were rolled into 0.040-inch thick sheets that were to be converted to sub-size flat tensiles or creep specimens. Ta-10W and PM molybdenum-44.5 rhenium flat extrusions were left in the as-extruded condition. The Ta

and Nb round extrusions were swaged to either 0.450-inch diameter rod or 0.275-inch rod. The 0.450-inch diameter Ta or Nb-base rods were converted into tube hollows that were subsequently formed into thin walled 0.250-inch diameter tubing. The 0.275-inch diameter swaged stock was machined to form 0.250-inch diameter end plugs for biaxial creep specimens. The arc cast Mo-47.5 rhenium round was swaged to ~0.780-inch diameter rod for tube hollow formation as well as thinner 0.275-inch diameter rod for end plug formation.

The details of these swaging and rolling steps are described more fully in sections H, I, and J below. However, the difference in behavior between the Group VB and VIB alloys that was alluded to in the previous section needs to be re-emphasized for a better understanding of the processes and parameters used. The Group VB (Nb and Ta) alloys typically exhibit Ductile-to Brittle-Transition Temperatures (DBTT) well below room temperature in the wrought condition. In fact, the DBTT of pure tantalum is near 0 K as can be seen in Figure 10, Reference (2). The DBTT for pure niobium is not as low but still remains well below room temperature. The addition of alloying constituents to increase strength or creep behavior usually degrades the DBTT of both niobium and tantalum alloys relative to their pure base-element. Welding causes additional degradation. Nonetheless, previous testing conducted in the late 1960s indicates that current JOYO candidate Ta and Nb alloys display DBTTs that remain below room temperature following welding, Reference (2). Tantalum alloys are especially forgiving to welding and display little degradation in their DBTTs (Reference (2)).

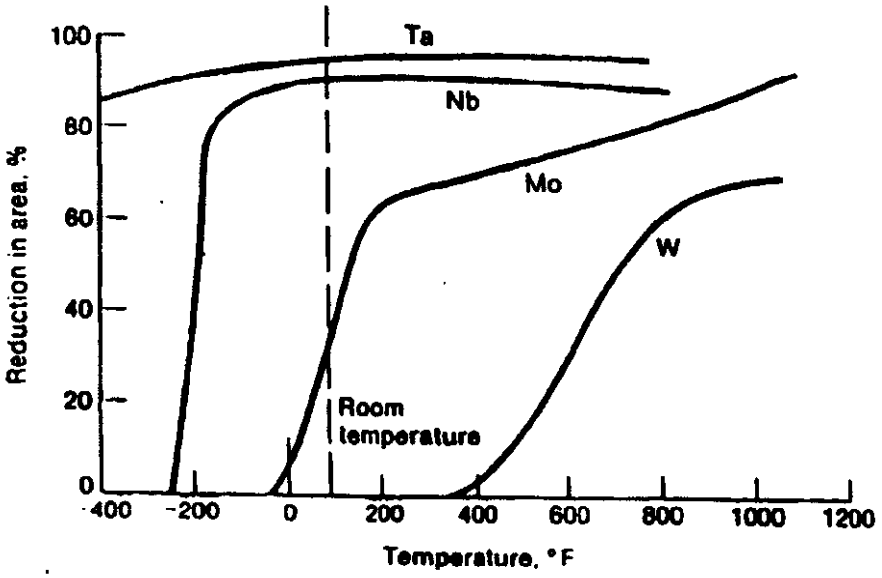

Figure 10: Ductile to Brittle Transition Temperature for Pure Refractory Metals (Reference 2).

Although it is not critical for an understanding of the processing rationale for these alloys, it is important to note from a usage and testing perspective that there are some subtle differences in the fracture mechanics between Nb and Ta alloys. Niobium alloys typically "display unarrested cracking and a classic, abrupt transition from ductile to brittle cleavage behavior," References (3 & 4). The tantalum alloys and their weldments in the aged condition do display shifts in transition behavior, but they usually fracture in a ductile intergranular mode and not in a brittle cleavage mode. Again, a transition exists for tantalum alloys, but it is gradual and would not require imposing a design limit, Reference (4).

While subtle differences in fracture behavior between niobium and tantalum-base alloys do exist, both of these elements and their alloys still exhibit a large measure of ductility in the wrought and welded

condition. As a result, once the as-cast structures of either alloy have been broken down and annealed, they can be readily rolled or swaged at room temperature. In-process anneals are only necessary for pure Ta and most tantalum alloys when the total reduction approaches 75-90%, Reference (5). Niobium alloys can be reduced to slightly smaller percentages before an in-process anneal is necessary. If equipment limitations are present, the Group VB alloys can be preheated to 500°F prior to initial rolling or swaging passes to soften the materials with little risk of oxidation.

This behavior is significantly different from that exhibited by the Group VIB (Mo and W) alloys. The DBTTs for pure molybdenum and tungsten are shifted well to the right in Figure 10. The DBTT for wrought molybdenum is close to room temperature and tungsten is well above. Welding significantly increases the DBTT of both pure elements and most of their respective alloys. There is one notable exception. Rhenium additions to both of these Group VIB alloys can significantly improve their ductility in the wrought and welded condition. When Naval Reactor involvement in the Prometheus mission was first initiated, the understanding of the NRPCT with respect to processing of molybdenum and in particular Mo-Re alloys can be summarized by the following. Most of the molybdenum alloys with DBTTs near room temperature require temperatures of 1200-1400 °C for initial secondary swaging or rolling passes. As the product thins, the molybdenum-base alloys can be processed at lower temperatures with the lower bound set by the DBTT of the particular alloy. Once the thickness of the sheet product or diameter of the bar stock has been sufficiently reduced, the molybdenum-rhenium alloys with rhenium contents greater than 44 w/o rhenium should be workable at room temperature. However, as the current program continued to evaluate Mo-Re, processing parameters had to be modified from those employed for pure molybdenum and TZM to achieve desired microstructures. The modifications will be detailed in later sections.

In summary, following ingot breakdown Nb and Ta alloys can be further broken down cold or with the addition of little heat, whereas molybdenum and tungsten alloys require significant heat input except for certain Mo-Re alloys.

G. Additional Preparation for Swaging and Rolling of Refractory Alloys

The rough bark surface finish (see Figure 11) remaining on the as-extruded rounds or flats after decladding, pickling, and annealing is not acceptable for further fabrication. The bark-like surface can fold-over during processing leading to surface oxide entrapment or entrapment of other contaminants such as swaging grease on the outer layers. The entrapment can extend to appreciable depths and would only be partially removed by subsequent pickling operations. PMTI typically takes special care to machine the outer surfaces of the rounds or flats to form a smooth surface prior to rolling or swaging.

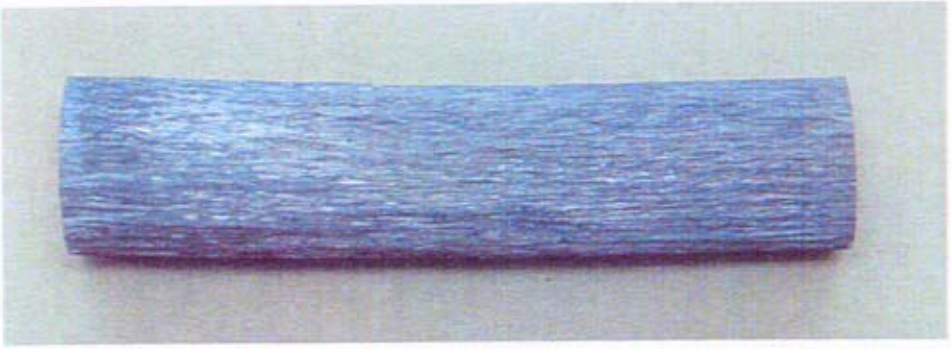

Figure 11: Rough surface remaining on a 1.3-inch diameter piece of T-111after cladding has been removed by pickling.

H. Swaging

Swaging was performed at PMTI using a hydraulic FENN 4-F swager. The 4-F unit is comprised of four dies that rapidly rotate and compress the material as the rod is slowly inserted by a technician holding the piece in a set of tongs. Figure 12 is a schematic of a swager.

The die sets are manufactured from high temperature tool steels to specific target diameters. A set of dies is typically changed after each pass to the next smaller set. Percentage reductions for each swaging pass vary depending on die availability, the strength of the material, the amount of spring-back, and the amount of work imparted to a specific piece prior to in-process annealing. The swaging process allows a fairly thick cylinder to be elongated and reduced to the proper diameter. The largest diameter rod that can be reduced at PMTI is slightly greater than 1.25 inches. The smallest diameter that PMTI can swage to is 0.200 inches. It should be noted, however, that the rod will undergo pickling and annealing which will reduce the diameter further.

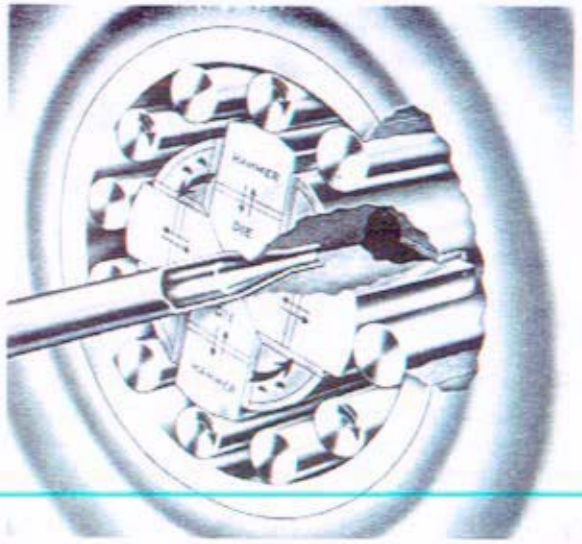

Figure12: Schematic of a swager similar to the FENN 4-F unit at PMTI.

An example of a typical reduction employed of the Nb or Ta-base alloys can be seen in Table 11 where the swaging parameters used for Ta-10W are listed.

Percentage reductions vary from 3-8%. The average percentage reductions for the Nb and Ta base alloys were approximately 4%. Early passes employed 500 °F heating to soften the material slightly. Note that the material was reduced ~ 85% before an in-process anneal was conducted.

Swaging of the Mo-47.5 rhenium alloy followed a similar reduction scheme. The molybdenum-47.5 rhenium alloy was preheated to 1300 °C in the hydrogen furnace prior to each pass. After the 1.2-inch diameter extrusion was reduced to a diameter of 0.800-inches, it was sectioned into two pieces approximately 16-18 inches long. The pieces were then annealed at 1550 °C and supplied to Rhenium Alloys to be formed into tube hollows and then drawn into tubing. Note that in-process anneals were not conducted during swaging of this alloy. The reduction scheme employed for this material was established prior to contact with Rhenium Alloys to establish the optimum processing parameters for this alloy.

Table 11: Swaging of Ta-10W bar stock

Ta-10W

Pass Number	Diameter	% Reduction	Temperature
1	1.1	5%	250°C
2	1.05	3%	250°C
3	1.015	2%	250°C
4	0.99	2%	250°C
5	0.97	5%	250°C
6	0.92	2%	250°C
7	0.9	7%	250°C
8	0.835	2%	250°C
9	0.82	7%	250°C
10	0.765	5%	250°C
11	0.725	6%	250°C
12	0.68	2%	Room Temperature
13	0.665	5%	Room Temperature
14	0.63	2%	Room Temperature
15	0.615	8%	Room Temperature
16	0.565	1%	Room Temperature
17	0.562	3%	Room Temperature
18	0.546	5%	Room Temperature
19	0.519	4%	Room Temperature
20	0.497	3%	Room Temperature
21	0.48	4%	Room Temperature
22	0.46	2%	Room Temperature
Anneal at 1250°C for one hour (85% reduction before anneal)			
23	0.45	7%	Room Temperature
24	0.42	7%	Room Temperature
25	0.39	4%	Room Temperature
26	0.375	7%	Room Temperature
27	0.35	6%	Room Temperature
28	0.33	6%	Room Temperature
29	0.31	-	Room Temperature

I. Rolling of Tantalum and Niobium-Base Alloys

T-111, ASTAR-811C, & FS-85:

The two tantalum-base alloys, T-111 and ASTAR-811C, as well as the niobium alloy, FS-85, were rolled to thicknesses of approximately 0.040-inches at PMTI using a 25-horsepower STANAT 2-high rolling mill. The rolls on this mill are 8-inches wide and were operated at a roll speed of 10 ft/minute for this program. A photograph of the actual mill is in Figure 13.

As noted above, once the as-cast structures of niobium and tantalum-base alloys are broken down and refined by extrusion, both alloy types can be processed through significant room temperature reductions before an in-process anneal is required. Heat, while not required, can be used to lower the yield strength and make it easier for initial reductions at thicker stages. The total amount of the final room temperature reduction imparted following the next-to-last anneal is believed to have an impact on final mechanical properties. To resolve this issue, two different schemes were employed for the breakdown of T-111, ASTAR-811C, and FS-85. The same relative rolling scheme was employed for all three alloys although different starting thicknesses caused some variations in actual percentage reductions.

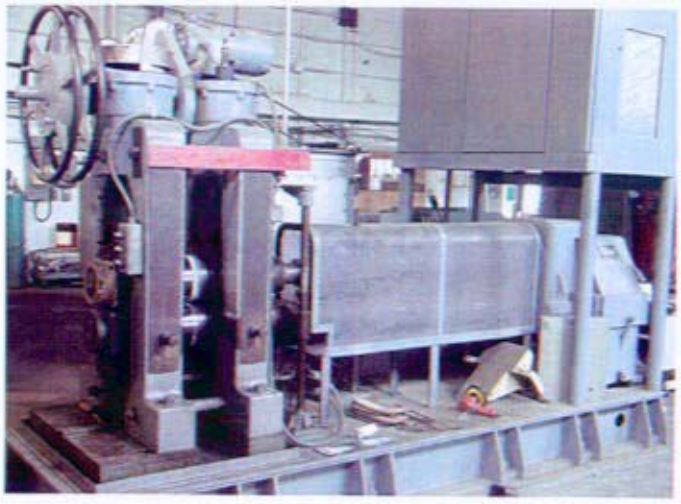

Figure 13: Photograph of the PMTI 2- high STANAT rolling mill used for RT reductions of Ta-base and Nb-base alloys as well as hot and cold rolling of Mo-Re alloys.

The details of the individual rolling schedules can be seen in Tables 12, 13, and 14.

Table 12: Rolling Schedule of T-111 Sheet

T-111

Pass Number	*Thickness*	*% Reduction*	*Temperature*
1	*0.53*	*9%*	500°C
2	*0.48*	*9%*	500°C
3	*0.435*	*9%*	500°C
4	*0.395*	*10%*	500°C
5	*0.355*	*15%*	500°C
6	*0.3*	*4%*	500°C
7	*0.287*	*2%*	500°C
8	*0.28*	*15%*	500°C
9	*0.237*	*10%*	500°C
10	*0.213*	*11%*	Room Temperature
11	*0.19*	*3%*	Room Temperature
12	*0.185*	*15%*	Room Temperature
13	*0.157*	*9%*	Room Temperature
14	*0.143*	*9%*	Room Temperature
15	*0.13*	*4%*	Room Temperature
16	*0.125*	*7%*	Room Temperature
Anneal at 1650°C for one hour			
17	*0.116*	*7%*	Room Temperature
18	*0.108*	*6%*	Room Temperature
19	*0.102*	*10%*	Room Temperature
20	*0.092*	*20%*	Room Temperature
21	*0.074*	*5%*	Room Temperature
22	*0.07*	*11%*	Room Temperature
23	*0.062*	10%	Room Temperature
24	*0.056*	11%	Room Temperature
25	*0.05*	-	Room Temperature

Table 13: Rolling Schedule of ASTAR-811C Sheet

ASTAR-811C

Pass Number	Thickness	% Reduction	Temperature
1	0.48	5%	500°C
2	0.457	4%	500°C
3	0.438	9%	500°C
4	0.397	10%	500°C
5	0.358	8%	500°C
6	0.33	14%	500°C
7	0.284	3%	500°C
8	0.275	15%	500°C
9	0.235	10%	500°C
10	0.211	10%	Room Temperature
11	0.19	4%	Room Temperature
12	0.183	15%	Room Temperature
13	0.155	8%	Room Temperature
14	0.143	9%	Room Temperature
15	0.13	5%	Room Temperature
16	0.124	6%	Room Temperature
Anneal at 1650°C for one hour			
17	0.116	9%	Room Temperature
18	0.105	7%	Room Temperature
19	0.098	8%	Room Temperature
20	0.09	4%	Room Temperature
21	0.086	9%	Room Temperature
22	0.078	6%	Room Temperature
23	0.073	11%	Room Temperature
24	0.065	9%	Room Temperature
25	0.059	7%	Room Temperature
26	0.055	5%	Room Temperature
27	0.052	-	Room Temperature

Table 14: FS-85 Rolling Schedule

FS-85

Pass Number	Thickness	% Reduction	Temperature
1	0.67	7%	500°C
2	0.625	7%	500°C
3	0.58	14%	500°C
4	0.5	15%	500°C
5	0.425	15%	500°C
6	0.36	15%	500°C
7	0.305	15%	Room Temperature
8	0.26	15%	Room Temperature
9	0.22	16%	Room Temperature
10	0.185	19%	Room Temperature
11	0.15	15%	Room Temperature
Anneal at 1400°C for one hour			
12	0.127	6%	Room Temperature
13	0.12	15%	Room Temperature
14	0.102	12%	Room Temperature
15	0.09	17%	Room Temperature
16	0.075	15%	Room Temperature
17	0.064	13%	Room Temperature
18	0.056	13%	Room Temperature
19	0.049	10%	Room Temperature
20	0.044	9%	Room Temperature
21	0.04	-	Room Temperature

A summary of the rolling schedule is listed below, which ignored the minor variations in starting thickness:

1. T-111, ASTAR-811C, & FS-85 – Roll from ~0.600-inch thickness to ~0.125-inch thickness (~75% total reduction)using 10% reductions at room temperature (RT) except for initial passes that preheated material to 500 °F before rolling.
2. Pickle to remove 0.001-0.002-inches & vacuum anneal for 1 hour.
3. Roll half of the material to a thickness of approximately 0.038-inches at RT using reductions of 10% per pass. (Total reduction ~ 72%). No further processing of this material would be required.
4. Roll the remaining half to ~0.052-inch (~ 40% total reduction from last anneal))
5. Pickle this half to remove 0.001-0.002-inch & vacuum anneal
6. Continue rolling to ~0.038-inches at R.T. using 10% per pass reduction
(Total reduction following the last anneal ~ 30%).

For this program, sheets of T-111, FS-85, ASTAR-811C, and molybdenum-47.5 rhenium were produced. There was no sheet production for Ta-10W; only tubing and end caps were made. However, if Ta-10W had been processed, a similar reduction schedule to that of T-111 and ASTAR-811C would have been followed.

All of the alloys rolled into sheet product yielded final rolled sheets that displayed either no edge cracking or minimal edge cracking. There was one exception. A single sheet of ASTAR-811C severely cracked during final passes. The rolling of this sheet had been initiated on the STANAT mill

and was moved to a LOMA 4-high foil mill for final rolling with the goal of improving final surface finish. This mill had not previously been used for production of refractory metals. Once the plate cracked, the other ASTAR-811C plates were returned to the STANAT mill and were rolled to final thickness without failure. It is not clear what caused the one plate to crack. Chemical evaluation of final rolled product indicated that the alloying constituents were in specification and that no interstitial contamination had occurred. A small undetected defect present within the plate may have been responsible. The response of the other plates as well as the successful tube drawing of this material suggests that this was an isolated incident. It also suggests that this ingot of ASTAR-811C demonstrates good fabricability consistent with ASTAR-811C produced in the 1960s and 1970s.

Figure 14 is a photograph of three as-rolled plates representing respectively, FS-85, T-111, and ASTAR-811C. The minor defects observed on the surfaces result from slight defects present on the surface of the rolls and were not a result of deformation problems. Note that for efficient production, PMTI typically processes both hot and cold rolled product on the STANAT mill using the same set of rolls. However, hot rolling of molybdenum typically mars the roll surfaces over time. Subsequent rolling of the ductile Nb and Ta alloys transfers these defects from the rolls to the in-process plates. If necessary, surface finish on cold rolled Ta and Nb product can be appreciably improved by changing to a new roll set before initiating final rolling.

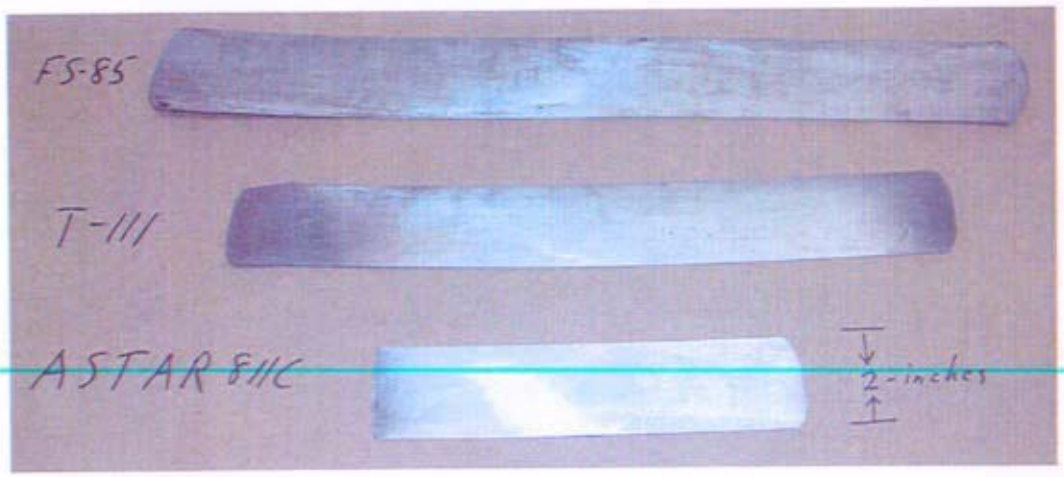

Figure 14: Photograph of as-rolled 0.040-inch thick plates of ASTAR-811C, T-111, and FS-85.

J. Rolling of Mo-47.5 Re

A 2-inch ingot of molybdenum-47.5 rhenium had been melted at PMTI and processed into plate stock prior to the start of production of JOYO specimens. This material had been subsequently supplied to ORNL and served as the basis for machining of in-reactor tensile specimens and control specimens exposed in the HIFR reactor. The material had been processed on the STANAT mill using a reduction schedule similar to that typically used for pure molybdenum or Mo-TZM. The schedule is listed below:

Initial process used to roll a 2-inch ingot of Mo-Re

1) Preheat in hydrogen furnace to 1200 °C.
2) Reduce material using ~10% passes (actual reduction significantly less).
3) Reheat after each pass at 1200 °C.
4) After material is reduced a total of 50%, lower furnace temperature to 1050 °C.
5) Continue ~10% passes with reheats after each pass at 1050 °C.

Following this breakdown scheme, a 1400-1500 °C anneal produced a partially recrystallized and very heterogeneous microstructure. The structure contained a mixture of both large and fine grains. This was not the equiaxed microstructure desired for final processed Mo-Re. As a result, Rhenium Alloys was contacted for suggestions on how to improve the final structure for the JOYO material. (Note that pure molybdenum, as well as most of its alloys, is typically placed into service with a stress relieved as-rolled or worked final microstructure.)

The technical director of Rhenium Alloys [Reference (6)] suggested one of two paths to improve the final microstructure. Both of these paths are used by Rhenium Alloys for the processing of commercial PM Mo-Re. One path consisted of cold rolling intermixed with short high temperature anneals at 1600 °C in a hydrogen furnace. This anneal is to be conducted when reductions in thickness total 20%. A second path consisted of rolling at 1400 °C intermixed with an identical in-process anneal. Total rolling reductions for this path should be limited to approximately 50% before conducting the in-process anneal. These two paths were used during rolling of the 3-inch diameter molybdenum-47.5 rhenium ingot. In addition, a third path was added by the NRPCT that combined portions of each of the other two. This third variant began with high temperature rolling using the second path parameters and then switched to the cold rolling process at a thickness of 0.080-inches. Cold rolling then continued until reaching the final thickness of 0.040-inches. These process variations are displayed in the flow sheet depicted in Figure 1.

Materials representing all three paths were successfully processed to a final thickness of 0.040-inches on the STANAT mill at PMTI. Minimal edge cracking was observed in each processing path as opposed to that sometimes observed for rolled pure molybdenum or molybdenum alloys such as TZM. Following the final passes, material representing each process path was annealed at 1550 °C to recrystallize the product. The 1550 °C anneal produced equiaxed microstructures that extended across the entire cross sectional thickness for each process. Resulting grain sizes after annealing were ranked in the following order: 1) mixed path (largest), 2) cold worked, and 3) hot or warm worked.

Initially it was believed that annealing of the final cold rolled material would form the smallest equiaxed grained structure. It was assumed that the un-annealed cold rolled structure would consist of elongated and very fine grains. Recrystallization of this structure was expected to produce a finer grain size than either of the other processes. This proved to be only partially true. In retrospect this is consistent with our understanding of cold and warm or hot working. Cold working typically introduces more dislocations and stored energy into a structure than does warm or hot rolling. The more stored energy imparted to a structure the lower is the starting temperature for recrystallization. In addition, the greater the dislocation density, the larger is the quantity of nuclei for recrystallized grain formation. Conversely, high temperature rolling imparts less energy to the piece and fewer dislocations. It also allows the material to partially recover during the preheating conducted prior to each pass. All of the paths used for rolling molybdenum- 47.5 rhenium appeared to result in the introduction of work that was both sufficient and equally spread throughout the thickness of each piece. However, the larger stored energy present within the cold worked structure apparently more than compensated for its own

smaller starting grain size as well as the much larger starting grain size of the entirely warm worked material. At the same time, both the mixed path and the cold worked path experienced the same total reduction at room temperature following the last in-process anneal. Thus the material processed via the mixed path contained the same amount of stored energy as did the entirely cold worked material. Combining this with an apparently larger starting grain size resulted in the largest grain size upon final annealing.

Note that the high temperature rolling schedule allows for a greater reduction for each individual pass as well as a greater total overall reduction before an in-process anneal is required. Rhenium Alloys also noted that the 1600-1625 °C in-process anneal should be limited to 15 minutes. Longer annealing times could result in abnormally large grains and cause cracking during subsequent passes. Rhenium Alloys also suggested monitoring of the hardness during rolling to ensure that process was correctly performed.

K. Preparation of Niobium and Tantalum Alloys for Tube Drawing

There are numerous methods that can be used to form tubing. The method selected for these alloys employed a cold drawing process that pulls a tube hollow through a circular die during a series of passes. A steel mandrel is encased within the tube hollow for all but the last 1-2 passes. The method was employed by True Tube, Inc, a vendor with considerable experience in forming niobium and tantalum-base refractory metal tubing.

The dimensions of the starting tube hollow are a function of several factors including: 1) annealing capability both at the tube drawing facility and at PMTI, and 2) total percentage reductions to produce the desired wall thickness. Existing furnace capability at PMTI dictated that the initial length of the tube hollow should be a maximum of 10-inches. Furthermore, the lack of any vacuum furnace capability at True Tube suggested that the process selected should not include an in-process anneal if an expedited process was desired. As a result, the dimensions of the starting tube hollow were set at a length of 10-inches, an outer diameter of ~0.400-inch, and an inner diameter of ~ 0.300-inch. Processing this size tube hollow into thin walled 0.250-inch diameter tubing should produce tubing with lengths exceeding 24-inches and with total wall reductions less than 80%. This percentage reduction should enable the draw sequence to be completed without shipping to an off-site vendor for an intermediate vacuum anneal although this premise still needed to be confirmed for these specific ingot melts. Note that longer tubing of a similar diameter could be formed at True Tube if larger diameter and longer tube hollows were formed and if additional annealing vendors were contracted for in-process vacuum annealing.

The 10-inch tube hollows for all of the niobium and tantalum alloys except Ta-10W were prepared from the round declad extrusions. Five to six tube hollows were formed for each alloy. Ta-10W was left in the as-swaged condition when the program was terminated. A detailed summary of the preparation of the tube hollows is described below. A supplement of this is located in Figures 2 and 3.

Formation of Nb and Ta-base Tube hollows

1. Vacuum anneal the declad & pickled round extrusions: Ta- alloys @ 1500 °C, FS-85 @ 1300 °C (1 hour).
2. Machine to remove bark-like surface on exterior.
3. Swage to a diameter of ~0.450-inch. No heating with the exception of initial passes where material was heated to 500 °F.
4. Cut to 10-inch lengths.

5. Centerless grind solid 10-inch long rods to a diameter of 0.400-inch.
6. Pickle & vacuum anneal as stated in step #1.
7. Electro-Discharge Machine (EDM) to remove inner plug thereby forming a
    a. cylinder with an inner diameter of 0.300-inch and an outer diameter of 0.400-inch.
8. Remove recast layer formed during EDM process by honing inner diameter to remove ~0.002-0.003-inches from the radius.
9. Pickle to remove ~0.001-inch additional from the diameter.
10. Vacuum anneal at 800 °C-1000 °C for 1 hour to remove any hydrogen absorbed during pickling.

L. Tube Drawing at True Tube, Inc for Nb and Ta-base alloys

Much of the following discussion is based on NRPCT observations occurring during a visit to the True Tube facilities located in Paso Robles, California, to witness tube drawing of an initial set of tube hollows representing T-111, ASTAR-811C, and FS-85, Reference (7).

The formation of tubing at True Tube extended over two campaigns. The initial campaign consisted of the formation of tubing from tube hollows representing T-111, ASTAR-811C, and FS-85. Two tube hollows representing each alloy were processed during this initial campaign. Objectives for the initial campaign included the following: 1) to determine if the reduction schedule selected was optimum for all alloys, 2) to acquaint new members of the NRPCT materials team to the True Tube process, and 3) to ensure that the total reduction process could indeed be conducted without including an in-process anneal. Prior to this effort, True Tube personnel had indicated that the niobium alloy, FS-85 might require an in-process anneal based on their experience years ago with fabrication of Nb-1Zr tubing for the SP-100 program. As will be discussed later, problems did occur with several of the tube hollows representing this alloy, but the reduction scheme was not believed to be a factor.

The observations detailed below for each alloy were based on direct observations by NRPCT engineers. With regard to the question of the appropriateness of the selected scheme for each or all alloys, the evidence suggests the reduction schedule was applicable for all alloys. Individual observations on each alloy suggested that minor differences in response may be present but that they were so slight that no process changes appear to be warranted when changing from one alloy to another.

True Tube personnel initiated the process by swaging one end of each tube hollow to form a short nose. The nose allows the tube hollow to be gripped and pulled through the tube drawing die. The nose of the tube hollow is under the highest amount of stress during the drawing process. It is likely that if cracking does occur, it will occur in the nose of the material.

Following formation of the nose, the tubes were cleaned and lubricated. Lubrication is a critical part of the process. It allows the tubing to be pulled through the die and prevents metal to metal contact between the die and the outer surface of the tube. Most tubing vendors employ their own so-called "witches brew" concocted and applied using methods that each considers proprietary. True Tube is not an exception. Much of their lubrication practice is based on lubricants manufactured by Hangstefers, a well known lubricant supplier. The initial lubrication was applied by dipping the tube hollow in a vat of lubricant and then hanging it vertically by the swaged nose to dry. Drying normally takes an hour and is followed by a quick visual inspection to ensure proper lubricant coverage for the entire part. A mandrel is then lubricated and inserted into the tube hollow. The lubricant applied to the mandrel had a consistency similar to motor oil. The composition of the mandrel was different from what has been used in the past. Typically a bronze/copper mandrel is employed; however, it had a

tendency to contaminate the tubing. Consequently, a steel mandrel was used in its place. A final lubricate consisting of "Ivory soap" was rubbed onto the outside of the tube hollow just before each pass. The same lubricants in the same sequence were applied to the tube hollow and mandrel, if used, prior to each pass.

Once the last lubricant was applied, the material was pulled through the die (drawn). The size of the die was varied for each pass depending on the percentage reduction desired. The same mandrel was used for the first four passes and was then changed for the fifth pass. The percentage reduction varied from ~16% to ~20% for each of the first five passes. The final pass (#6) involved only a 10% reduction. The first five passes reduced both the diameter and wall thickness of the tube hollow. Reductions for all six passes totaled approximately 68%. All three alloys were processed using the same reduction schedule. For each pass, the nose end of the tube hollow and the encased mandrel were simultaneously gripped allowing both to be pulled through a circular shaped tool steel die using a hydraulically operated draw bench. The mandrel was removed following each draw by slowly passing the tube hollow between two rotating hardened steel wheels also known as a reel roll. The wheels, both rotating counterclockwise, struck the tube hollow uniformly around its entire circumference and along the entire length of the tube hollow. This resulted in a very slight stretching of the tube wall so that the mandrel could be easily removed. After every reel roll, a very slight burnishment or polishing could be seen on the outer diameter of the tube.

After the first draw, rings were observed on the outer diameter of several of the tube hollows. True Tube indicated this was caused by direct contact with the die as a result of lubrication breakdown. This problem was easily solved by belt-sanding the outer diameter of the tube and polishing the die. Belt-sanding slightly roughened the outer surface and allowed more lubricant to be loaded onto the surface. This problem was specifically found on a tube of ASTAR-811C. Belt-sanding also was an effective way of removing small surface defects on the outer surfaces. As the tubes representing each alloy elongated, they would slightly warp. It was necessary that the tube be straight each time it was drawn. Therefore following each pass, the tubes were hand straightened, sanded, cleaned, and then lubricated. It was also necessary to re-swage the end after the nose began to straighten and narrow. This newly swaged end allowed the tube to draw without severe cracking.

The last pass for all alloys omitted the mandrel. This limits most of the reduction on the last pass to the overall diameter and causes little change in final wall thickness. Its omission also eliminates the need for reel rolling and thereby improves the final surface finish and reduces the variation in final tube dimensions.

One final general observation arose during this initial campaign. Following its completion, True Tube personnel indicated that some of the minor cracking observed near the nose areas of several tubes might have been due to lubrication breakdown. They suggested using a modified lubrication process that employs the thicker or more viscous lubricant that True Tube uses for nickel base tube formation. The modified lube was indeed used on several of the second campaign tube hollows. However, no change in behavior was noted. Minor cracking around the nose area was still observed at the same frequency noted during the first campaign.

FS-85 tube formation

FS-85 (Nb -11W - 27.5Ta- 0.85 Zr) was the only material to experience severe cracking during the initial campaign. After the second draw, one tube hollow cracked at several places at the nose of the tube and one of the cracks then propagated halfway along the length of the tube. The crack actually led to the severing of the tube in half. The remaining half remained intact and was processed

successfully through the remaining passes as was the second tube hollow of this composition. Both experienced some minor cracking around the highly worked nose piece during one or more passes. Once the cracked nose was removed, drawing proceeded as usual. The cause of the drastic failure has not been identified definitively. However, metallographic, chemical, and SEM evaluations suggest two strong possibilities. As previously noted, this material experienced in-process anneals at 1300 °C, including those used during tube hollow formation. This resulted in a partially recrystallized and highly textured microstructure that had not been softened to the desired extent. A second possible contributing cause could have been due to the incomplete removal of the brittle recast layer formed during EDM removal of the center section of the tube hollow. Gross chemical differences or interstitial contamination were ruled out as causes. A more detailed evaluation of this failure is provided in Reference (8).

T-111 tube formation

T-111 (Ta-8W-2Hf) behaved in a very ductile manner. Only slight cracking at the nose of the material occurred in one of the tubes on the fifth draw.

ASTAR-811C tube formation

ASTAR-811C (Ta-8W-1Re-0.7Hf-0.025C) is known for its high temperature creep strength. Out of all the refractory alloys that were drawn at True Tube, this material exhibits the highest room temperature ultimate strength and yield strength. As previously noted, one of the ASTAR-811C plates severely cracked during rolling at PMTI. This created some doubt about the fabricability of this alloy and/or this particular ingot. The success with tube drawing minimized this concern. In summary, ASTAR-811C only had one trim per tube due to cracking at the nose. Some minor surface defects were found on ASTAR-811C tube B; however, the problem was corrected by belt sanding.

A photograph of a typical tube hollow and finished piece of tubing is provided in Figure 15. The draw schedule employed for all alloys is listed below in Table 15.

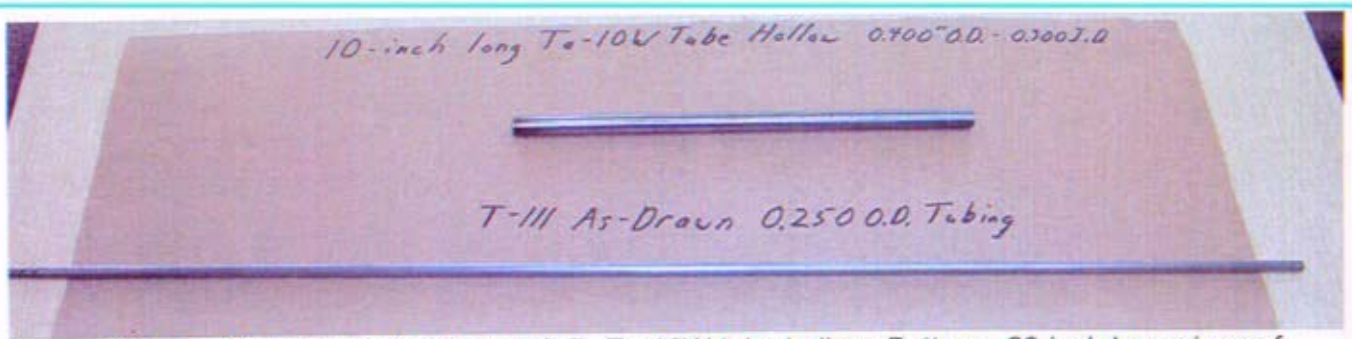

Figure 15: Top -10-inch long 0.450-inch O.D. Ta-10W tube hollow. Bottom - 23-inch long piece of 0.250-inch diameter piece of finished T-111 tubing.

Table 15: Tube Forming Parameters used by True Tube for T-111, ASTAR-811C, and FS-85 Tube production

All alloys	Draw #1	Draw #2	Draw #3	Draw #4	Draw #5	Draw #6
Die size dia. (inches)	0.345	0.33	0.316	0.304	0.275	0.25
Mandrel size dia. (inches)	0.25	0.25	0.25	0.25	0.225	None
% reduction per pass	19.25	17.91	19.49	19.92	16.43	10.00
Total % reduction	~20	~36	~47	~57	~64	~68
Wall thickness (inches)	0.0475	0.0400	0.0330	0.0270	0.0250	0.0250

M. Tube Drawing at Rhenium alloys for Arc Cast Mo-47.5 Re

Rhenium Alloys formed the arc cast molybdenum-47.5 rhenium into thin walled tubing at their facilities using equipment they had acquired approximately two years earlier from TECOMET. The latter vendor had previously been the major supplier of LCAC tubing within the U.S. but had exited the business. The acquired TECOMET facilities supplemented an existing Rhenium Alloys tubing line that produced pure molybdenum and Mo-Re tubing with similar dimensions but yielding much poorer surface quality along with much larger dimensional variations.

The tubing was formed as a development project by Rhenium Alloys since this was the first time this material (Arc cast Mo-Re) had been tube drawn. They employed two slightly different processes. The first, denoted as plug drawing, employs a small plug that is inserted into the inner diameter of the tube hollow. During tube drawing, the plug is maintained in a position just before the die as the tube hollow is pulled from through the die. The drawing bench for both processes is hydraulically operated. For both processes the individual operating the draw bench also uses a torch to heat the tubing as it passes through the die. Estimated temperature of the heated tubing is ~500 °F. The temperature of the tubing is periodically checked with a temple stick. The second process employed plug drawing for the first two passes and then switched to drawing with a mandrel. Similar to the True Tube process used for the Nb and Ta alloys, a mandrel is encased within the tube as it passes through the die. Both of the Rhenium Alloy processes are outlined below:

Process Path #1 to form molybdenum-47.5 Rhenium tubing at Rhenium Alloys

Starting size-0.750-inch O.D. X 16-inches solid rod
↓
1) EDM rod to form cylinder with 0.375-Inch I.D.
↓
2) Centerless Grind O.D. to a 0.625-inch dia.
↓
3) Remove recast layer on I.D. by pickling, machining
↓
4) ~25% reductions per pass using plug drawing.
Manually heat material with a torch during drawing.
↓
5) Reduce 25% on 2nd Pass using plug drawing.
Manually heat with torch.
↓
6) Anneal in H_2 at1625 °C for 20 minutes.
↓
7) Repeat steps #4, #5 & #6 until at final diameter (0.250-inch O.D.) and wall thickness(0.030-inch).

Process Path #2 to form molybdenum-47.5 Rhenium tubing at Rhenium Alloys

Repeat steps #1 through #6 of Process #1
↓
Insert mandrel and continue same reduction
and annealing sequence as above.
(Different size mandrels are employed after each pass or series of passes.)

Both processes produced acceptable tubing. The first process, employing plug drawing, formed tubing with a slightly better surface finish on the interior diameter.

N. Machining and Final Preparation of Tensile Specimens:

A limited number of sub-size tensile samples were sectioned and machined from the final as-rolled strip representing T-111, ASTAR-811C, FS-85, and molybdenum-47.5 rhenium. The quantities are listed in Table 2. No samples were tested. The tensile specimens were left in the as-rolled condition. In addition, a small number of flat creep samples were sectioned and machined from the as-rolled molybdenum- 47.5 rhenium alloy. A copy of the tensile machining drawing is provided in Figure 16.

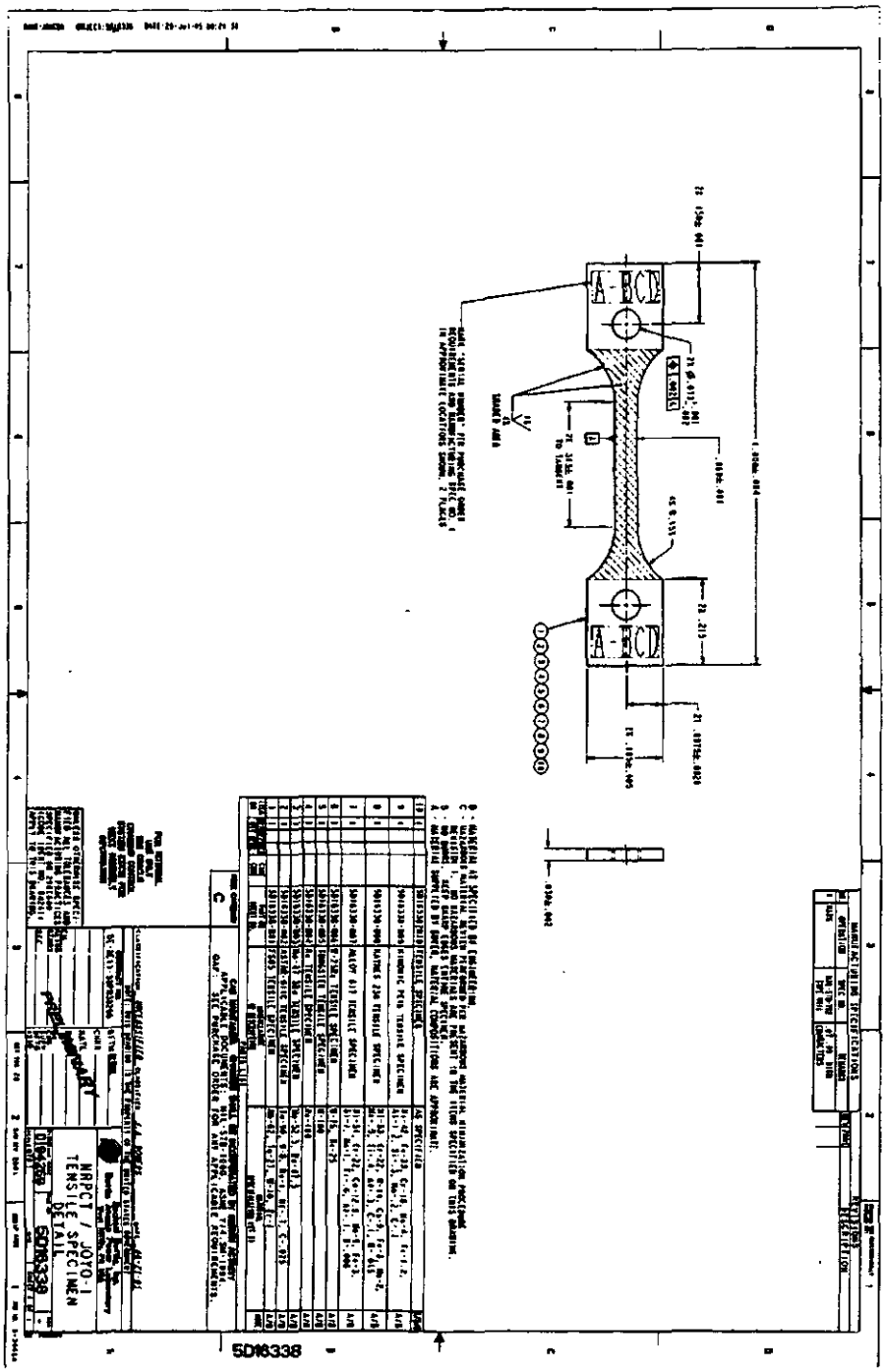

Figure 16: Tensile Specimen Drawing

End plugs for several of the alloys were machined from the swaged 0.275-inch diameter rod stock. The end plugs were machined according to Figures 17 and 18. Figure 19 illustrates the assembly of a biaxial creep tube. Figure 20 shows a flow chart of biaxial creep sample processing. Following machining, a significant number of end plugs had small cracks typically located near the center of each plug. The problem is further described in the next paragraph.

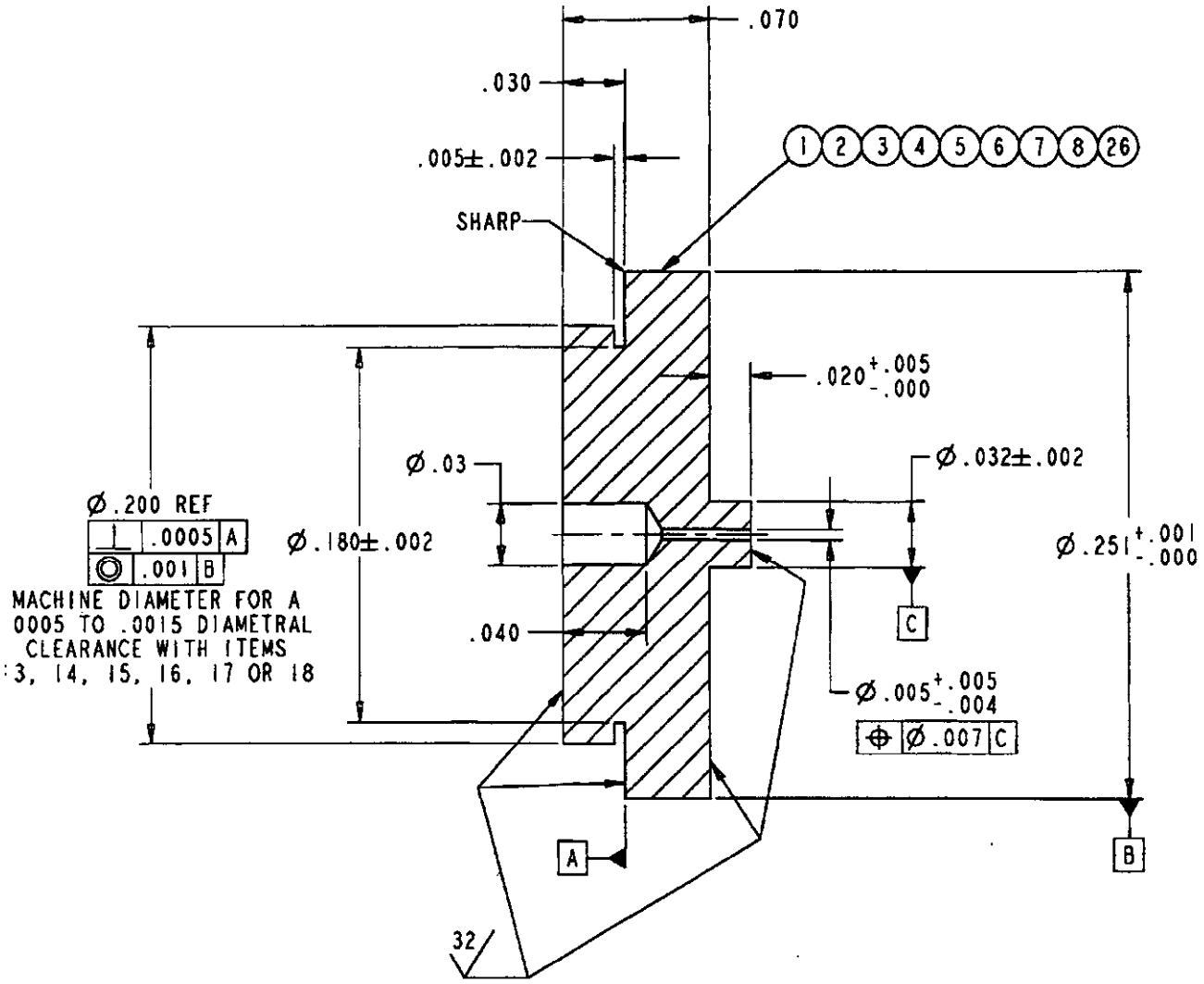

Figure 17: Top End Plug for Biaxial Creep Specimen According to Drawing 5D15996 (NRPCT/JOYO-1 Biaxial Creep Specimen Assembly)

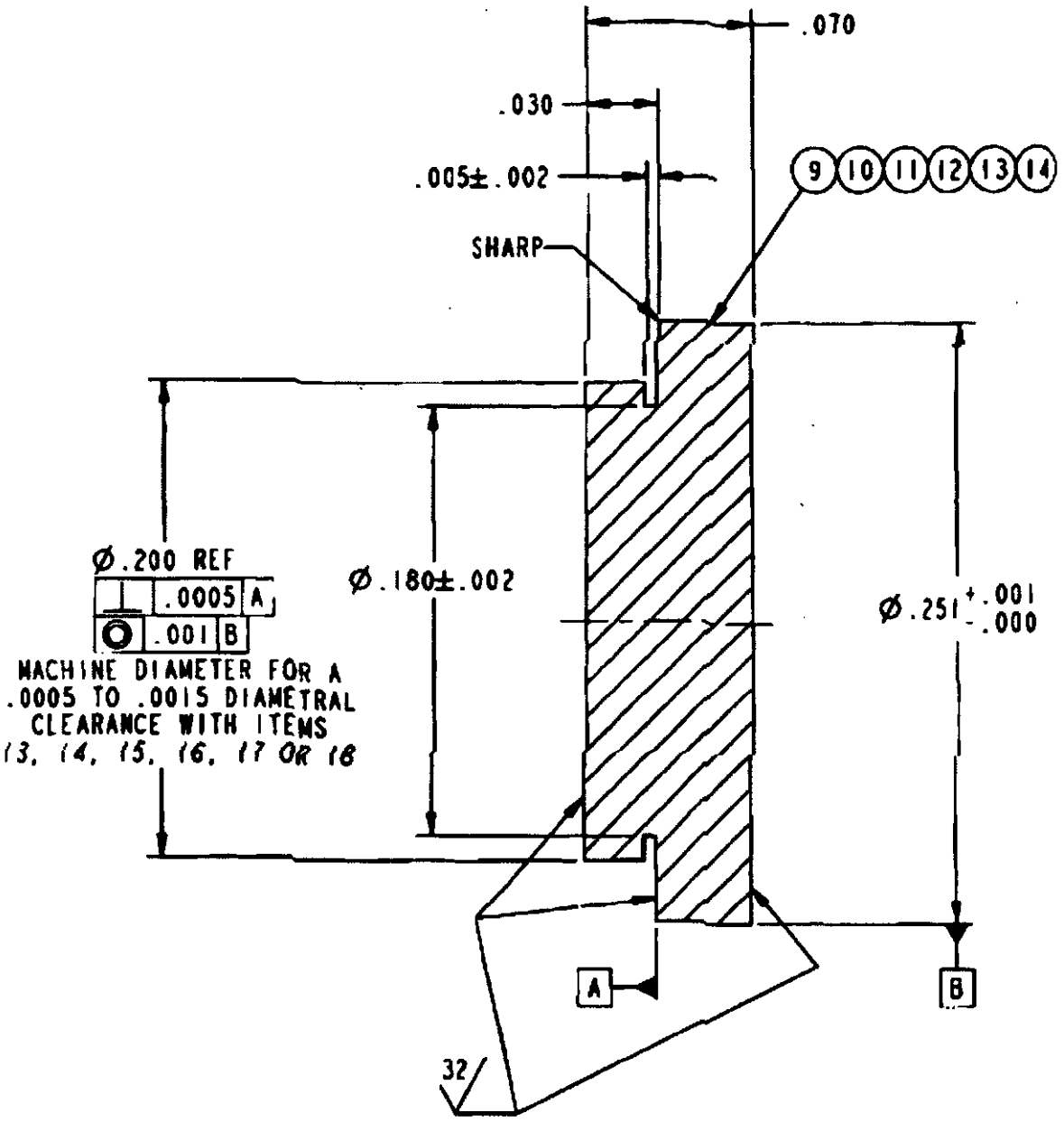

Figure 18: Bottom End Plug for Biaxial Creep Specimen According to Drawing 5D15996 (NRPCT/JOYO-1 Biaxial Creep Specimen Assembly)

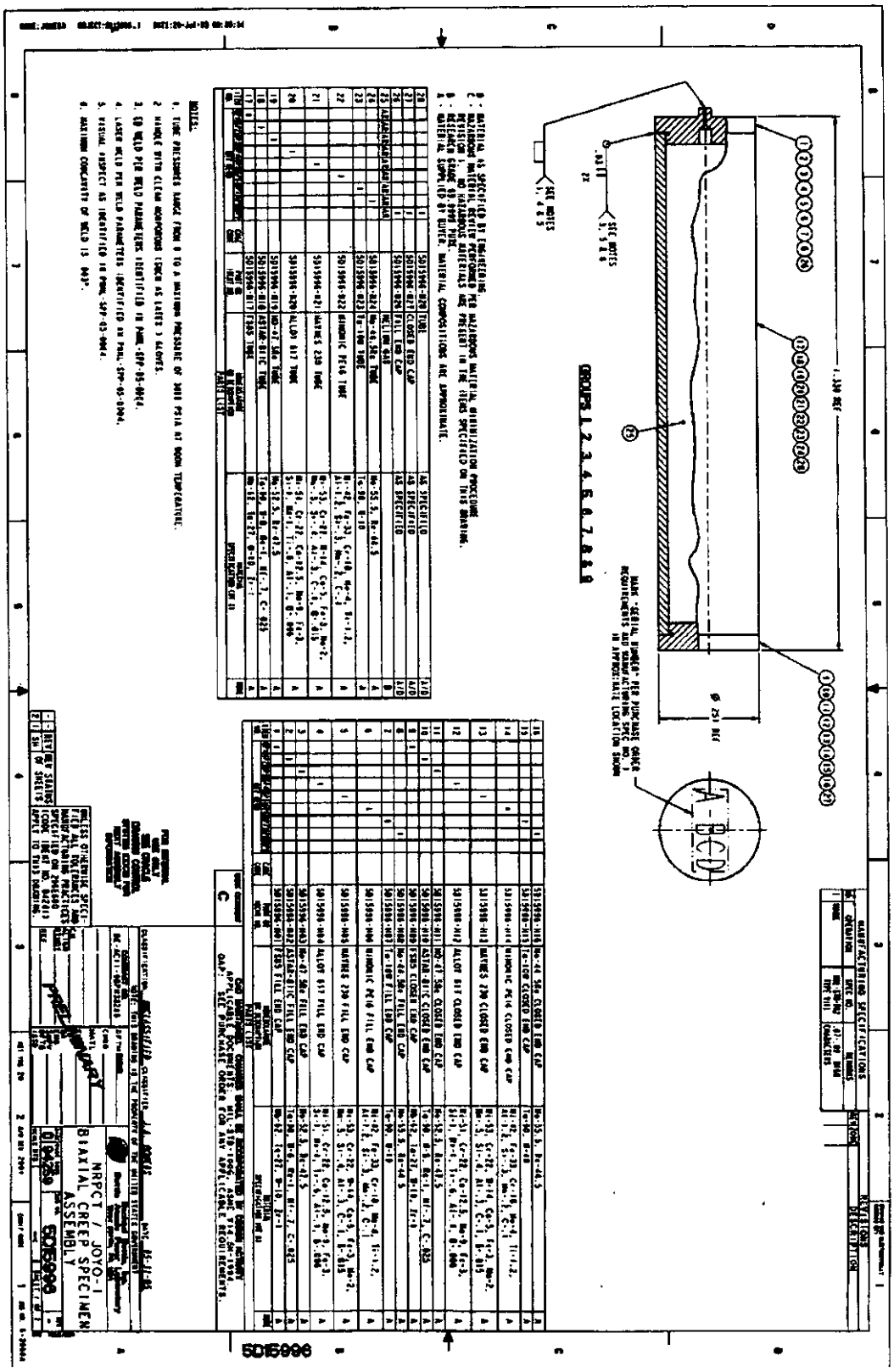

Figure 19: Assembly drawing of a biaxial creep sample

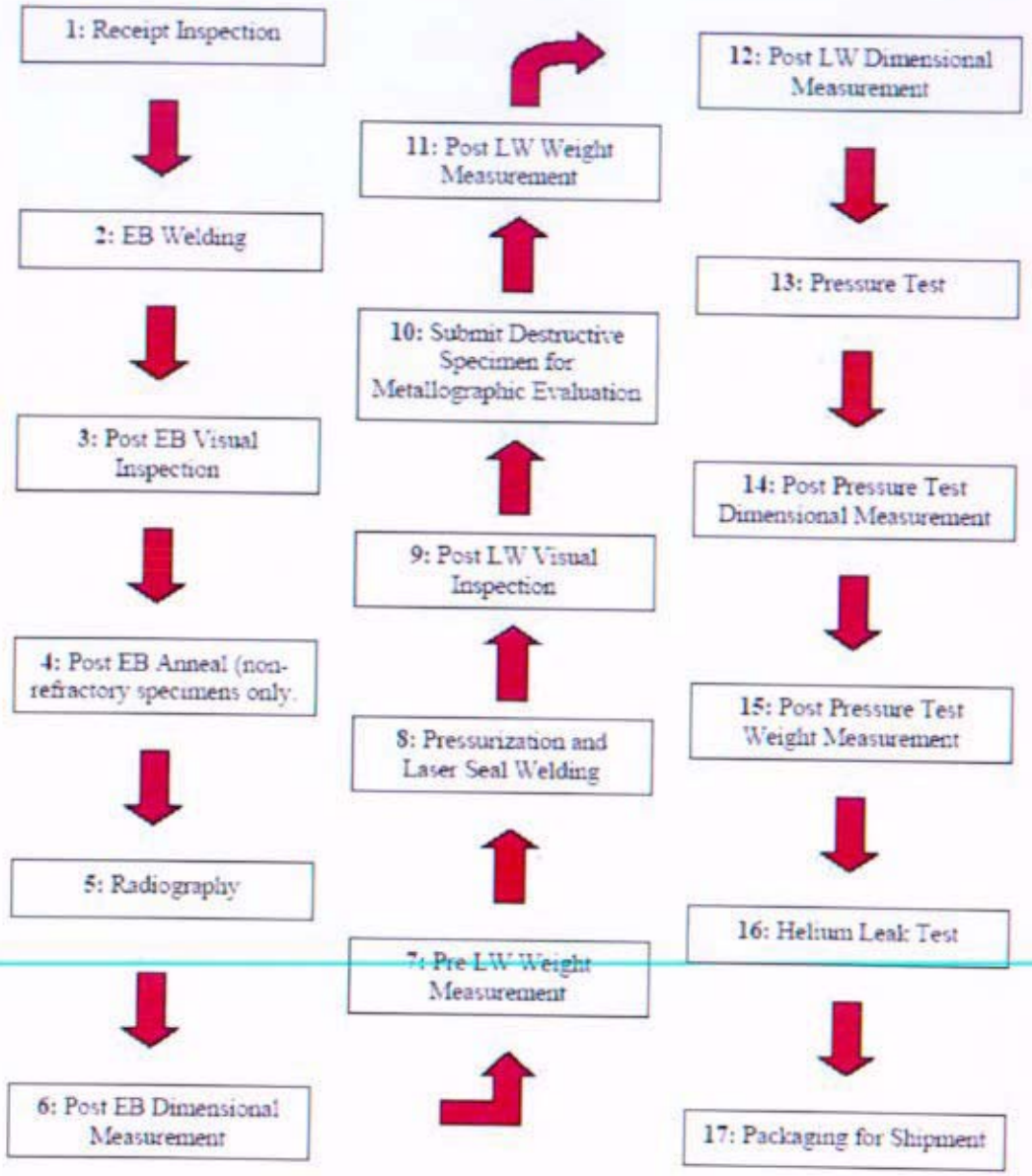

Figure 20: Production Biaxial Creep Specimen Fabrication Flowchart

O. Summary of Processing Difficulties

Most of the following items have been discussed in earlier sections dealing with a specific processing step. They are summarized briefly along with a resolution, if known.

1.) Cracked end plugs for Biaxial Creep Assembly

The end plugs from several different alloys exhibited small cracks following final machining and pickling. The cracks were usually located near the center of each plug. Although a definitive cause has not been established, an SEM evaluation of several failed ASTAR-811C end plugs strongly suggests that ingot pipe present at the top of the final melt ingots was the probable cause. A shortage of material resulted in usage of portions of the as-extruded rounds that represented material originally located very near the ingot top. The top of the ingot containing pipe is usually discarded to prevent the pipe from being processed into product and leaving a defect in the middle of the product. However, removal of the portion of the rounds containing pipe is a judgment call based on the apparent depth visible from the nose end of the extrusion. If a portion of the ingot containing pipe was inadvertently swaged into bar stock and then machined into end plugs, the defect location would be consistent with this location. Radiography of the extrusions prior to sectioning would have minimized this problem, Reference (8).

2) Cracked FS-85 tubing and tube hollows

Several FS-85 tube hollows cracked during initial passes at True Tube, Inc. A metallographic evaluation indicated the two following probable causes that either singly or in combination may have caused the cracking. 1) The 1300 °C annealing temperature, employed in tube hollow formation, was too low to fully recrystallize and soften the microstructure prior to the room temperature tube drawing reductions. 2) The appearance of several of the cracks suggested that the EDM recast layer produced during tube hollow formation may not have been completely removed. This would have left an as-cast somewhat brittle structure that may also have been contaminated with copper. See Reference (8) for a detailed evaluation.

3) Cracked plate of ASTAR-811C

One plate of ASTAR-811C severely cracked during rolling. The cause is not clear. Other ASTAR-811C plates were successfully rolled. Furthermore, tubing representing this same ingot was successfully drawn. Chemical analysis did not detect any abnormalities. A local chemical in-homogeneity or other defect or inclusion may have initiated the crack.

P. Final Machining, Processing, and Assembly of Biaxial Creep Specimens at Vangura, PMTI and Hanford Facilities.

A major objective of the JOYO test program was to determine the in-reactor creep behavior of the primary candidate alloys employing pressurized biaxial creep samples. The 0.250-inch diameter tubing formed either at True Tube or Rhenium Alloys was to form the basic building block for these specimens. A finished biaxial creep specimen consists of a 1.25-inch long piece of 0.250-inch diameter tubing from one of the candidate alloys plus two 0.250-inch diameter end plugs welded onto each end of the tube. The top end plug contains a small through hole that is used to pressurize the specimens with high purity helium and then is seal welded shut. Drawings of the respective components are included as Figures 17, 18, and 19. A photograph of the actual biaxial creep components as well as a final welded specimen is included in Figure 21.

Figure 21: Top - Individual biaxial creep components. Bottom - Final welded biaxial creep specimen.

Specimen end plug machining was subcontracted to Vangura Tool, a local vendor with experience in machining of refractory metals. Tube sectioning and final pickling of both the tube sections and end plugs were conducted at PMTI as was the final annealing of individual components. The PNNL organization was subcontracted to conduct final assembly and inspection of these specimens. Final assembly consisted of the following: 1) attachment of the two end plugs to the 1.25-inch long tubing section using electron beam welding, and 2) pressurization with high purity helium and laser seal welding. Assembly was followed by various inspection and characterization steps to assure the specimens were acceptable for in-pile testing. A flow sheet of the processing and inspection scheme is provided in Figure 20. The program at PNNL was to consist of three phases: Phase 1- weld development and equipment upgrading; Phase II- weld and process qualification; and Phase III- assembly and inspection of actual production specimens. The program was terminated before the completion of Phase II. However, an abbreviated weld qualification was conducted to capture work conducted to that point. The results of this effort have been thoroughly documented in Biaxial Creep Specimen Fabrication Close-out Report, Reference (9). A summary of the results, as well as fabrication guidelines and issues at PMTI, Vangura, and PNNL are provided below:

The final annealing temperatures used at PMTI for biaxial creep components shipped to PNNL that experienced the abbreviated weld qualification can be seen in Table 16. The components included those representing the tantalum base alloys T-111, ASTAR-811C, as well as the Nb-base alloy, FS-85.

Table 16: Final Annealing Temperatures

Alloy	Vacuum annealing temperature used for final processed biaxial creep components shipped to PNNL
T-111	1650 °C (1 hour)
ASTAR-811C	1650 °C (1 hour)
FS-85	1400 °C (1 hour)

Guidelines and issues regarding end plug machining, tube sectioning, and biaxial creep component processing at Vangura and PMTI.

1) The biaxial creep components consisting of a top and bottom end plug plus a 1.25-inch long section of tubing need to be final processed as a matched set. This will ensure the biaxial creep components can be assembled and fixtured in the weld glovebox with the tight fit-ups necessary to form high quality EB weldments. Preferably the components should be supplied to the welding rig so that a "snap fit" is required to insert the plugs into the end of the tubes.

2) In addition to a "snap fit," both the tube and the end plug should exhibit sharp corners extending circumferentially around their outer surfaces at their points of contact. This is the point where the EB weld beam first impinges on the specimen. An examination at 1x with the final processed end plugs fully inserted into the final processed tube should reveal little evidence of a visible juncture between the end plug and tube section. Note that these corners must be machined to a greater sharpness than is invoked by the standard drawing tolerances that specify machining of a sharp corner. Sharp corners will minimize weld concavity.

3) Furthermore, the end plugs should be machined slightly oversize to allow final pickling of the end plugs to a size so the "snap fit" is achievable. However, the amount of metal removal must be minimized to ensure that the as-machined "sharp" corners remain so. It is thereby critical to balance the amount of material needed for adequate clean-up against the need to maintain sharp corners and a tight fit. Inadequate metal removal during pickling of end plugs for weld development on this program may have contributed to the inconsistent appearance of laser seal welds observed during the abbreviated weld qualification effort.

4) The narrow diameter hole included in the top end plug for final specimen pressurization must be a drilled hole and not one formed by an EDM process. The hole is too narrow to allow cleaning processes to remove the recast layer formed by the EDM process. In addition, many EDM vendors employ a copper electrode, a contaminant which can lead to embrittlement of many of the refractory metal welds at test temperatures. The presence of either the recast layer or copper contaminant makes it impossible to consistently close the hole using laser welding.

5) The end plugs and tube sections used for weld development were pickled as matched sets at PMTI. The make-up of the pickling solution depended on the alloy (see Table 9). The end plugs and the matched end plugs always represented the same alloy. However, if Phase III had been initiated, scarcity of end plugs for the ASTAR-811C alloy as a result of cracking would have required the substitution of Ta-10W end plugs. This should not have caused a problem during fabrication or testing. The similar Ta-10W and ASTAR-811C alloys are readily weldable and interchangeable. The weld formed between the Ta-10W end plug and the ASTAR-811C tube should have been comparable in strength to an all ASTAR-811C weldment. Furthermore, the biaxial creep specimens are designed so that the stresses occurring within the welded regions are much less than those occurring within the tube body. Therefore some degradation in weld strength would still be acceptable. An evaluation of calculated stresses present in a welded and pressurized Haynes 230 biaxial creep specimen confirmed that the weld region experienced a much reduced stress level than that of the tubing, Reference (9). A final point to note is that a refractory metal weldment typically exhibits strengths that are comparable to a similar sized wrought product of the same alloy, Reference (10). Thus there is not a reduction factor that must be incorporated into the calculated strength of a refractory metal weldment, as required for many other metals.

Results of abbreviated weld qualification at PNNL

1) The vendor was successful in developing EB welding parameters for the three refractory alloys they were provided. These included the Nb alloy, FS-85, and the Ta-base alloys T-111, and ASTAR-811C. Processing of the Ta-10W material did not proceed to the point where a weld qualification could be conducted. However, the expectation is that the EB weld parameters developed for the two tantalum alloys, ASTAR-811C and T-111, would also have been applicable to Ta-10W.

2) The EB weld parameters developed for the FS-85 alloy included a final cosmetic pass to form a smooth outer weld surface. The employment of this "repair weld" would not have been a problem for production weldments of this alloy since it is highly weldable and typically exhibits an as-welded DBTT well below RT. Similarly, weldments of the tantalum-base alloys in this program exhibit DBTTs well below RT and could have been repair welded, if needed. However, the cosmetic pass is not desirable for either of these alloy types or the biaxial creep concept. These specimens were intended to be inserted in an environment where a premature failure resulting from a poor weld was not an option. The PNNL welding engineer and weld technician both indicated that with further effort and development of weld parameters, EB weldments of this alloy, which would not require a cosmetic pass, could most likely be formed.

   One should note that it is not clear if a cosmetic or repair weld could be employed for welding of biaxial creep components fabricated from the molybdenum-rhenium alloys. The DBTTs of weldments representing either pure LCAC molybdenum or alloys such as TZM are typically at or above RT. Repair weldments within these molybdenum-base materials are thus very, very difficult to make without forming cracks in the actual weld or adjacent HAZ. However, weldments of the molybdenum-rhenium alloys, especially those with higher rhenium contents, may not have this limitation. Unfortunately, work to evaluate this issue had just been initiated when the program was terminated.

3) The effort to form laser closure weldments was not as successful. Many of the seal welds exhibited by the alloys yielded a variety of shapes ranging from flat to sloping to the expected cone shape. Several exhibited cracks or incomplete fill. The reason(s) for the inconsistency is not clear. PNNL suggested that inadequate cleaning or oversize drilled holes could be causes. It is known that several sets of end plugs employed were only flash pickled for this effort suggesting that the surfaces and especially the interior of the small filling hole experienced minimal cleaning to remove surface oxide and other contaminants. If these contaminants are not removed, successful welding would be highly problematical.

Q. Characterization of Material

Limited characterization was performed prior to termination of Naval Reactors' effort on the project. This effort consisted mostly of chemical analysis of some but not all of the final product as well as a limited metallographic and recrystallization study.
1) Chemical analysis

Completed chemical analysis is provided in Table 6. The final alloying and interstitial levels appear to be satisfactory with the exception of oxygen in the arc cast molybdenum-47.5 rhenium alloy.

Mo-47.5 Re

The final product contained oxygen in the 40 ppm range higher than the <20 ppm desired. This level appeared at the ingot stage and continued through to the final product. The evidence suggests that the added oxygen may have been introduced at the melting stage although this is not clear. The lack of an extrusion canister combined with incomplete removal of sidewall defects may have played a role. Starting oxygen levels of the rhenium and molybdenum used in initial electrode fabrication were both less than 20 ppm. Melting, if properly performed, should not increase these levels. There were no apparent crucible leaks during any of the initial or final melts although a trace output of the vacuum levels present during the final melt revealed a very erratic behavior. At the time the behavior was attributed to a faulty vacuum gage.

Regardless of the cause, the effect of this level of oxygen on Mo-Re is not understood totally. For pure LCAC molybdenum the desired oxygen level is ~10 ppm, which should be combined with a carbon level that produces a C/O atom ratio greater than 2:1. If this is achieved, then the LCAC molybdenum exhibits good welding characteristics. The Mo-Re material contained oxygen at the much greater level of 40 ppm and was combined with a similar carbon level to produce a C/ O atom ratio very close to 1.

To provide some idea of the quality of the high oxygen Mo-Re with respect to welding, bend samples representing weldments of this alloy were fabricated and tested. A Bead-on-Plate (BOP) weldment of the suspect material was formed along the length of a 1-inch wide 0.040-inch thick plate centered on the plate width. Small bend samples with dimensions of 1T X 12 T X 24T (i.e., T= plate thickness) were then sectioned from the plate with the BOP oriented parallel to the length of each specimen and again centered on the width. The bend samples were then tested in accordance with Reference (11) to provide a rough approximation of the DBTT of the weldment. The test procedure entails cooling a bend sample to a specific temperature using liquid nitrogen while the specimen is suspended over a gap in the bend fixture shown in Figure 22.

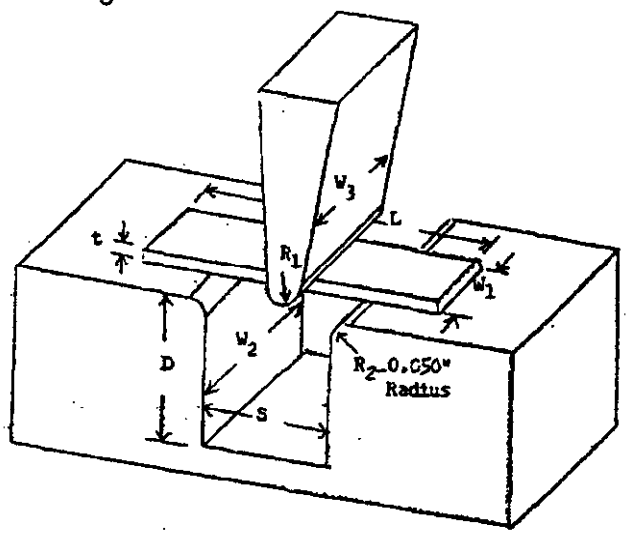

Figure 22: Schematic of Bend Test Fixture

The specimen ends are free. Once the sample has been stabilized at the test temperature, a punch is lowered at a slow, predetermined rate until it contacts the specimen at its midpoint and causes the specimen to bend. Testing is continued (lowering of the punch) until either the specimen breaks or

bends to form an angle of at least 90° and less than 105°. If a visual inspection of the bent sample reveals no visible cracks, then the material is deemed ductile at that temperature, and the process is repeated at a lower temperature. The spread in temperature between the lowest failure temperature and the lowest success temperature provides a broad measure of the DBTT for that material in the as-welded condition. The testing resulted in a DBTT of approximately -100 °C. An earlier test of wrought product representing the same high oxygen material produced a DBTT of close to -180 °C. Both are excellent values. Note that bend testing of weldments made in pure molybdenum and exhibiting proper C and O levels usually produces DBTT that are well above RT. Thus at first cut the slightly elevated oxygen level did not appear to degrade the weld behavior of the material.

However, an earlier evaluation of the bend properties of melted Mo-Re buttons containing similar rhenium levels and lower oxygen levels resulted in minimal change in the DBTT of weldments compared to the wrought product. Both DBTTs were close to -180 °C. However, carbon levels in these buttons were slightly higher than this material, thus improving the C to O ratio and perhaps aiding its weld behavior. The evidence is thus inconclusive as to whether C and O play a similar role in the welding characteristics of this material as they do in pure molybdenum. Nonetheless, the current high oxygen Mo-Re still exhibits excellent welding behavior. Increased carbon or lowered oxygen may further improve the behavior, but additional work is needed to determine the validity of this premise.

2) Metallographic Evaluation

A limited metallographic evaluation was conducted on in-process and some of the final processed material. The photomicrographs accompanying this evaluation are provided in Figures 23-57. ASTAR-811C (Figures 23-33), T-111(Figures 34-45), FS-85(Figures 46-51), and Mo– 47.5 Re (Figures 52-57).

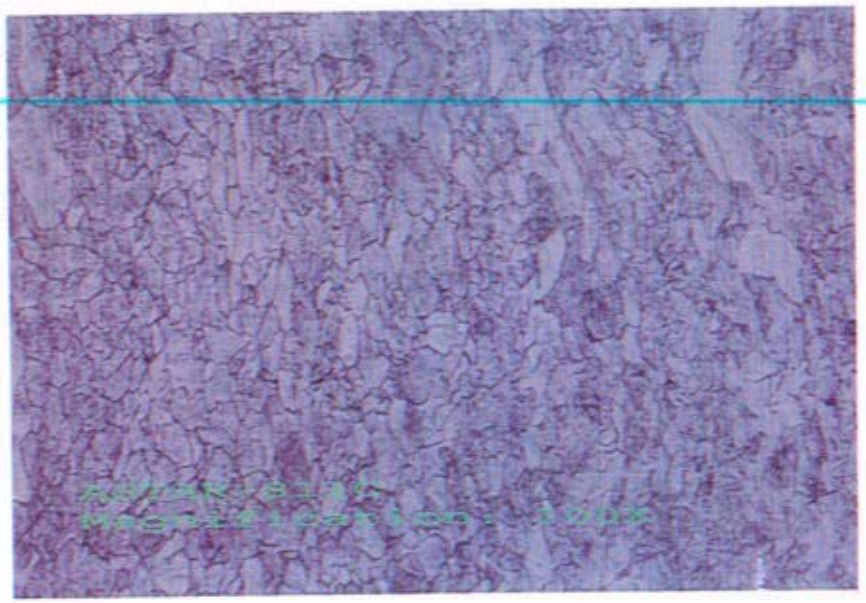

Figure 23: ASTAR-811C, as-rolled condition, 0.125-inch thick (Transverse)

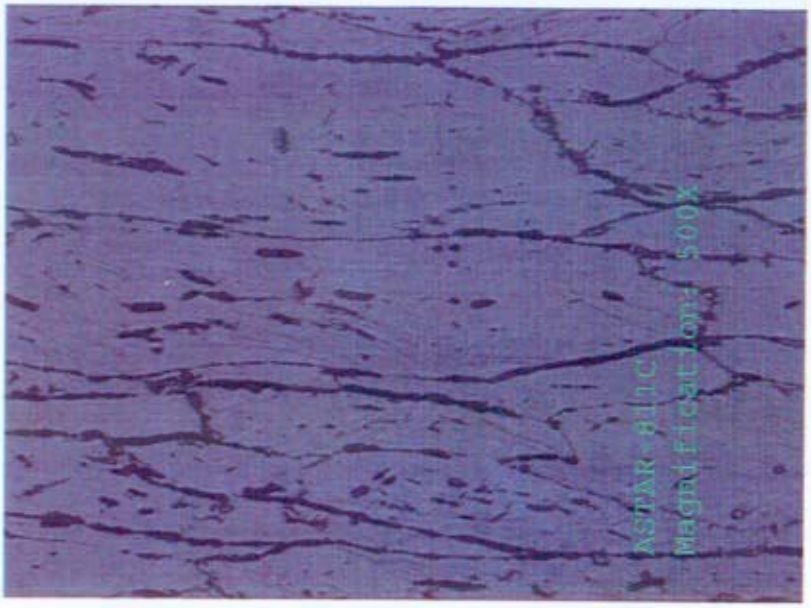

Figure 24: ASTAR-811C, as-rolled, 0.050-inch thick
(Longitudinal direction)

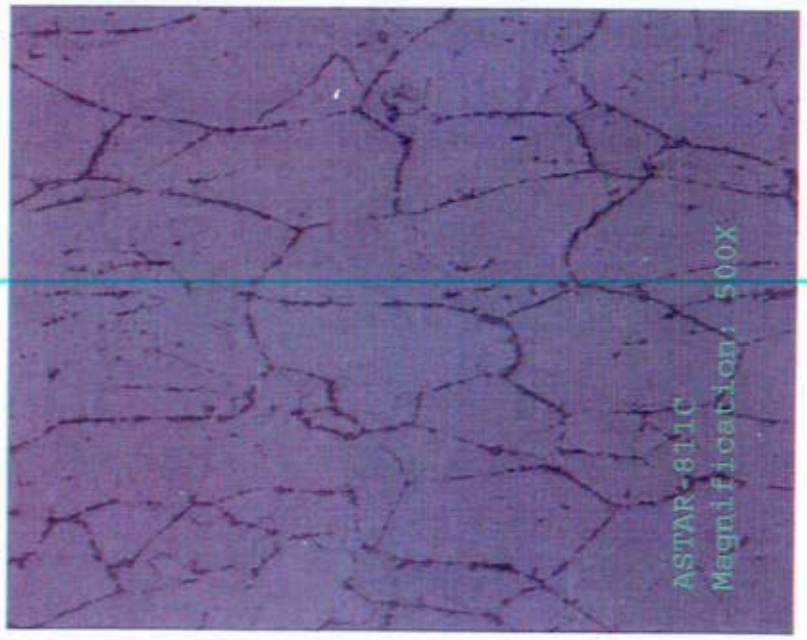

Figure 25: ASTAR-811C, 0.050-inch thick sheet, annealed at 1500 °C
(Center- longitudinal direction)

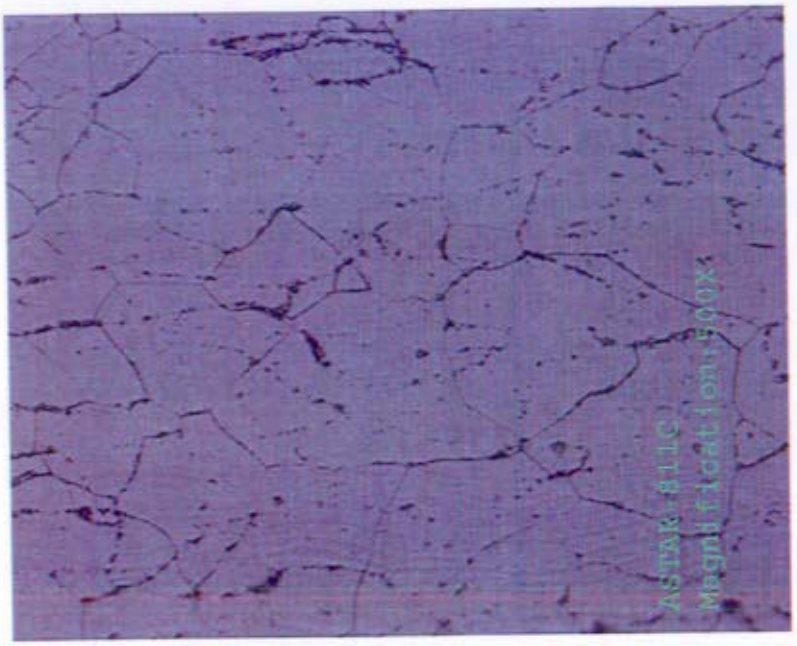

Figure 26: ASTAR-811C, 0.050-inch thick sheet, annealed at 1550 °C
(Edge- longitudinal direction)

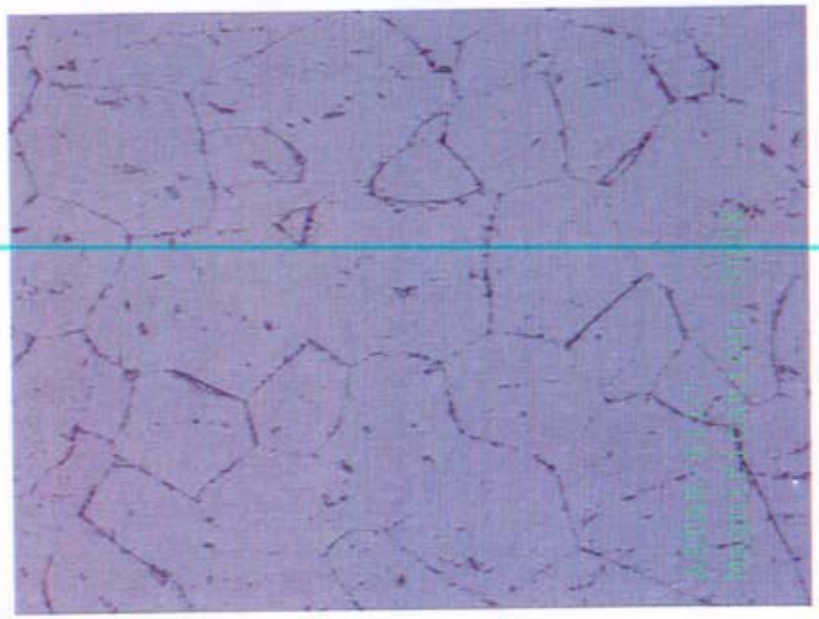

Figure 27: ASTAR-811C -0.050-inch thick sheet, annealed at 1600 °C
(Center- longitudinal direction)

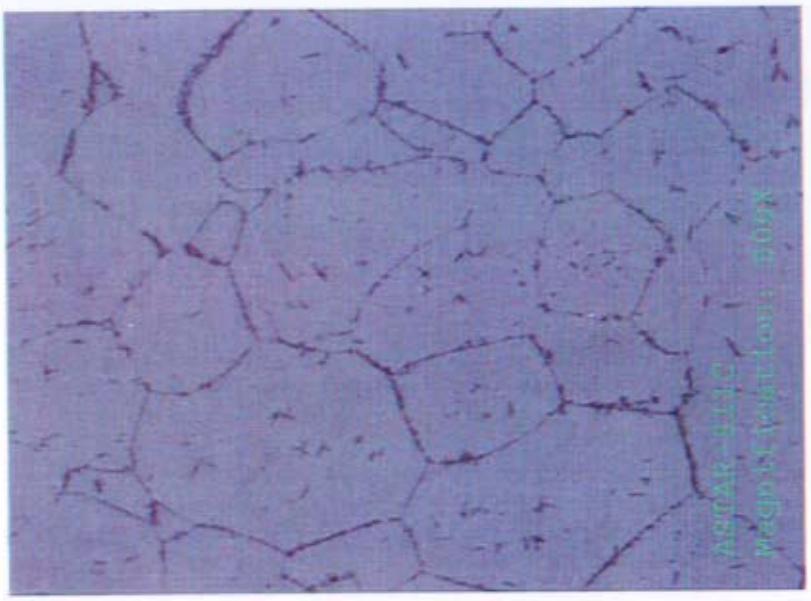

Figure 28: ASTAR-811C, 0.050-inch thick sheet, annealed at 1650 °C
(Center- longitudinal direction)

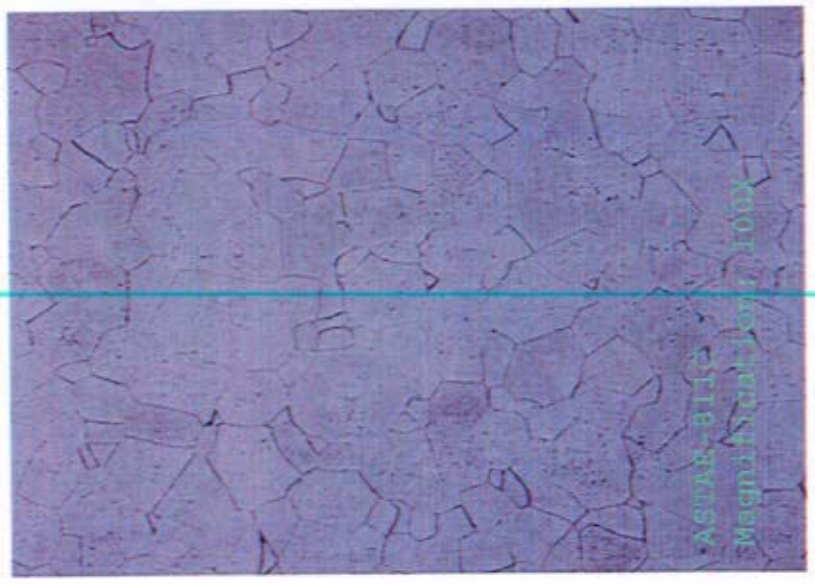

Figure 29: ASTAR-811C, 0.050-inch thick sheet, annealed at 1700 °C
(Longitudinal direction)

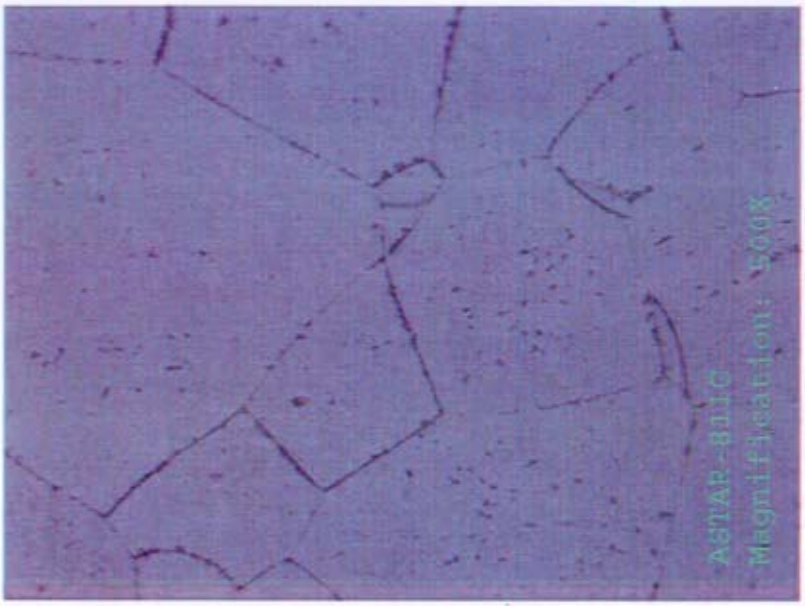

Figure 30: ASTAR-811C, 0.050-inch thick sheet, annealed at 1700 °C
(Edge-longitudinal direction)

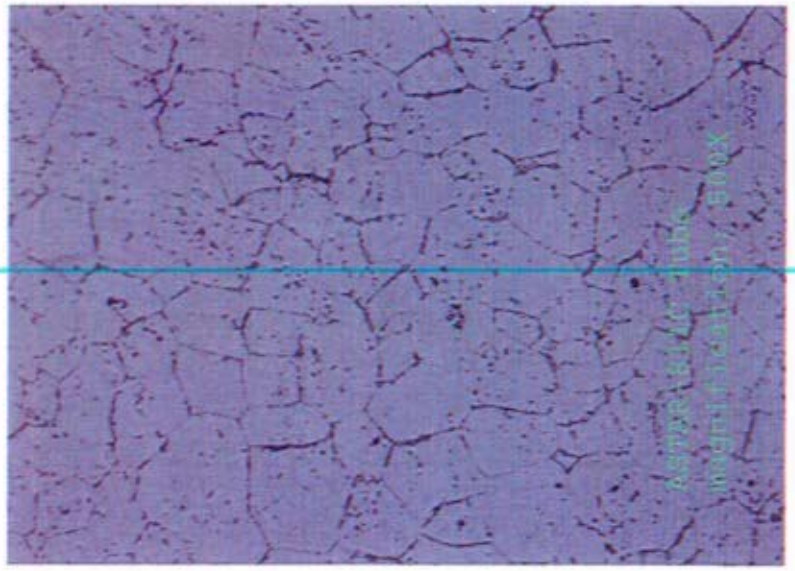

Figure 31: ASTAR-811C, tubing, annealed at 1600 °C
(Transverse direction)

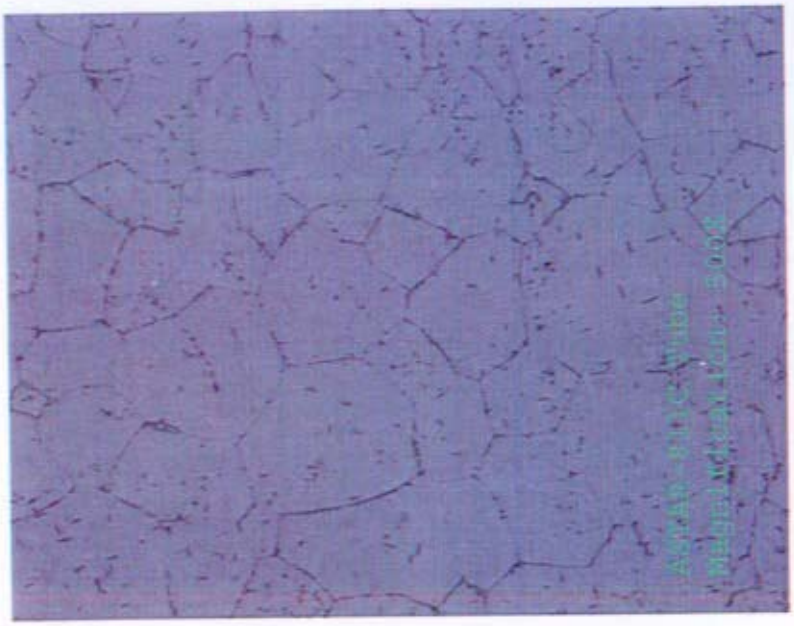

Figure 32: ASTAR-811C, tubing, annealed at 1650 °C
(Center–transverse direction)

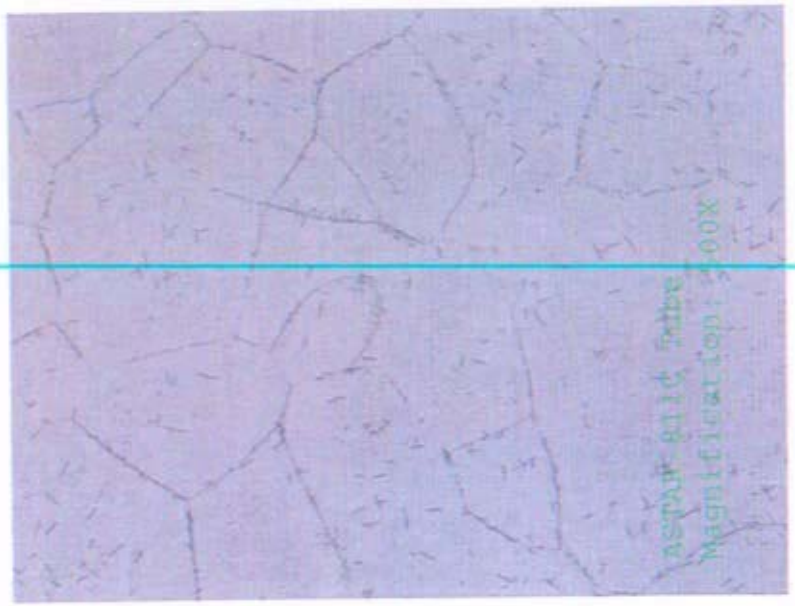

Figure 33: ASTAR-811C, tubing, annealed at 1700 °C
(Center-transverse direction)

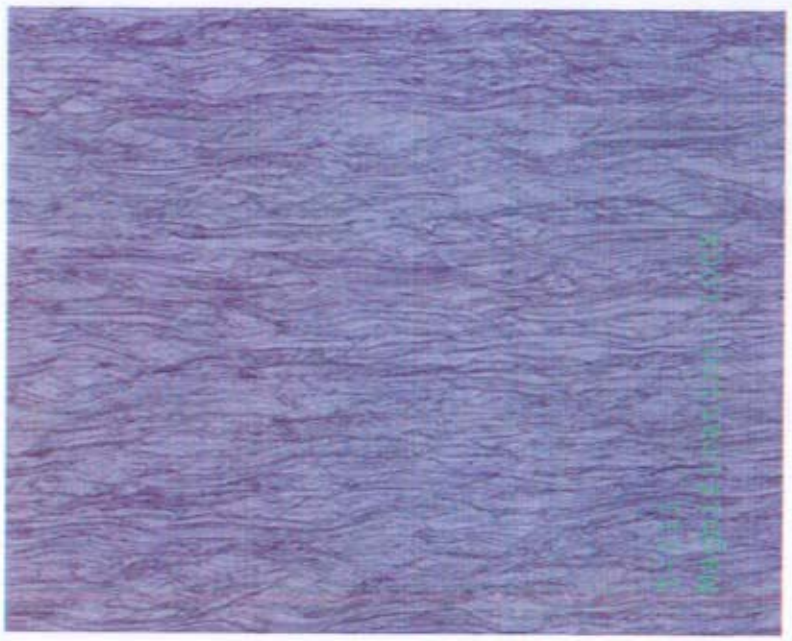

Figure 34: T-111, 0.050-inch thick sheet, as-rolled condition
(Center-longitudinal direction)

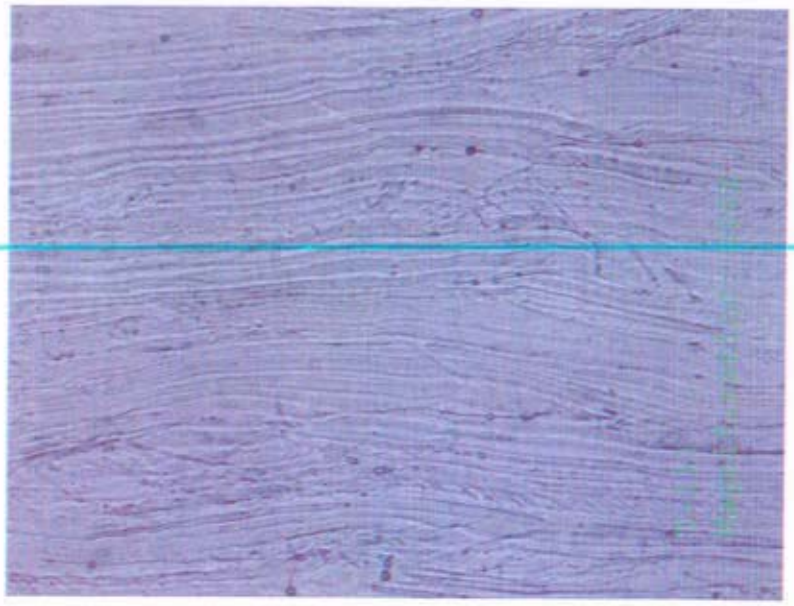

Figure 35: T-111, 0.050-inch thick sheet, as-rolled
(Center-longitudinal direction)

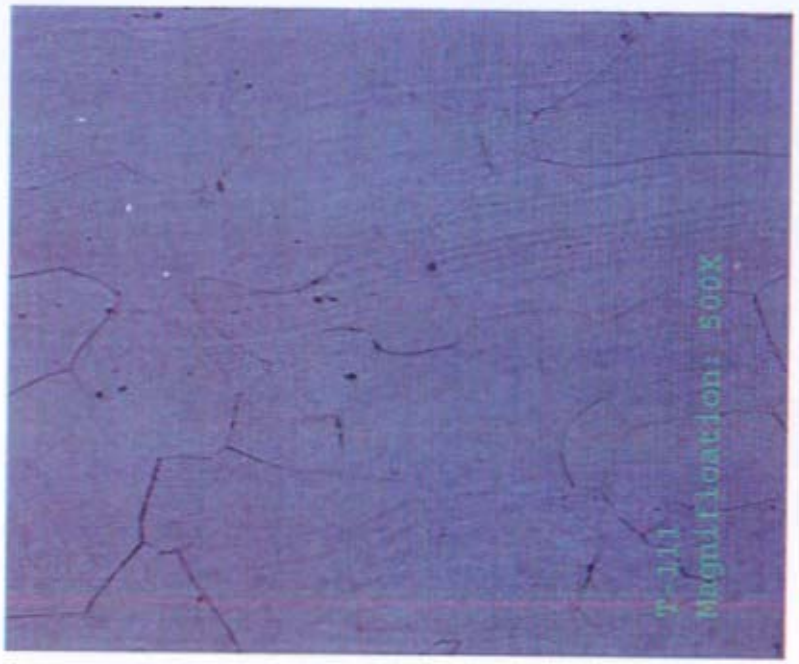

Figure 36: T-111, 0.050-inch thick sheet, annealed at 1550 °C
(Center-longitudinal direction)

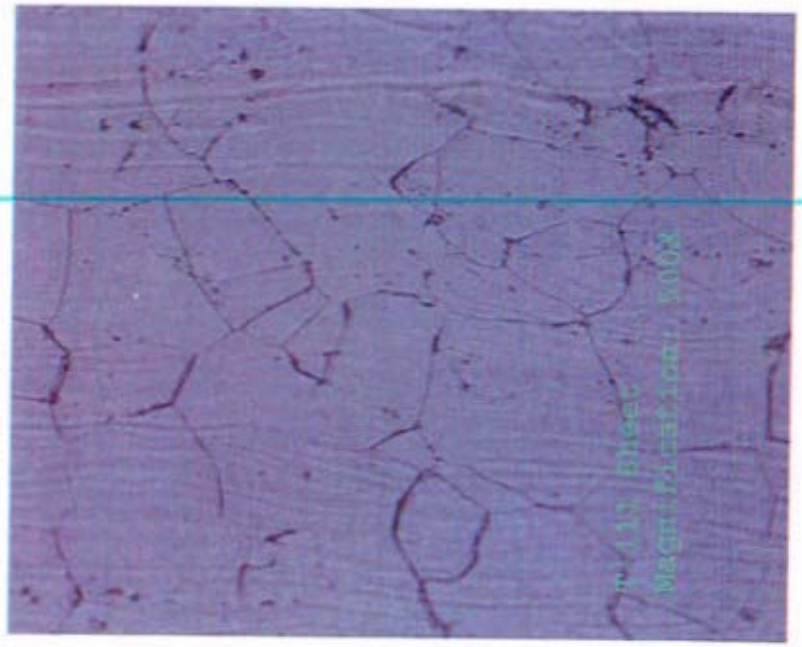

Figure 37: T-111, 0.050-inch thick sheet, annealed at 1550 °C
(Edge-longitudinal direction)

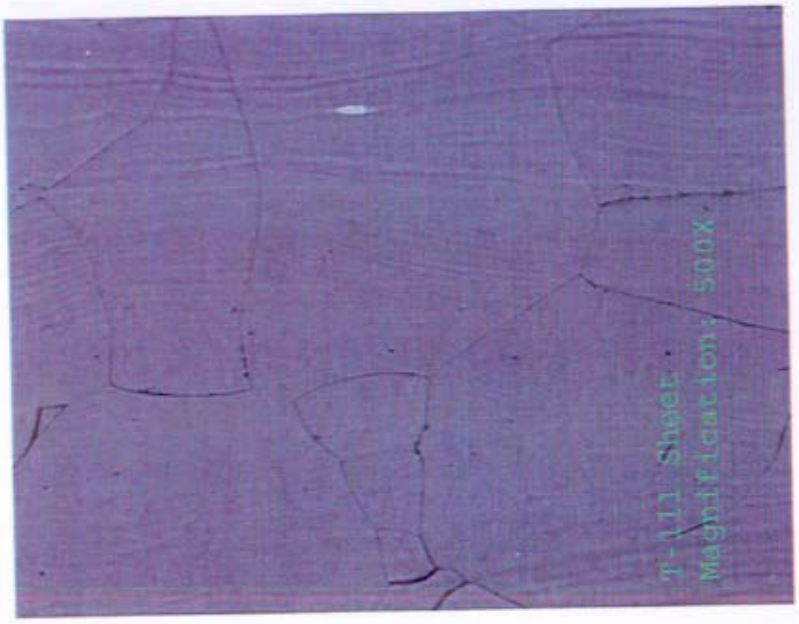

Figure 38: T-111, 0.050-inch thick sheet, annealed at 1600 °C
(Center-longitudinal direction)

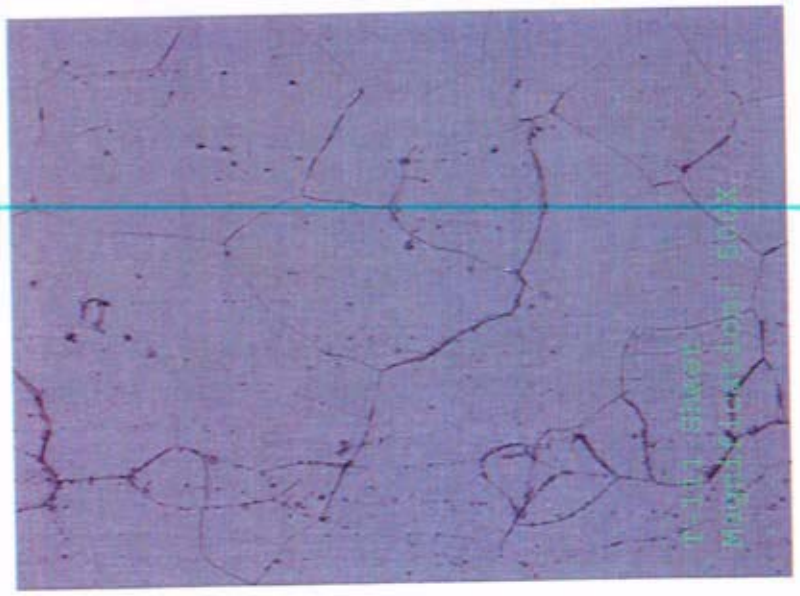

Figure 39: T-111, 0.050-inch thick sheet, annealed at 1600 °C
(Edge-longitudinal direction)

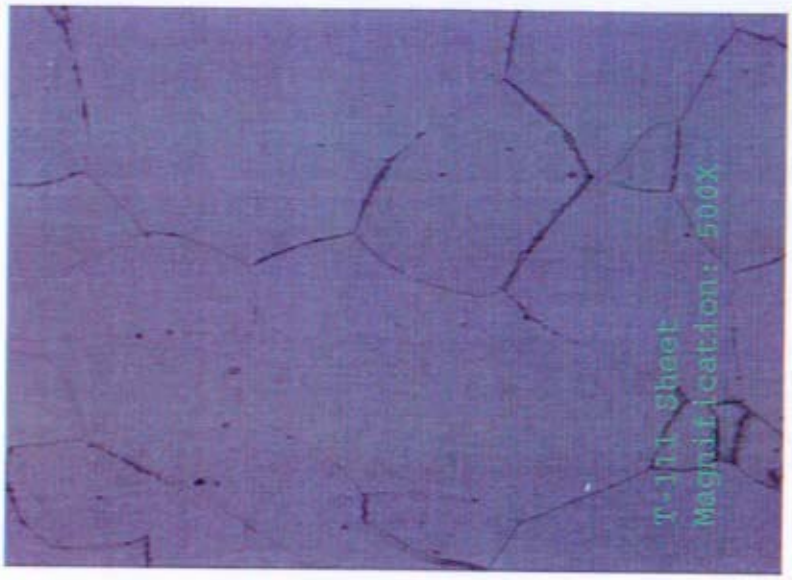

Figure 40: T-111, 0.050-inch thick sheet, annealed at 1650 °C
(Center-longitudinal direction)

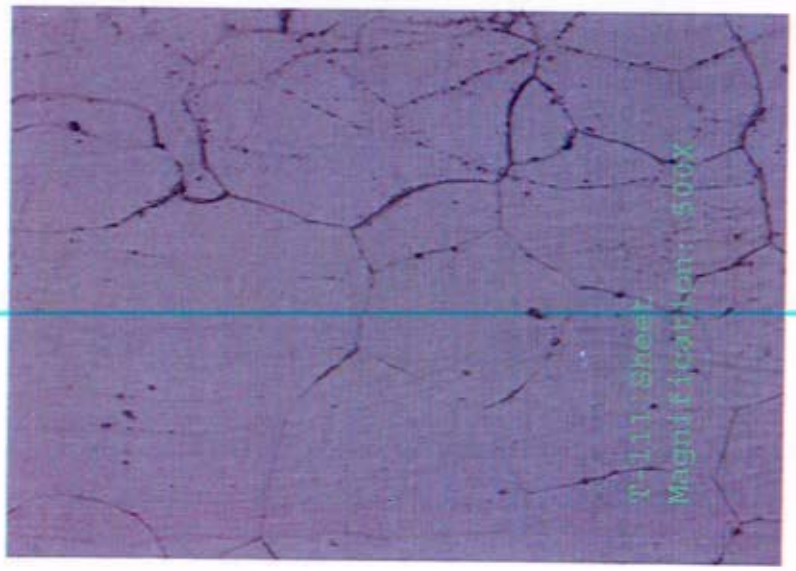

Figure 41: T-111, 0.050-inch thick sheet, annealed at 1650 °C
(Edge-longitudinal direction)

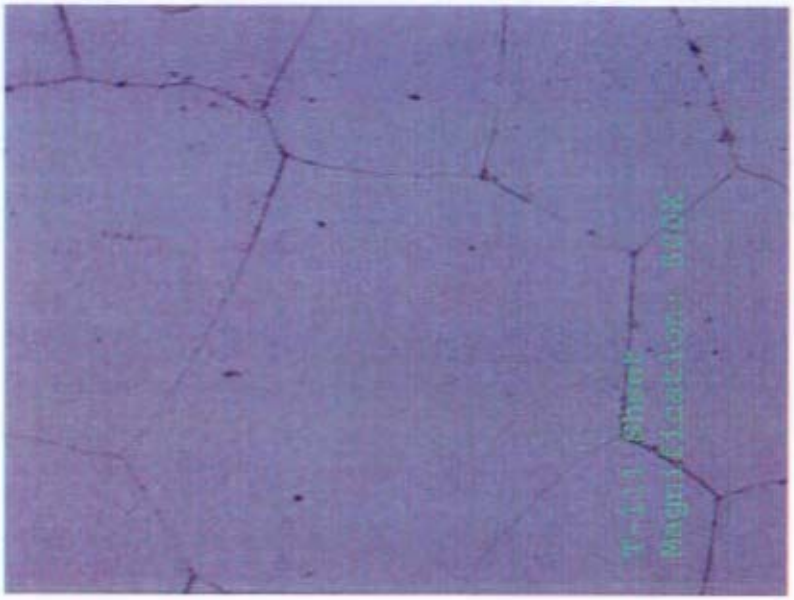

Figure 42: T-111, 0.050-inch thick sheet, annealed at 1700 °C
(Center-longitudinal direction)

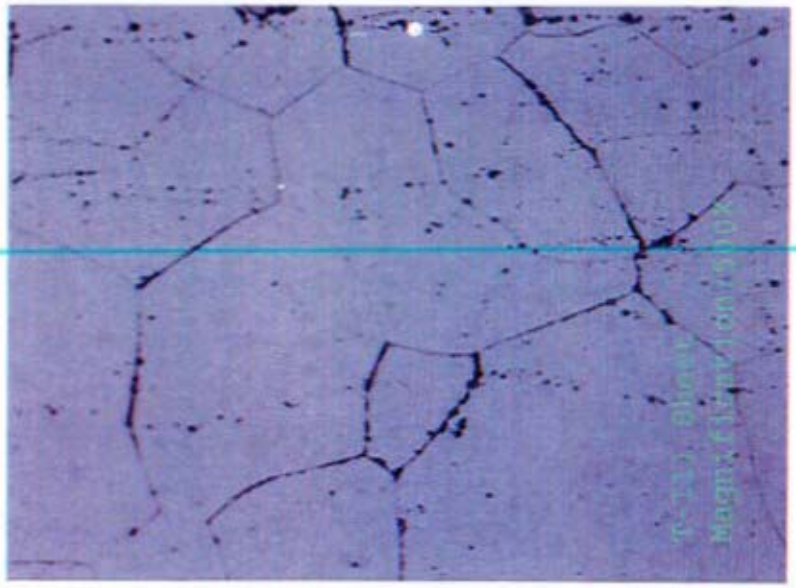

Figure 43: T-111, 0.050-inch thick sheet, annealed at 1700 °C
(Edge-longitudinal direction)

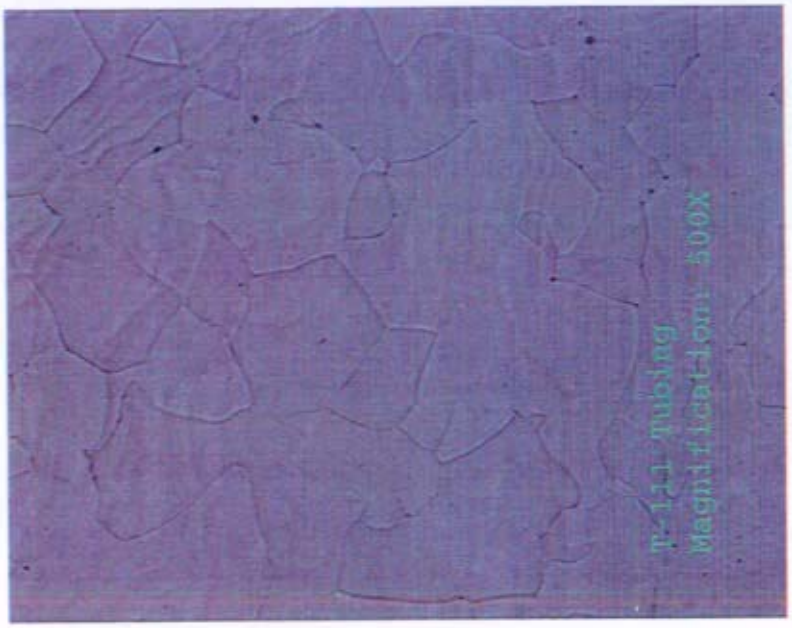

Figure 44: T-111, as-honed tube shell annealed at 1500 °C
(Center –transverse direction)

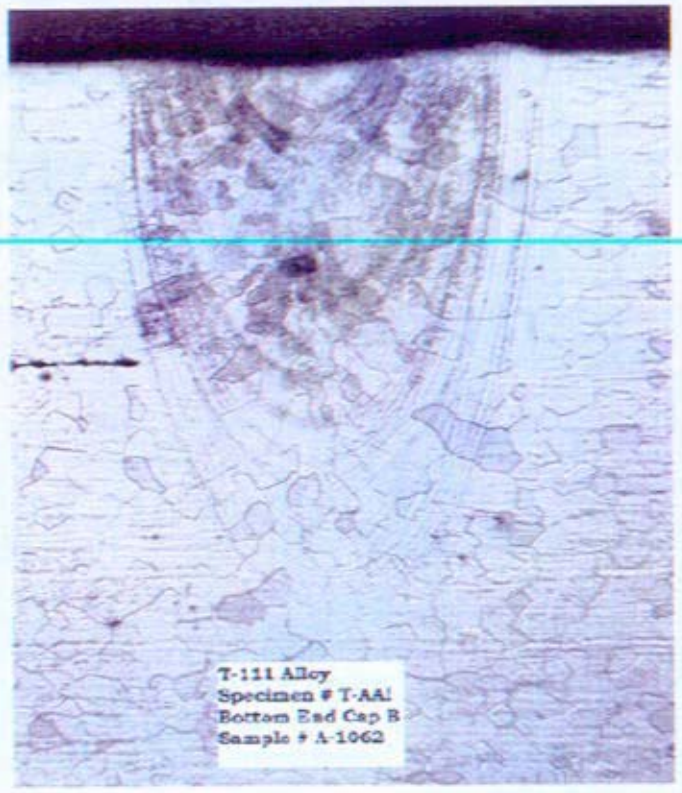

Figure 45: T-111, welded biaxial creep specimen. Tube is at the top left- end plug is bottom

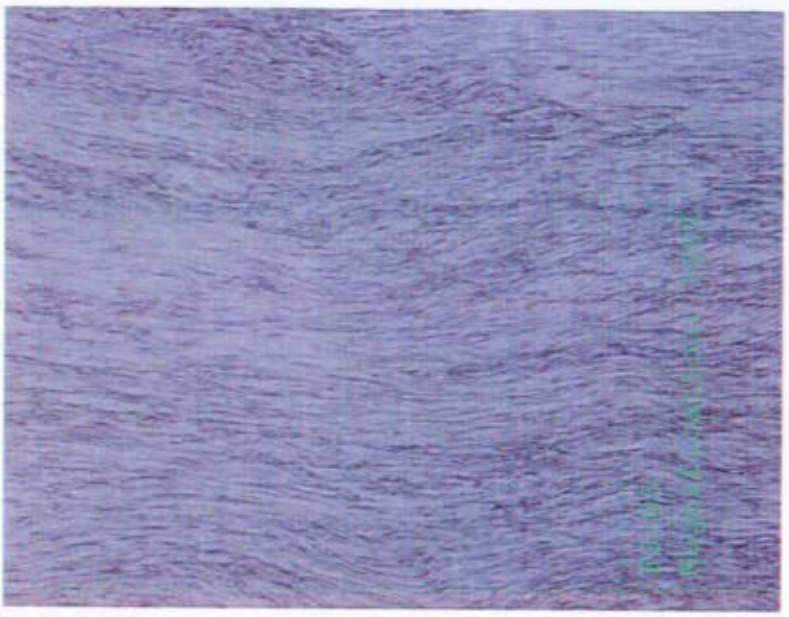

Figure 46: FS-85, 0.150-inch thick sheet, as-rolled condition.
(Transverse direction)

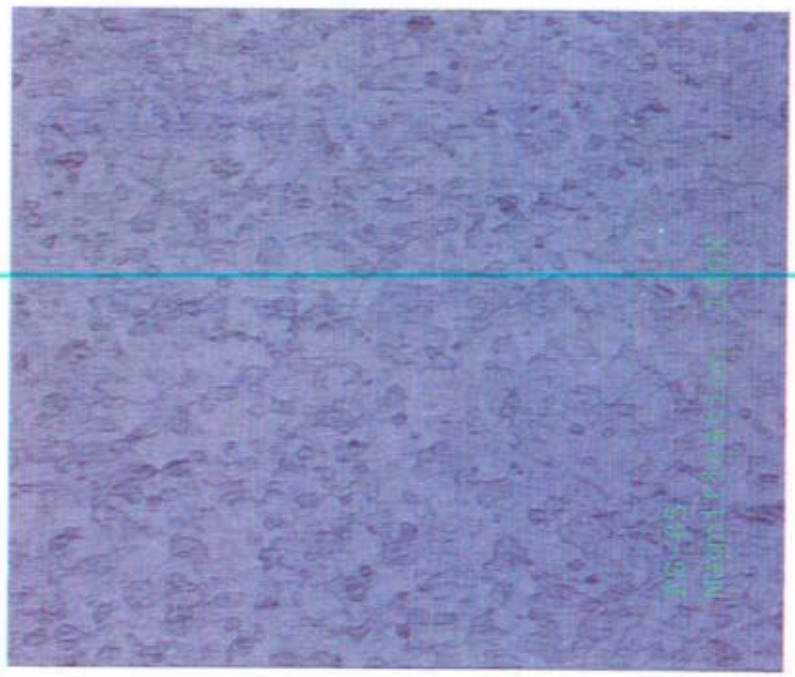

Figure 47: FS-85, 0.064-inch thick sheet, annealed at 1400 °C
(Center –transverse direction)

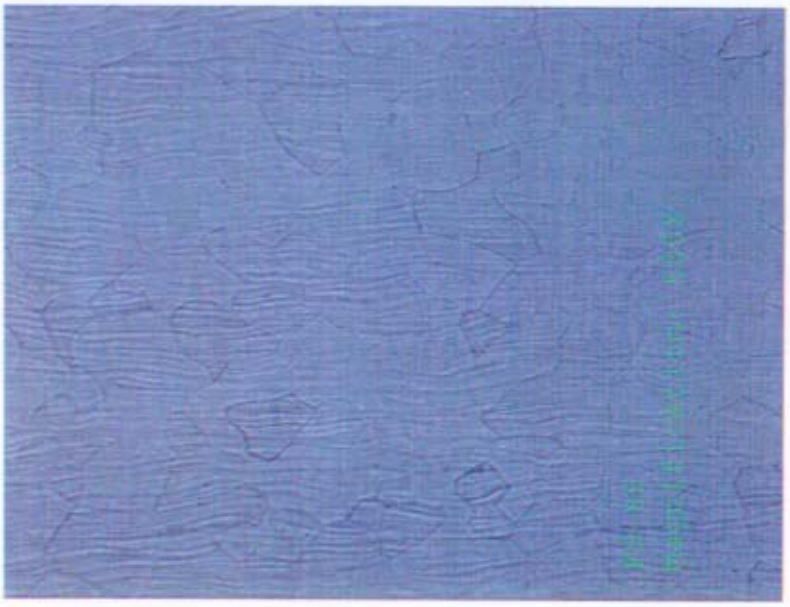

Figure 48: FS-85, 0.064-inch sheet, annealed, at 1400 °C
(Edge –transverse direction)

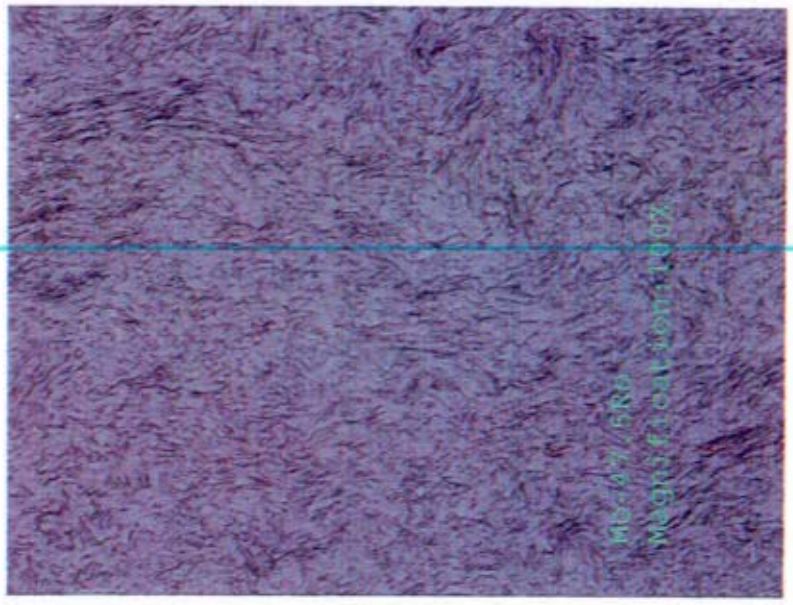

Figure 49: FS-85, as-honed, tube shell, annealed at 1300 °C
(Center – transverse direction)

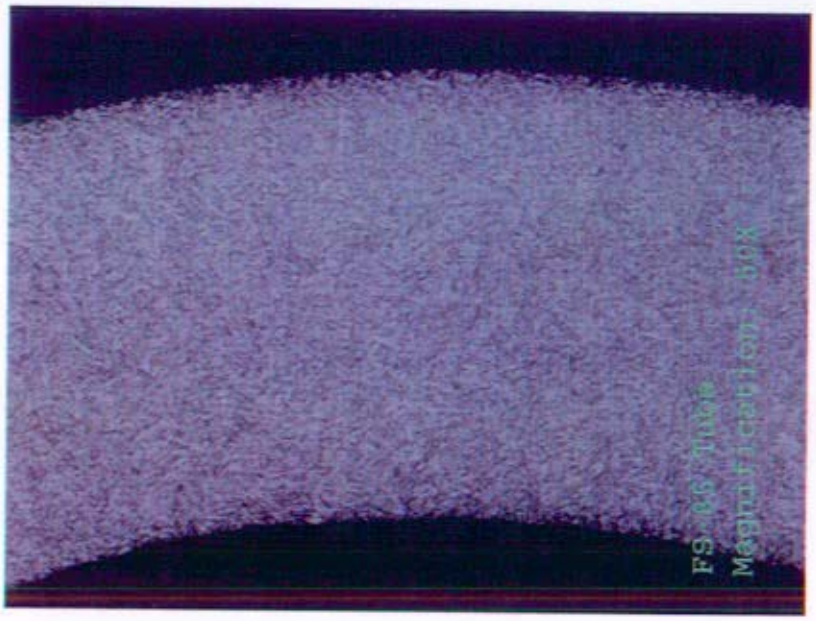

Figure 50: FS-85, as-drawn tubing, annealed at 1300 °C
(Transverse direction)

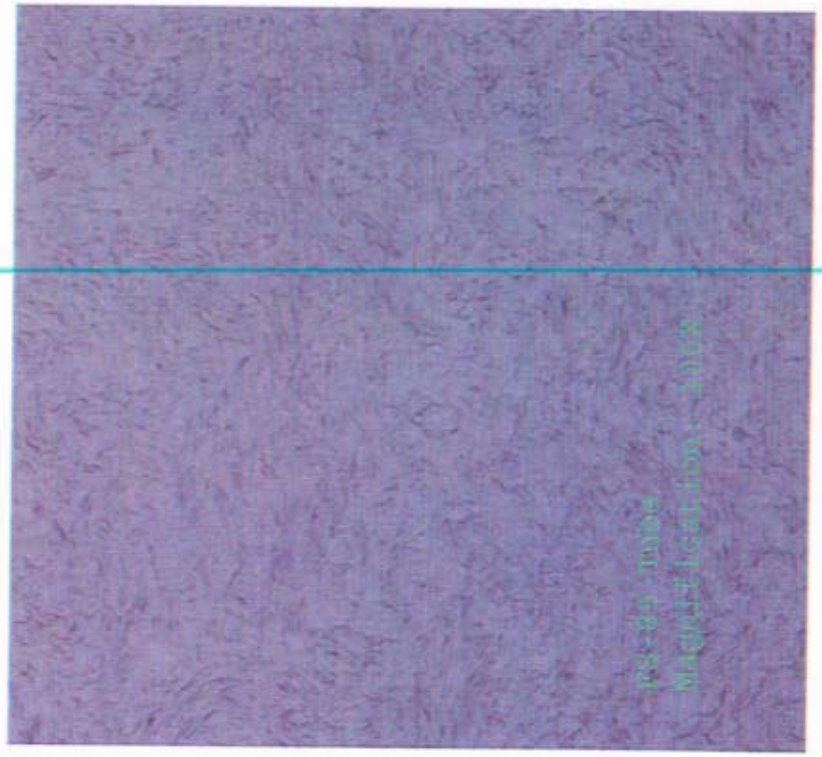

Figure 51: FS-85, as-drawn tubing, annealed at 1350 °C
(Transverse direction)

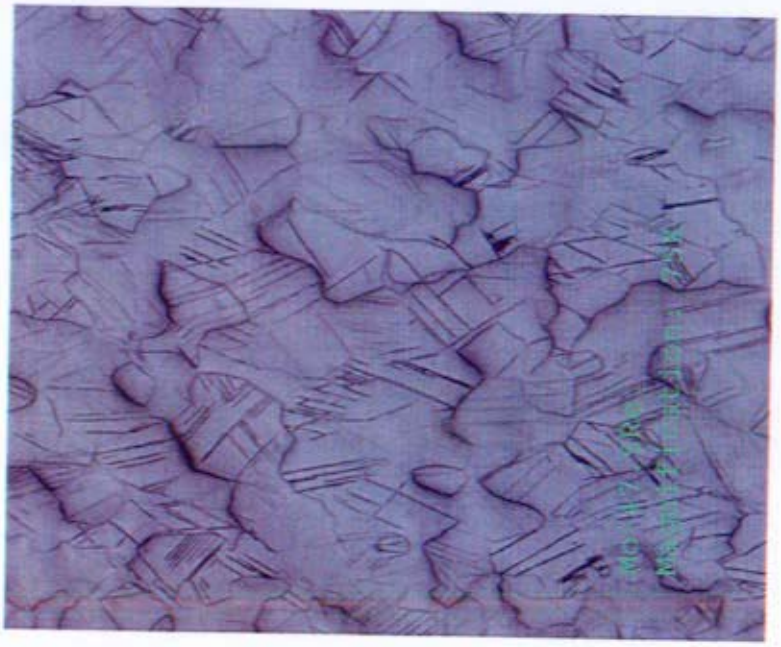

Figure 52: Mo-47.5 Re, arc cast, cold rolled, 0.040-inches thick (Longitudinal direction)

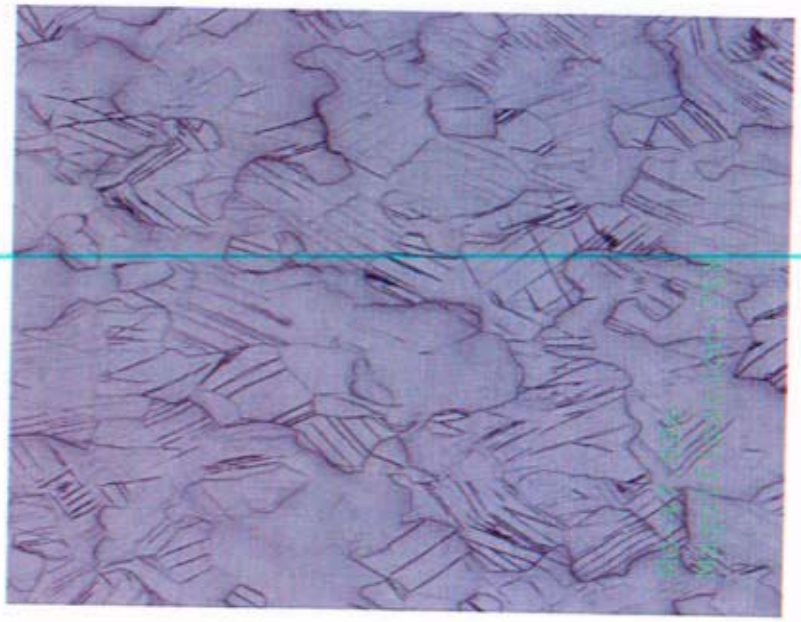

Figure 53: Mo-47.5 Re, arc cast, and 0.040-inch thick sheet. Rolled at 1425 °C to 0.080-inch – cold rolled to 0.040-inch. (Longitudinal direction)

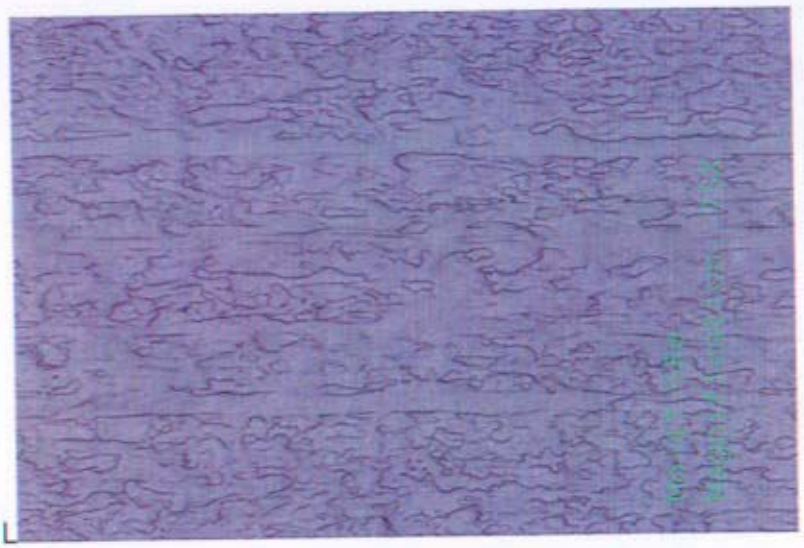

Figure 54: Mo-47.5 Re, arc cast, rolled to 0.040-inch at 1425 °C.
(Longitudinal direction)

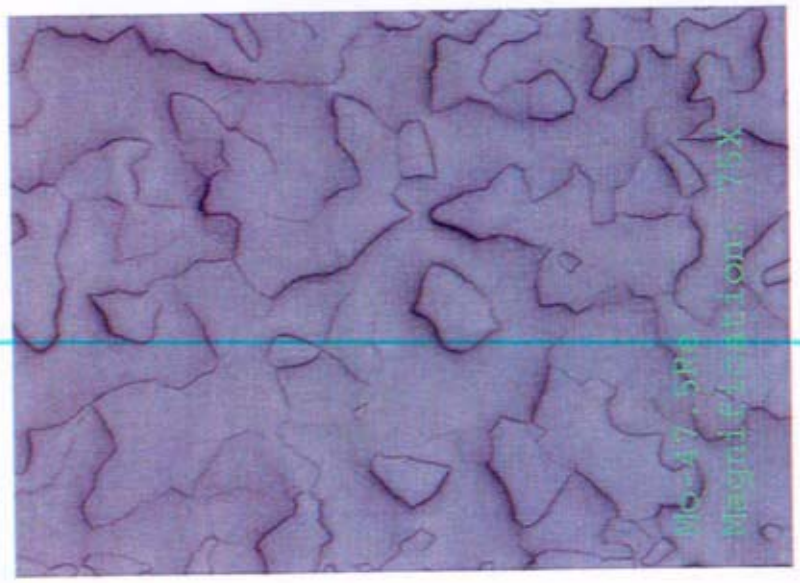

Figure 55: Mo-47.5 Re, arc cast, cold rolled to 0.040-inch and annealed at 1550 °C
(Longitudinal direction)

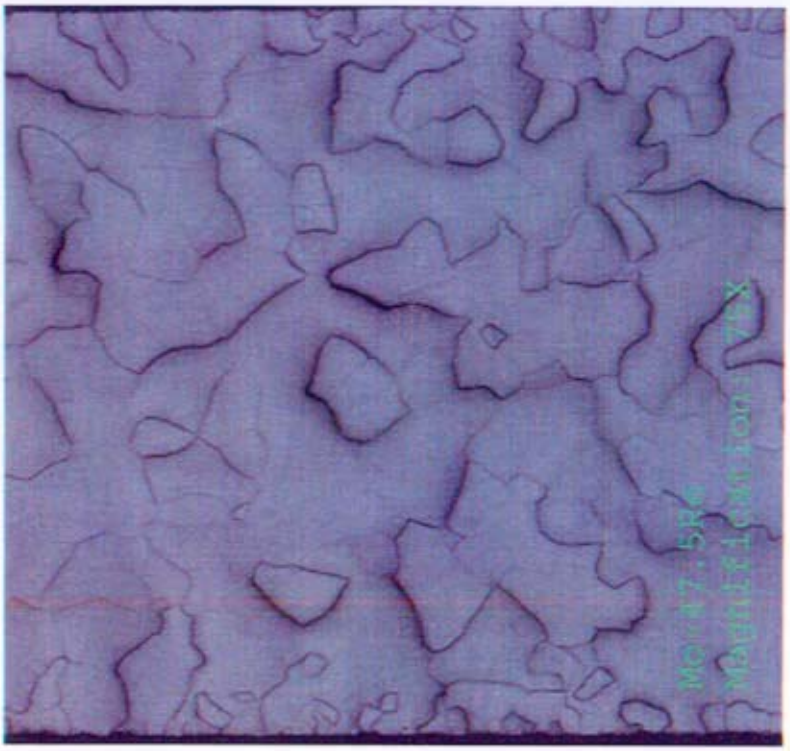

Figure 56: Mo-47.5 Re, arc cast, rolled to 0.080-inch at 1425 °C. Cold rolled to 0.040-inch, annealed at 1550 °C (longitudinal direction)

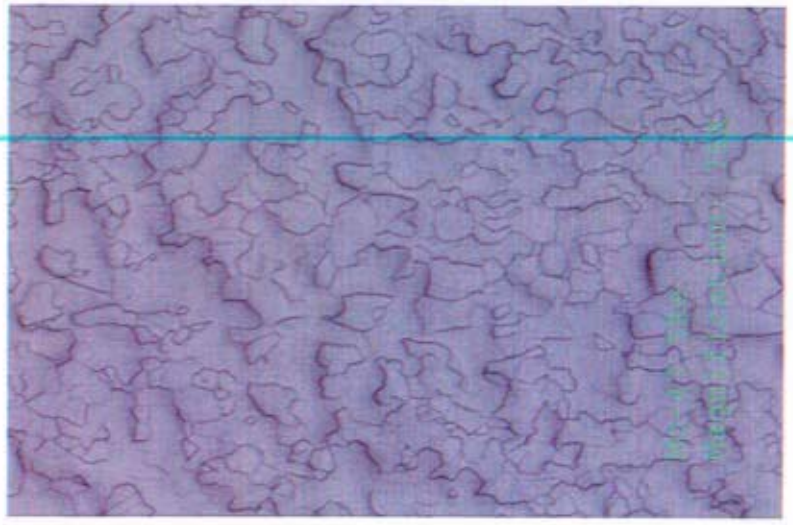

Figure 57: Mo-47.5 Re, arc cast, rolled to 0.040-inch at 1425 °C, annealed at 1550 °C (Longitudinal direction)

Generally in-process and final structures appear to be consistent with expectations. In addition, comparisons were made to previous efforts to fabricate T-111 and ASTAR-811C that were conducted in the early 1960s and 1970s and documented in References (4, 12, &13). The microstructures

developed on these ingots compared favorably to the previous T-111 and ASTAR-811C. There were some exceptions; they are discussed below along with general observations:

The ASTAR-811C microstructure in either the annealed or the rolled condition exhibits a large density of precipitates that are presumed to be mainly carbides. This is consistent with the addition of 250 ppm carbon to the base alloy. The carbides are further assumed to be of the type Ta_2C based on a review of the pseudo phase diagram (Figure 58) taken from Reference (12).

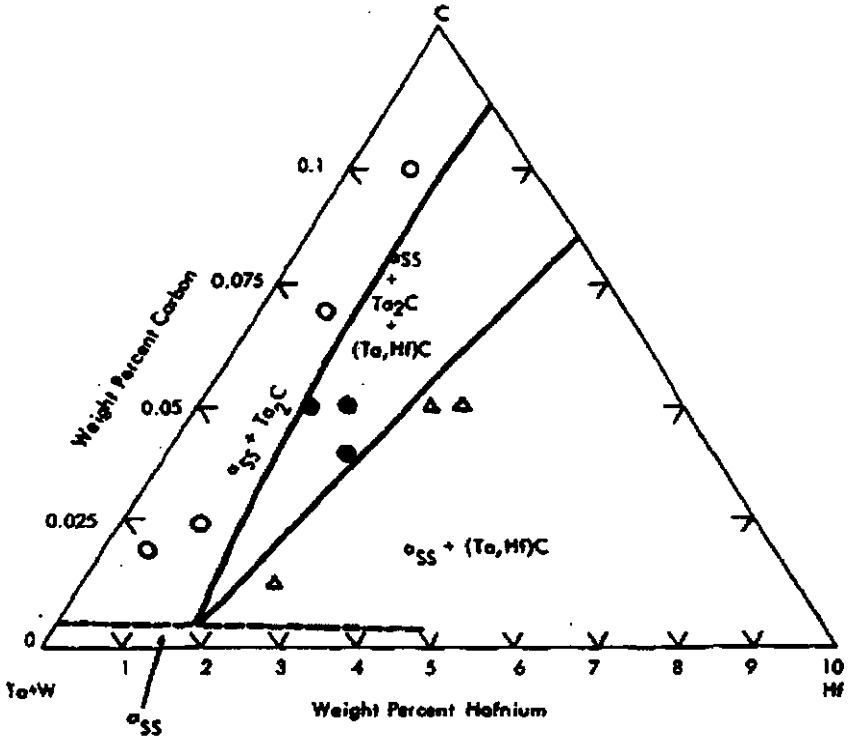

Tantalum Rich Corner of the (Ta+W)-Hf-C Psuedo Ternary Phase Diagram 2400°F Isotherm

Figure 58: Ternary Phase Diagram

Furthermore, microstructures of heat treated ASTAR-811C, provided in this 1967 review, were very similar in appearance to those of the current effort.

The carbides are located both at the grain boundaries and within the matrix. A one hour recrystallization study of final rolled plate and final processed tubing, conducted over the temperature range of 1500 °C to 1700 °C, resulted in minor changes in the carbide structure for both rolled plate and tubing. Both products experienced identical changes in both carbide morphology and increases in carbide density as the annealing temperature was increased.

Note that the carbide solvus temperature for 250 ppm carbon is reported to be well in excess of the highest temperature, which these specimens experienced, Reference (12).

The T-111 alloy is essentially a solid solution strengthened alloy. Carbon is not included as an alloying addition. Thus the expectation is that the structure should be relatively clean with an occasional carbide or oxide precipitate resulting from combination of hafnium with the small amounts of carbon, oxygen, and nitrogen present within the starting material. Aging of T-111 will modify the clean structure and cause additional precipitates to form at grain boundaries and at dendrites. A study of aged and un-aged T-111 weldments and base metal suggested that the precipitates observed at the grain boundaries were of the type Ta_2C and those at the dendrites were of the type W_2Hf. However, the authors indicate that the evidence was inconclusive as to their actual composition, Reference (4).

Regardless, the expectation was that a relatively clean microstructure should be normal for this T-111 material following a short term anneal. Indeed, the microstructures representing the center of the thin rolled plates fabricated for JOYO met this expectation. They were essentially clean with only an occasional precipitate. However, near the edges of final processed and annealed plates, as well as the edges of annealed tubing, increased levels of precipitation were observed (Figures 37-44). The increase extended inward several mils from the outer surfaces of the two products. This suggests that the final anneal may have been conducted in a poor atmosphere, or that insufficient material was removed during the previous pickle operation. Both sample types were processed through pickling at the same times and were annealed within the same series of furnace runs thus providing some evidence that the rationale is plausible. Note that the as-machined surfaces of the tensile specimens machined from these same plates were well below the surface of the final rolled plates. Thus, whether the problem occurred during the anneal for this heat treatment study, or occurred as a result of insufficient pickling, the contamination would not have been an issue for tensile samples machined from the mid-thickness of these same plates. The same statement cannot be made for the tubing samples. The surface of the as-drawn tubing minus material removed during a subsequent pickle operation is the final surface of a biaxial creep specimen. However, a metallographic evaluation of a T-111 biaxial creep sample that experienced the abbreviated weld development reported above did not reveal any surface contamination. The photomicrograph (Figure 45) includes both weld and HAZ within the tubing, as well as within the attached end plug. The respective outer surfaces, admittedly viewed at a relatively low magnification, do not exhibit surface contamination. This observation suggests that the problem was a final processing one, and thus limited solely to the material processed for the heat treating study. Nevertheless, future users of this material should carefully evaluate the surfaces of both T-111 tubing and plate product for evidence of contamination.

FS-85 is essentially a solid strengthened alloy although the addition of the reactive element zirconium causes a small amount of dispersion strengthening. Zirconium will combine with the small levels of the interstitial elements present in the as-melted material to form low levels of carbides, oxides, and nitrides. Despite their presence, a final processed and annealed structure should be relatively clean. Again as noted above for T-111, aging can cause additional precipitates to form in FS-85 weldments and base material. The same study referenced for T-111, (Reference 4), postulated that the precipitates formed during aging were of two types. Those at the grain boundaries were believed to be Nb_2C and those at the dendrites were believed to be W_2Zr. However, for the short term annealed FS-85 of the current study only isolated precipitates were expected.

That expectation was met. The only controversy with this alloy was the temperature required to recrystallize this material. A photomicrograph of the as-honed tube hollow for this alloy, Figure 50, is shown to be in the as-worked condition. A 1300 °C anneal conducted two steps earlier was expected

to recrystallize the material (Section I.K.) For comparison, a photomicrograph of a honed T-111 tube hollow is included in Figure 44. A subsequent annealing study conducted after the FS-85 tube hollows had been processed into tubing (~68% wall reduction) provided further verification that the 1300 °C anneal did not recrystallize this alloy.

Three different processes were used to produce final plate product for the arc cast molybdenum-47.5 rhenium as previously described. The as-rolled structures are considerably different for two of the three. Both materials cold rolled a final 20% following their last anneal exhibit a highly twinned structure superimposed on the remnants of the grain structure formed during the high temperature in-process anneal at 1600 °C. Twinning is commonly seen in cold worked and annealed Mo-Re alloys, Reference (14).

FURTHER DISCUSSION OF INDIVIDUAL PROCESSING STEPS AND COMPARISON TO COMMERCIAL VENDORS

A. Melting

Figure 59: Leybold-Heraeus AC Arc Melter at PMTI. Maximum power input is 5000 amps. Maximum melt diameter for refractory ingots is ~4 inches.

A1) AC melting

As noted above, PMTI melted the alloys as consumable electrodes with a Leybold-Heraeus arc furnace powered by an AC current. This is contrary to most large scale melting facilities that melt with a direct current (DC) arc furnace. The main advantage of an AC arc is that the melted ingot is more homogeneous than a comparable DC melted ingot. The AC arc imparts more power to the melt than a comparable DC melt. Indeed the AC melt is often described as a "violent melt." When viewed, the liquid metal splashes vigorously, thoroughly mixing the contents. This phenomenon is caused by the physics of the alternating current. An AC current changes polarity 60 times a second. This alternation in current increases the power distribution which not only allows high melting point materials to liquefy, but it also causes the liquid metal to mix, homogenizing the ingot. A DC current is an AC current that has been rectified. It has a constant polarity during the entire lifetime of the melt. Due to its constant polarity, a DC arc furnace does not allow the liquid metal to mix as thoroughly.

However, the impact of the AC current is not limited to the molten pool. The AC current also causes constituents contained in the electrode to melt at a similar rate even if they exhibit a wide disparity in melting points, Reference(1). This may not always be the case for DC melted ingots, especially small, rapidly melted ingots. It has been the experience of the undersigned that it is very, very difficult to homogenize small DC melted ingots containing constituents with widely different melting points. Repeated consumable DC melts do not improve the homogeneity. Larger DC melts with a larger molten pool may be able to overcome the disparity in melting points. Despite the AC arc furnace's ability to homogenize an ingot whose constituents exhibit a wide disparity in melting points, a second melt should be conducted to ensure this characteristic.

A2) Difficulty in achieving exact composition and weight

The difficulty in achieving exact weights or chemical levels can be appreciated if one observes the variety in shape and length of residual electrodes that remain when melting of a specific electrode has been terminated (See Figure 60). The termination of a melt is based on interaction of the melting technician and a second technician viewing the melt through a small quartz glass located just above the melt furnace. When the electrode appears to have almost entirely melted or if the molten metal is approaching the crucible top, the "call" is made to terminate the melt. The problem is that it is difficult to judge the electrode length when viewing from directly above through a narrow window. Even if a camera is used to assist the melt technician, the camera location (right above), causes the same visual dilemma. Regardless of when the melt is called, the use of a sandwich electrode where the alloying constituents are evenly distributed along the entire length of the crucible would still ensure a relatively homogenous melt if the electrodes melted evenly. However, the variety of the shapes shown below reveals that the electrodes do not melt evenly.

Figure 60: Electrode stubs.

The power input causes different portions of the electrode to melt at different rates causing different yields and shapes. This phenomenon in turn causes variations in composition. However, the variations when melting sandwich type electrodes are usually insignificant. It should thus be emphasized that development of the sandwich electrode for melting of refractory alloys especially when combined with AC melting (Reference (1)) has alleviated much of the difficulty in achieving desired compositions. The deviations caused by the variation in electrode remnant shapes are relatively minor.

A3) Ingot hot topping

Hot topping is a technique that is used to prevent severe piping defects from evolving at the top of the final melt ingot. During the final stages of the second (final) melt, the melting current is reduced, slowing the melt process. This increases the depth of the molten pool and slows ingot solidification. The goal is to reduce the pipe or void which forms at the top of the ingot as the ingot solidifies and shrinks. Even with this "hot topping" technique, some length of pipe almost always forms at the top of the ingot. This pipe is usually centered on the ingot top and extends to a depth of ½-inch or greater. If this pipe isn't removed after the melting process, further processing can cause defects to evolve in the material. Complications due to this issue can be found in Reference (8) where several biaxial end caps were rejected due to centerline cracks as was discussed in Section I.

Once the material is melted, the ingot is taken out of the copper chill mold and conditioned. The piping is usually cut off with a band saw unless it is a Mo-Re alloy. Since Mo-Re work hardens at a rapid rate, a high pressure water jet is typically used to section this material. Following removal of the pipe, approximately 10% of the ingot is machined off due to imperfections on the walls of the ingot, piping, or to remove the flashing. Imperfections on the exterior walls of the ingot range from copper contamination to a rough surface. A lathe is used to rid the ingot of these imperfections. The term wet wall" is used to define an ingot that has a smoother refined surface. This can be achieved by lining the copper mold with refractory metal foil of the same base composition as the electrode and then melting the electrode rapidly. The drawback of melting the electrode quickly is that the material will not be efficiently homogenized. It is best to be concerned with the homogeneity of the melt rather than the surface finish of the ingot. Figure 61 shows the difference between a wet wall and a rough wall.

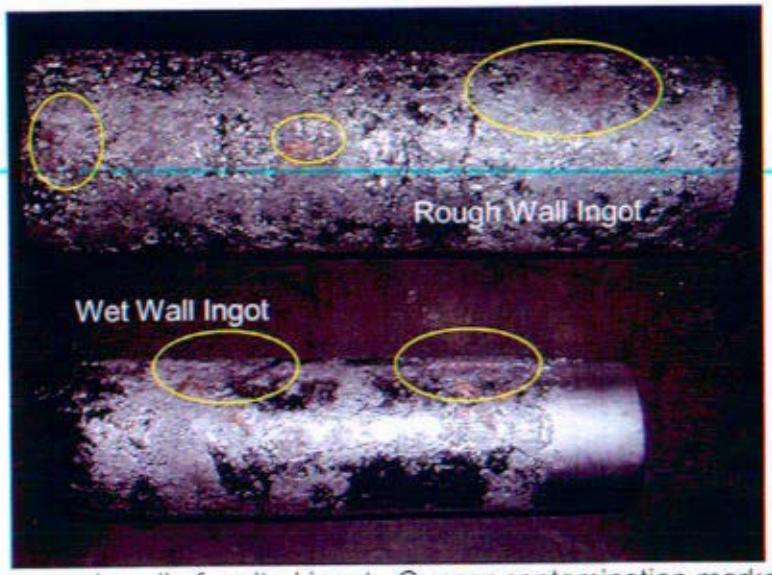

Figure 61: Wet wall vs. rough wall of melted ingot. Copper contamination marked in yellow occurred during ingot removal from copper crucible

The surfaces of both ingots in Figure 61 were contaminated with copper when they were removed from the soft copper crucible following melting. Despite the difference in surface finish, both wet and rough walled ingots appeared to pick-up similar levels of copper during ingot removal.

B. Extrusion

B1) Historical Basis for Extrusion

Typically most commercial iron or nickel base alloys are forged to break-down the large-as cast grain structure of the final melted ingot. However, extrusion where the material (clad or unclad) is forced through a die after preheating to a high temperature remains a primary method for breakdown of the high strength tantalum alloys as well as molybdenum and molybdenum-rhenium alloys. This is based on several factors. Part can be attributed to the lack of a commercial forging infrastructure that combines high strength forges with furnaces capable of heating to the high temperatures necessary to adequately soften a large refractory metal ingot and allow it to be worked.

However, with respect to the tantalum alloys containing hafnium, metallurgical reasons also dictate that extrusion must be used. Following the final melt of large tantalum-base ingots containing hafnium such as ASTAR-811C, both the large molten pool and ingot size cause the ingot to very slowly solidify and cool to room temperature. This slow cooling allows the hafnium to segregate to the grain and dendrite boundaries. The hafnium dramatically weakens these ASTAR-811C boundaries when they are placed in tension. Consequently, forging, a process that combines both tensile and compressive forces can cause the ingot to crack and even shatter into pieces. However, the extrusion process employs only compressive forces during breakdown and can overcome the inherent weakness of the hafnium enriched grain and dendrite boundaries. Once the as-cast structure is broken down and the grain structure is significantly refined, hafnium is not an issue. At this point ASTAR-811C as well as all of the Group VB alloys(Nb and Ta) can be further broken down via swaging or rolling with little or no heat input and with no risk of cracking.

Surprisingly this is not an issue for small (4-inch or smaller) diameter Ta ingots containing hafnium, Reference (15). Apparently the smaller molten pool occurring during melting of the smaller diameter ingots results in a fast enough cooling rate that segregation of hafnium to the grain boundary is minimized. As a result forging has and can be employed for their breakdown.

B2) Ingot Orientation for Extrusion

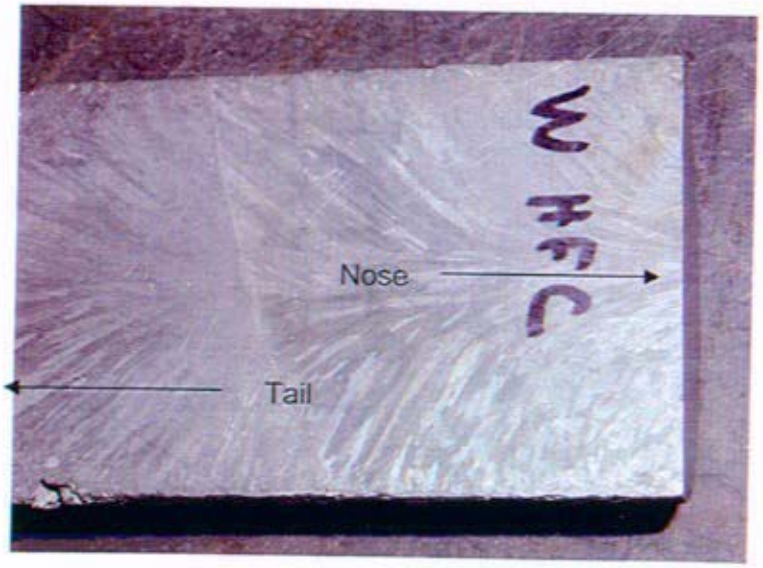

Figure 62: Orientation of grains in ingot. Top of the ingot is to right.

The microstructure shown in Figure 62 reveals the elongated grain structure that forms at the top of the ingot with the grains angled towards the top of the ingot. The grain structure at the ingot bottom or tail can be seen to diverge away from the ingot bottom. The ingot should thus be extruded nose first so that the compressive forces of the extrusion process continue to push the grain structure in the same direction that they are currently oriented. If the ingot were extruded tail first the compressive forces of the process would not be so aligned and the ingot could fray apart during extrusion. Therefore, when loading the ingot into the canister, it is important to have the top of the ingot as the nose of the extrusion.

C. Comparison of Processing Experienced by these Laboratory Size Ingots to that Expected for Larger Commercial ingots of the Same Compositions

A major concern for any testing program predicated on small laboratory size ingots is that test results obtained from material representing these ingots may not be representative of results generated from testing of larger commercial ingots of the same alloys. Differences, if they occur, may be caused by differences in melt practice, by cooling rate differences during final ingot solidification as well as at later process steps, by differences in material breakdown procedures because of equipment limitations or because of a lack of a general understanding of proprietary commercial practices. This program was intended to evaluate these issues since these smaller ingots were to serve as forerunners for larger size commercial ingots that were to be procured for most of the alloy compositions listed in Table 1. Comparison of results and behaviors between laboratory and commercial alloys was intended to be a primary objective of the program.

Documented below is an incomplete listing of the key differences in manufacture that were expected between the small ingots of this report versus the larger commercial ingots that were to be procured by the NRPCT for testing, evaluation, and fabrication studies. The listing is incomplete because the procurement process for the large ingots had only just been initiated when Naval Reactor's effort was terminated. A better understanding of the differences would have been possible once production of these ingots had ensued and NRPCT personnel had witnessed their melting and processing. The listing below is based on limited discussions with Contracting personnel at the commercial vendors as well as with other knowledgeable individuals in the limited refractory metal community. The discussion below also provides a snap shot of existing US refractory metal infrastructure in the 2005 -2006 time frame.

C1) Melting practice for Nb- and Ta-base ingots

Wah Chang is the only US refractory metal vendor with the capability to arc melt complex niobium and tantalum-base refractory alloys such as FS-85 and ASTAR-811C. They purify the starting refractory elements (Ta, Nb, and W) with an electron beam (EB) melting process to reduce the interstitial contaminants to single digit levels. The refractory elements are then combined with lower melting constituents such as hafnium or zirconium and double arc melted using DC current to form 10-inch diameter or slightly larger ingots. Other vendors such as Cabot have the capability to EB melt an alloy based solely on refractory alloys such as Ta-10W, but they do not have the capability to arc melt an alloy containing lower melting point constituents as would be needed for FS-85 and ASTAR-811C.

The laboratory size ingots were arc melted using AC current as 3-inch diameter ingots as has been discussed. The starting stock used in electrode fabrication was obtained from Wah Chang and is presumed to have experienced the same processing as would have been employed for starting stock

employed by Wah Chang for large size ingots. The employment of AC melting is not believed to be an issue. AC melting, as noted, improves the chemical homogeneity of small ingots relative to the same size DC melted ingots. However, the much larger molten pool present during DC melting of the 10-inch diameter commercial ingots would serve the same function.

One difference that can't be discounted is that of the cooling rate occurring during solidification of the final melt ingot. This was already alluded to in a previous discussion concerning the historical basis for extrusion where it was noted that hafnium segregation is an issue for large diameter ASTAR-811C ingots but apparently not for smaller diameter ingots. There may be other unknown chemical elemental differences resulting from the size differences. Previous experience indicated that later ingot breakdown and secondary processing should erase these differences occurring at the melt stage, but that was still to be determined.

The Ta-10W laboratory ingot was arc melted at PMTI using EB melted W and Ta as electrode constituents. Negotiations hadn't been finalized, but the large Ta-10W ingot that was to be procured from Wah Chang most likely would have been final melted using EB melting. The Ta and W would be melted and homogenized solely within the EB melter. This should not have been an issue because the AC consumable melt process should have little effect on this binary alloy where each element is mutually soluble within the other. The microstructures of the laboratory and commercial size ingots could be different following melting, but the overall elemental homogeneity would have been similar. Later processing would be expected to obliterate any ingot microstructural differences.

C2) Melting or formation practice for Mo-Re alloys

The primary US producer for molybdenum -rhenium alloys is Rhenium Alloys located in Elyria, Ohio. Another vendor, Schwarzkopf, located in Holliston, MA is limited strictly to production of molybdenum-41 rhenium in addition to a number of other molybdenum and tungsten alloys. Both vendors fabricate their respective Mo-Re alloys using a PM process. The major concern with employment of a PM product as a structural material is that welding of PM material to form structural joints may result in significant weld porosity, Reference (16). As a consequence, the NRPCT was evaluating both arc melted molybdenum-47.5 rhenium and PM molybdenum-44.5 rhenium for structural applications. The expectation was that an arc melted material would be required if this alloy type continued as a candidate. However, both vendors have only PM capability. The only US vendor with the capability and experience to possibly melt a commercial size ingot of molybdenum–rhenium is probably H.C. Starck at their facilities located in Coldwater, Michigan. They currently are the only US based melter of pure molybdenum and molybdenum alloys. It is believed that H.C. Starck would not have any serious technical reservations with regard to melting and processing of Mo-Re. Potential contamination of the Coldwater facilities by rhenium, an element they do not normally handle, would most likely be their major concern. However, it must be emphasized that this is only conjecture because H.C. Starck has not been approached officially about their interest or capability in melting this alloy.

C3) Ingot breakdown procedures for Ta- and Nb-base alloys

All of the ingots included in this program were broken down using extrusion at WPAFB. The majority were clad in molybdenum during this procedure. However, Wah Chang took partial exception to this procedure during preliminary contract discussions for the large ingot order. They recommended forging for the initial breakdown of the Ta-10W and FS-85 alloys. They indicated that they currently break-down large 10-inch diameter Ta-10W ingots using forging and were confident it would provide an acceptable product. Furthermore, they believed that they have sufficient experience with Nb alloys such as Nb-1% Zr so that they would also recommend forging for the initial breakdown of the FS-85

alloy. Later processing for tubing to be formed from all alloys would employ extrusion albeit at much smaller diameters.

Wah Chang also noted that if a molybdenum canister were to be employed for ASTAR-811C, as specified in the original inquiry, then this would cost considerably more than had been estimated. However, it was recognized by all that extrusion was the only viable method for breakdown of the ASTAR alloy for the reasons previously listed. Wah Chang lacks this process capability and would have to subcontract this step to H.C. Starck at their Coldwater facilities. Wah Chang has dealt with Starck in the past for similar efforts and did not expect any contractual issues for this route. However, attempts by Wah Chang to find a vendor that would encapsulate the ASTAR-811C in molybdenum for extrusion at 3000 °F were only partially successful. Recent cost increases by molybdenum suppliers as well as material scarcity resulted in vendor responses to the Wah Chang inquiry that approached $100,000 (2005 dollars). As a result, it had been tentatively agreed by both parties that a much cheaper mild or stainless steel canister could be substituted. The substitution would cause the extrusion temperature to be lowered to 2200 °F-2300 °F because of the lower temperature capability of the steel. Furthermore, the ingot would have to be wrapped in molybdenum foil prior to encapsulation to prevent contamination by the elemental constituents within the steel. Technically these modifications were not expected to be an issue because several early developmental ingots of ASTAR-811C had been successfully extruded using a similar approach during much earlier development efforts for this alloy. The undersigned had also successfully extruded a 4-inch diameter ingot of this alloy in the late 1990s using these same modifications.

Do's and Don'ts for Refractory Metal Processing

The refractory metals when processed correctly possess unique capabilities. However, they are prone to contamination from a variety of sources during processing or usage that can drastically degrade their properties. There sources include but are not limited to the following: 1) employment of a less than pristine atmosphere during welding and annealing resulting in interstitial contamination with oxygen, nitrogen or carbon, 2) contact with non-refractory metals during welding and annealing with the resultant transfer of non-refractory metals to the refractory metal, 3) copper contamination occurring during melting or Electro-Discharge-Machining (EDM) for those refractory alloys containing zirconium or hafnium, 4) improper cleaning of these alloys prior to annealing or welding operations, and 5) omission of a vacuum anneal for the niobium and tantalum-base alloys following acid pickling thereby causing hydrogen absorption and contamination. Each of these areas is briefly described below. Note that all of the vendors employed in this effort had extensive experience in processing of the refractory alloys and were familiar with the precautions required for their processing discipline.

A) Vacuum Annealing, Hydrogen Annealing, and Inert Gas Exposure Practices

Annealing of the refractory metals is a critical step in the fabrication of these materials, required either to allow continued processing of the alloys or to place them in the optimum metallurgical condition for final usage. However, if this process step is not correctly conducted, severe degradation in the final product properties will occur. Interstitial contamination with oxygen or nitrogen leading to embrittlement may be the primary concern, but it is not the only concern. Contamination with other elements such as carbon can occur from use of non-refractory heating elements or from small oil leaks from vacuum diffusion pumps. Furthermore, contact need not be direct for the contamination to occur. Thin films of non-refractory metals deposited during previous annealing runs and not removed by a furnace bake-out can cause contamination of refractory metals annealed at later times.

The problem of interstitial contamination with oxygen or nitrogen is most severe for the refractory alloys based on the Group VB refractory elements (Nb and Ta), but it is also a concern for those based on the Group VIB elements (W & Mo). The contamination can occur at vacuum levels that many commercial annealing vendors employ for annealing of non-refractory metals. The sources of contamination include system leaks, out-gassing of the furnace hot systems, or out-gassing from the metal being annealed. The problem is a complex one and has been the subject of many studies that are beyond the intent of this paper. However, a brief prospective is warranted because of its importance. An excellent review was conducted by H. Inouye of ORNL in the late 1960s and is documented in Reference (17). The paper indicates that the contamination process for refractory metals is a function of the incident rate of the potential contaminant on the metal's surface multiplied by the sticking probability. The sticking probability is a small fraction of the incident rate and decreases as the system (metal and contaminate) approach equilibrium. System pressure, the interstitial equilibrium content within the metal, furnace temperature and pressure, and even the alloying constituents within the base metal all have an impact. For instance, if an element lowers the solubility level of an interstitial within an alloy, then most probably the element will form a precipitate with the interstitial. This would result in relatively greater contamination than that for the pure element annealed under the same furnace conditions. The paper also notes that contamination is not the only issue for improper annealing of refractory metals. Degassing or decarburization are also possibilities depending on 1) starting interstitial levels within the material, 2) system pressures, and 3) annealing temperatures. Again the subject is complex; however, more than a superficial understanding of the subject is required if these alloys are to be annealed successfully.

While the overall subject may be complex, the explanation for the relative difference in behavior between the Group VB Nb and Ta alloys and the Group VIB alloys is easier to understand. The much greater tendency for the Nb and Ta alloys to become contaminated during annealing can be rationalized in terms of their relative solubilities for C, O, N, and H as listed below in Table 17. The Nb and Ta alloys are observed to exhibit large solubilities for the respective interstitials, whereas Mo and W exhibit almost no solubility.

Table 17: Interstitial Solubility within Refractory Metals based on Estimates of Equilibrium Solubility at the Temperature where Diffusion D= 10^{-11}cm^2 /s, Reference (18).

Element→ Interstitial ↓	**Nb**	**Ta**	**Mo**	**W**
Oxygen	1000 ppm	300 ppm	1.0 ppm	1.0 ppm
Nitrogen	300	1000	1.0	<0.1
Carbon	100	70	<1.0	<0.1
Hydrogen	9000	4000	0.1	N.D

This difference in affinity has a significant impact on both the quality and type of environment that the two refractory metal Groups can be exposed to either during the annealing process, long-term high temperature testing, or during final deployment. The consequences include the following:

1) Molybdenum and its alloys can be annealed for either short periods or exposed long term when the vacuum level is maintained in the mid-10^{-5} torr regime with little risk of contamination.
2) Likewise, molybdenum can be exposed for long periods at high temperatures within inert gas environments with little risk of contamination as long as moisture and oxygen levels are maintained in the low single digit ppm levels.

3) Whereas Nb and Ta can be exposed for short term anneals in the mid-10^{-5} torr level with minimal increases in interstitial contamination, long term vacuum anneals or extended testing require appreciably better vacuum levels. Both require vacuum levels to be maintained at or below 10^{-8} torr if interstitial contamination is to be avoided. The consequences of long term exposure at only marginally lower levels in the 10^{-6} torr range versus that in the 10^{-8} range were noted in Reference (19) for T-111. A relatively short 200 hour exposure in an unbaked system at 1370 °C evacuated with a diffusion pump resulted in appreciable increases in both carbon (from oil in the vacuum pump) and oxygen levels. In contrast, a T-111 specimen tested in high vacuum evacuated with a sputter ion system maintained a constant interstitial level.
4) Long term exposure of Nb and Ta alloys in a flowing and replenished inert gas system is also to be avoided. As noted by Inouye in Reference (17), to prevent contamination of Nb and Ta and their respective alloys within an inert gas environment at high temperatures, it is necessary to maintain oxygen and nitrogen at amounts that are below the level of detection for available instrumentation. This statement made in the 1960s is still valid today. It should be acknowledged that long term exposure of Nb and Ta elements and their respective alloys can be made within a closed inert gas system where the total contamination is limited by the initial starting contaminant level within the inert gas if the initial burden or contamination level is not too high.

More detailed guidelines are listed below to ensure that all sources of contamination are minimized during vacuum annealing of these materials.

1) All refractory metals to be vacuum annealed shall be freshly pickled.
2) The furnace heating elements shall be of a refractory metal composition.
3) The furnace atmosphere for short term anneals when at temperature shall be 5×10^{-5} torr or better. For longer anneals involving testing of thin niobium or tantalum specimens, the vacuum level shall be at or below 10^{-8} torr.
4) The furnace leak rate should be checked prior to use to ensure that a small system leak is not present, which could be masked by an excellent or oversized vacuum pumping system. The leak rate shall be checked with the vacuum system shut-off and shall be less than 5×10^{-3} torr-liters/min.
5) All products shall be completely wrapped in thin refractory metal foil during annealing to further reduce any chance of contamination. Note that rather than acting as a getter, the main function of the foil is to slow the rate of contact, Reference (17). Thus it is critical to tightly wrap.
6) Refractory and non-refractory materials shall not be annealed in the same furnace run. It is also desirable that refractory metals be annealed in a furnace limited solely to refractory metals. If this is not possible, then before annealing refractory metals, the furnace shall be baked out for 1 hour minimum at a temperature 100-200 °C hotter then is intended for the annealing of the refractory metal.
7) An ultra-high vacuum unit (10^{-8} torr or better) that employs a sputter ion system for maintenance of the final vacuum atmosphere shall be sealed and placed under a vacuum when the system is not in use. This will minimize absorption of moisture within the vacuum pumping system and shorten the time required to achieve test temperature when placed in usage. This practice will also appreciably extend the lifetime of pumping components.

PMTI employs two different types of vacuum furnaces for annealing of refractory metals. The first is a so-called brew furnace employed for anneals requiring only moderate vacuums

(~1 x10^{-6} torr), and the second is an ultra-high vacuum unit where the atmosphere can be lowered to 10^{-8} torr and even the 10^{-9} torr range with longer exposures. The ultra high vacuum unit is typically used for long term aging runs and has been used in the past for extended biaxial creep specimen testing. A photograph of the brew furnace is shown in Figure 63 while the ultra-high vacuum unit is shown in Figure 64.

Figure 63: Photograph of two Brew furnaces at PMTI. The one on the left is limited solely to annealing of refractory metals. The furnaces employ tungsten heating elements enclosed with neoprene seals. The furnaces can be evacuated with diffusion pumps to vacuum levels as low as 1x 10^{-7} torr. The heat zones measure 3-inches in diameter with heights of 6-inches and can be heated to maximum temperatures of 2200 °C.

Figure 64: Photograph of two ultra-high vacuum aging furnaces at PMTI. Both are used strictly for refractory metals. They have Ta heating elements and can achieve temperatures as high as 2000 °C. Vacuum levels in the 10^{-8} to 10^{-9} torr levels can be maintained for long term anneals using metal to metal copper sealing rings in combination with sputter ion pumping systems. The heat zones are approximately 3-inches in diameter with a height of 10-inches.

Another option for annealing of molybdenum and Mo- Re alloys is to use a furnace heated by the ignition of "dry" hydrogen flowing through its interior, Reference (20). If the anneal is long enough and the temperature high enough, surface oxides will be reduced and removed. It is also the experience of the undersigned that long term anneals within the PMTI furnace at its maximum usage temperature will reduce both oxygen and carbon levels at appreciable levels below the surface and even throughout the material if the annealing period is sufficiently long. The depth and amount of C and O removal is a function of diffusion kinetics and thus depends on both temperature and time at temperature. Diffusion down the grain boundaries is the controlling factor. The hydrogen furnace is also useful for preheating of molybdenum and molybdenum-rhenium during rolling or swaging operations. However, this furnace is not an option for use with Nb or Ta alloys. They will hydride very quickly within a hydrogen environment. Photographs of the interior and exterior of the PMTI hydrogen furnace are provided in Figure 65.

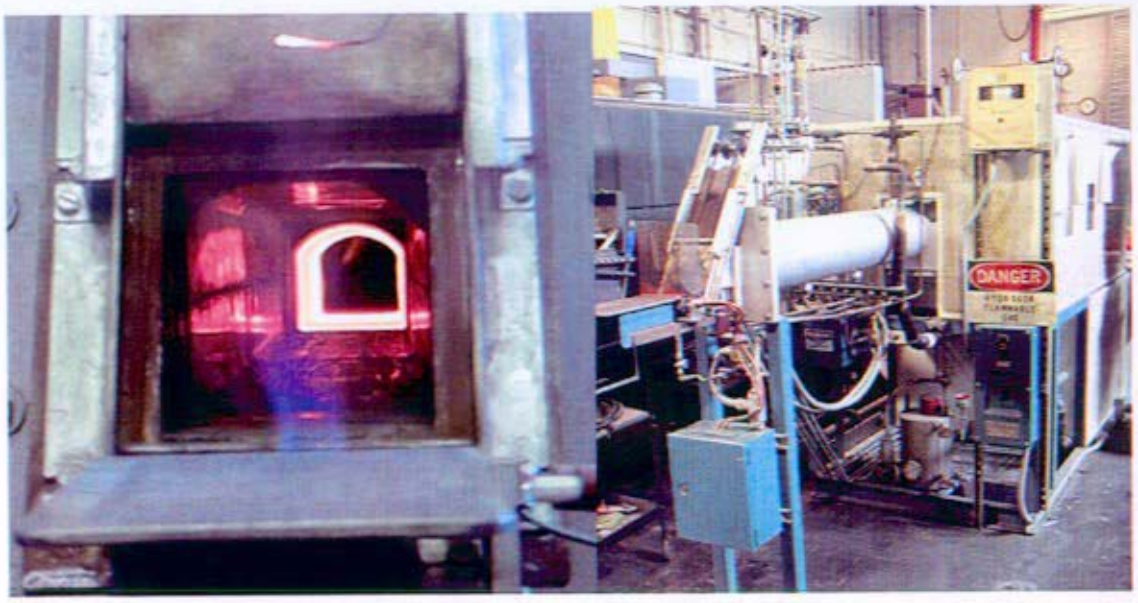

Figure 65: Interior and exterior views of hydrogen furnace at PMTI used for annealing, as well as preheating for rolling or swaging of molybdenum and molybdenum-rhenium. The CM400 series furnace has a 4-foot long 3-zone hot region. Normal operation flows "dry" hydrogen through the 4-inch x 4-inch cross sectional area at ~ 5 cubic feet per hour. Maximum temperature is 1600 °C.

B) Welding Practices:

All of the normal welding methods including GTAW, electron beam, and laser can be used to weld the refractory alloys. However, to prevent contamination, the guidelines listed below should be followed. These guidelines were established early in the development of refractory metals, Reference (21). Additional guidance is provided in References (16, 22, and 23). A typical set-up for a glove-box used at PMTI for GTAW welding is also depicted in Figure 66.

1) All refractory metals to be welded shall be in a freshly pickled condition.
2) Refractory metals and lower melting non-refractory metals shall not be welded in the same load to prevent the lower melting materials from depositing on and contaminating the refractory alloys.
3) The weld chamber shall be evacuated into the mid 10^{-5} torr level or better before initiating an EB weld or before introducing the inert gas required for GTAW. The leak rate of the weld chamber shall be checked to ensure that a small leak is not present. The leak rate shall comply with that noted above for annealing.
4) Even with evacuation into the 10^{-5} torr level, moisture and oxygen probes are recommended to ensure that both levels remain below 5 ppm. If probes are not available, bake-out lamps should be employed for several hours during the final stages of evacuation.
5) Weld fixturing shall employ refractory metal foil or refractory metal inserts between non-refractory metal components and the refractory metal piece to be welded.

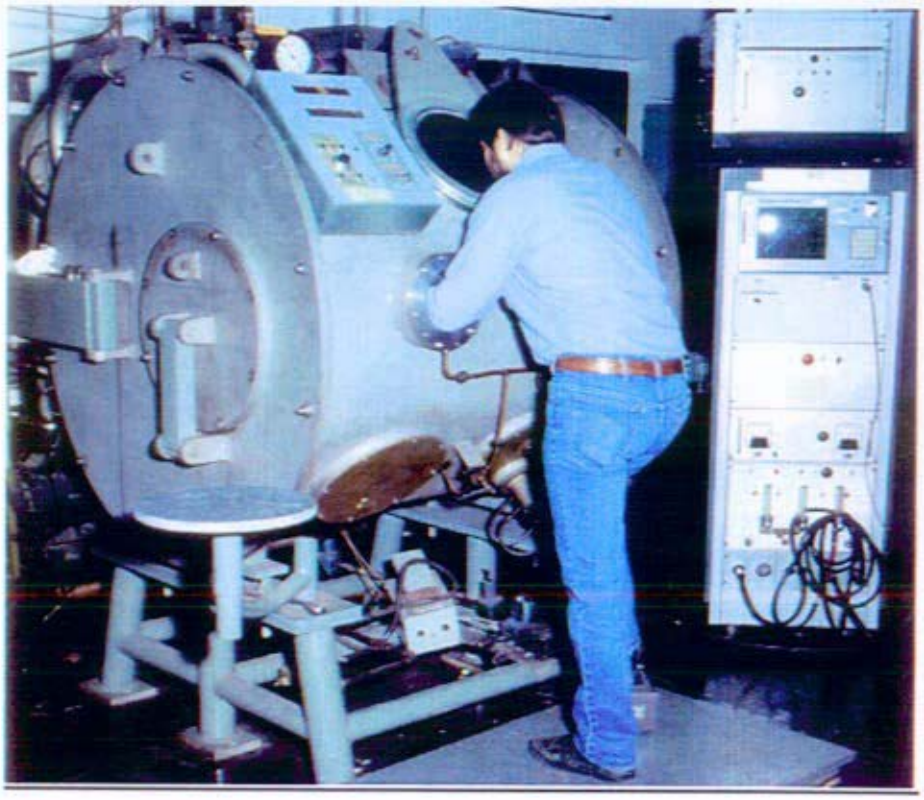

Figure 66: Photograph of glove-box used for GTA welding at PMTI. The glove-box can be evacuated to levels approaching 10^{-6} torr prior to backfilling with inert gas. The box includes bake-out lamps to drive moisture contents down into the single digit ppm levels, if required. This glove-box was used to weld the electrodes required for initial and final melts on this program.

C) Contact and Contamination with Non-Refractory metals

Parts A and B in this section stated that contact with refractory metals should be avoided during welding and heat treating. Part D (below) states that minor levels of copper contamination during melting of niobium or tantalum alloys containing zirconium or hafnium can lead to total degradation of high temperature properties. However, contamination with non-refractory metals is not a concern limited strictly to melting, annealing, or welding processes. Contamination can come at any step in the process. It is impossible to avoid contact with all non-refractory metals during processing. It will occur during machining with carbide tool bits or other machining materials. Rolling on steel or cast iron rolls can not be avoided during rolling to final thickness. Thus it is critical that the alloys be cleaned or pickled to remove any probable contaminant after each of these steps. Removal of 0.001-inch and preferably 0.002-inches per surface is recommended during pickling. Furthermore, any step in a process that has the possibility of embedding a foreign particle in the surface at levels beyond the depth removed by pickling must be carefully monitored to ensure that this has not occurred.

The consequences of contamination of the refractory alloys can be seen in Table 18, which lists the lowest melting points for various combinations of refractory alloys with potential contaminants such as Fe, Cr, Ni, and Cu.

Table 18: Eutectic Melting Points for Various Metals in Contact with Refractory Metals

LOWEST MELTING POINTS(°C) IN VARIOUS BINARY SYSTEMS

	W											
W	3407	Re										
Re	2830	3180	Ta									
Ta	3014	2695	3014	Mo								
Mo	2617	2444	2617	2617	Nb							
Nb	2467	2424	2467	2297	2467	Hf						
Hf	1950	1840	2130	1879	2068	2227	V					
V	1910	1910	1910	1910	1860	1456	1902	Cr				
Cr	1860	1857	1760	1827	1671	1500	1785	1857	Zr			
Zr	1798	1593	1822	1578	1743	1852	1265	1372	1852	Fe		
Fe	1533	1533	1342	1454	1372	1302	1468	1516	948	1536	Ni	
Ni	1495	1453	1330	1317	1175	1132	1203	1345	961	1427	1453	Cu
Cu	1085	1085	1085	1085	1085	970	1085	1076	886	1085	1085	1085

= The Elements Generally Identified as "The Refractory Metals"

Many of the listed eutectic temperatures are well below intended usage temperatures for these alloys. This suggests that failure via a large number of potential mechanisms is possible if inadvertent and undetected contamination of these refractory alloys does occur. Numerous examples of a processing faux pas for the Nb-1%Zr alloy are provided in Reference (24), which provides an excellent description of what happened during processing of this alloy for the SP-100 program.

D) Hydrogen Removal for Tantalum and Niobium-Base alloys

The niobium and tantalum-base alloys have a large affinity for hydrogen even at room temperature. Consequently, they may absorb an appreciable amount of the hydrogen generated during acid pickling. The hydrogen should be removed prior to further processing via a one hour vacuum anneal at 800 °C or hotter.

E) Copper contamination of niobium or tantalum alloys containing hafnium or zirconium

1) Copper contamination during melting

Niobium and tantalum alloys containing zirconium or hafnium as alloying constituents can have their high temperature mechanical properties drastically degraded if they are inadvertently contaminated by small levels of copper. The hafnium or zirconium will combine with the copper contaminant to form low melting eutectics that embrittle grain boundaries. The copper levels at which these properties can be degraded are so low that they lie below the detection limits for most chemical analytical procedures. The levels at which problems occur are also less than current specifications allow.

Thus, if it is suspected that the electric arc has strayed and struck the side of the copper mold during either the initial or the final arc melt, then the integrity of the ingot is suspect. Indeed if *the arc has struck the side wall, copper contamination will most likely have spread throughout* the ingot. The only solution is to re-melt the ingot using Electron Beam (EB) melting to remove the copper. This must be followed by chemical reanalysis, re-addition of alloying constituents,

and double consumable arc melting to both homogenize the ingot and to ensure that the lower melting alloy constituents (i.e., Zr, Hf) depleted during the EB re-melting have been returned to their intended levels.

2) Copper contamination during Electro-Discharge-Machining (EDM)

Copper electrodes are typically employed in this process although other alloys or elements such as molybdenum can be used. Regardless of what electrode material is employed, the recast layer has to be removed by a combination of honing, machining, and pickling. If not, and especially for refractory alloys containing zirconium and hafnium, as noted above, the copper contamination occurring with use of a copper electrode will dramatically degrade high temperature mechanical behavior. As was previously discussed, incomplete removal of the recast layer and associated copper may have played a role in the cracking of several FS-85 tube hollows during early passes at True Tube, Inc.

Summary:

This report describes in detail the processing experienced by the refractory metals T-111, ASTAR-811C, Ta-10W, FS-85, and several molybdenum–rhenium alloys prior to termination of Naval Reactor's effort on the Prometheus Program. Sufficient detail is provided to allow an understanding of the rationale for many of the processing steps unique to these materials as well as how these steps are to be conducted to avoid material contamination. The report was written from the perspective of a processing engineer to aid this understanding. Additional objectives are to: 1) allow future engineers to complete the processing of archived materials that were stopped in mid-process, and 2) allow future engineers to test final processed specimens and remain confident about the individual specimen's pedigree.

ACKNOWLEDGEMENTS:

The assistance of many individuals was crucial in the effort necessary to melt and process these materials on an expedited basis. Thanks especially to Jim Carr, Tim Delahanty, Harry Grubich, and Bal Patil of PMTI. However, beyond these individuals there is a special individual who for a number of years has provided the advice, wisdom, and special expertise required to understand and successfully process these unique but touchy materials. Thanks Bill (i.e., R. W. Buckman).

REFERENCES:

1) R.L. Ammon and R.T. Begley, "Pilot Production and Evaluation of Tantalum Alloy Sheet," Summary Phase Report, Part II, WANL-PR-M-004, June 15, 1963, Prepared under Navy, Bureau of Navy Weapons, Contract NO w 62- 0656-d
2) W.R. Clough and A.S. Pavolic, Trans. Am. Soc. Materials, Vol.52, 1960.
3) G.G. Lessmann, "Determination of Weldability and Elevated Temperature Stability of Refractory Metal Alloys," NASA-1607 dated August 1970.
4) G.G. Lessmann and R.E. Gold, "Determination of Weldability and Elevated Temperature Stability of Refractory Metal Alloys," NASA CR-1608, September 1970.
5) "Refractory Metals Fabrication Technology as Applied to Fusion Reactors," BNWL-2053 dated July 1976
6) Private communication with Todd Leonhardt of Rhenium Alloys on June 24, 2005
7) "Witnessing of trial fabrication runs of FS-85, T-111, and ASTAR-811C tubing at True Tube Inc., " B-MT (SRME)-31, issued June 2005.
8) "Failure Analysis of Cracked FS-85 Tubing and ASTAR-811C End Caps," B-MT (SRME)-58, dated February 9, 2006.
9) "Biaxial Creep Specimen Fabrication Close-out Report "B-MT (SRME)-50, dated February 9, 2006.
10) G.G. Lessmann and D.R. Stoner, "Welding Refractory Metal Alloys Space Power System Applications" WANL-SP-009 dated November 15 1965.
11) Evaluation Test Methods for Refractory Metal Sheet Material, MAB-192-M dated April 22, 1963, Issued by Materials Advisory Board to the National Academy of Sciences- National Research Council
12) R.W. Buckman and R.C. Goodspeed, "Development of Precipitation Strengthened Tantalum Base Alloys," WANL-PR (Q0 -017 for period 6/19/63 to 8/20/67).
13) R.E. Gold, "Investigation of High Temperature Fracture of T-111 and ASTAR-811C," WANL-PRVVV-003 dated April 1971
14) J.C. Carlen and B.D. Bryskin, "Concerning Sigma Phase in Molybdenum-Rhenium Alloys," Journal of Materials Engineering and Performance, Vol 3(2), April 1994, ASM International
15) Private communication with R. W. Buckman on 12/2005
16) A.J. Bryan, "Joining of Molybdenum Base Metals and Factors Which Influence Ductility", Bulletin 312, February 1986, Welding Research Council
17) H. Inouye," Interactions of Refractory Metals With Active Gases in Vacua and Inert gas Environments" from Proceedings of A Symposium on Metallurgy and Technology of Refractory Metals in Washington D.C. in April 1968
18) R.W. Buckman, "Alloying of Refractory Metals," From "Alloying," ASM book edited by Walter, Jackson and Sims
19) R.W. Buckman, "Operation of Ultra High Vacuum Creep Testing Laboratory," Transactions of Vacuum Metallurgy Conference, 966, American Vacuum Society, 1967
20) J. Shields and J. Dahl, "Heat Treating of Refractory Metals and Alloys," Vol. 4, ASM Handbook
21) G.G. Lessmann and D.R. Stoner, "Measurement and Control of Weld Chamber Atmospheres," Welding Journal Supplement, 44(8), 337-S to 346-S August, 1965
22) T. J. Moore, P.E. Moorhead, and K.J. Bowles, " Specifications for Cleaning, Fusion Welding and Post-heating Tantalum and Columbium Alloys, NASA Technical Memorandum-NASA TM X-67879 dated July 1971
23) A. J. Moorhead, J.R. Distefano, and R.E. McDonald, "Fabrication Procedures for Unalloyed Molybdenum," Nuclear Technology, Vol. 24, October 1974
24) Peter Ring, "SP-100 Materials and Fabrication Technology Lessons Learned, "SP-100 Program Information Release #1199 dated March 31, 1994

Attachment B: Raw Material Certifications

H.C. Starck(Ohio),Inc.
460 Jay Street
Coldwater, MI 49036
Tel: (517) 279-9511
Fax: (517) 279-9512

To Ross Luther 6479

MATERIAL CERTIFICATION REPORT
DATE :21-AUG-01 PAGE 1 OF 1

BECHTEL BETTIS INC.
PITTSBURGH MATERIALS TECH.
1801 RT 51 SOUTH
PA 15025

Customer PO : 2110290
S.O. Number : 21-38026-1-2
Line Number : 1
Part Number : 32200.62500RLBA
Description : CSM ABL-4 MO BAR LC

Heat/Lot # : C25774-0.625

Dye Penetrant - PASS
Dimensional - PASS
Surface Finish - PASS

STANDARD CHEMISTRY

STDC #: 44656 Heat/Lot#: C25774

C	=	.007	%
FE	=	.0023	%
MO	>	99.97	%
N2	=	.0004	%
NI	<	.001	%
O2	=	.0013	%
SI	<	.001	%

DPH 10KG LOAD

DPH #: 44506 Heat/Lot#: C25774-0.625

DPH 10KG LOAD > 235 < 240 DPH

Longitudinal Tensile Test

LTEN #: 44507 Heat/Lot#: C25774-0.625

ELONGATION	> 34	%
ULTIMATE STRENGTH	> 98.9 < 99.3	KSI
YIELD STRENGTH	> 85 < 86	KSI

The undersigned authorized representatives of H.C. Starck(Ohio),Inc., certify that the above information is correct and that all requirements of the above specifications have been met.

Prepared By: R. Welk Approved By: R. Welk

CSM INDUSTRIES, INC.
360 Jay Street
Coldwater, MI 49036
Tel: (517) 279-9511
Fax: (517) 279-9512

MATERIAL CERTIFICATION REPORT
DATE :08-JUN-01 PAGE 1 OF 1

BECHTEL BETTIS INC.
PITTSBURGH MATERIALS TECH.
1801 RT 51 SOUTH
PA 15025

Customer PO : 2110290
S.O. Number : 21-38026-1-1
Line Number : 1
Part Number : 32200.62500RLBA
Description : CSM ABL-4 MO BAR LC

Heat/Lot # : C25629-0.625

Dye Penetrant - PASS
Dimensional - PASS
Surface Finish - PASS

X0022CT

STANDARD CHEMISTRY STDC #: 43822 Heat/Lot#: C25629

C	=	.006	%
FE	<	.001	%
MO	>	99.97	%
N2	=	.0003	%
NI	<	.001	%
O2	=	.0002	%
SI	<	.001	%

DPH 10KG LOAD DPH #: 44178 Heat/Lot#: C25629-0.625

DPH 10KG LOAD	> 236 < 241	DPH

Longitudinal Tensile Test LTEN #: 44179 Heat/Lot#: C25629-0.625

ELONGATION	> 34 < 35	%
ULTIMATE STRENGTH	> 99.4 < 104.3	KSI
YIELD STRENGTH	> 84.7 < 88.6	KSI

The undersigned authorized representatives of CSM Industries, Inc., certify that the above information is correct and that all requirements of the above specifications have been met.

Prepared By: Jerry Parker Approved By: Jerry Parker

RHENIUM ALLOYS, INC.

1329 Taylor St.
P.O. Box 245
Elyria, Oh 44036-0245
Voice (440) 365-7388
Fax (440) 366-9831

MATERIAL CERTIFICATION

DATE: August 29, 2004

SOLD TO: Bechtel Bettis Inc.
814 Pittsburgh-McKeesport Blvd.
West Mifflin, PA 15122

PURCHASE ORDER: 3002177

MATERIAL: Rhenium Rod

This is a shipment against your order # 3002177 which completes the requirement for the Rhenium rod 0.500" diameter. The Rhenium rod meets the requirements to your attachment specification on P/O 3002177 for pure rhenium.

Lot number R-1455

Todd Leonhardt
Director of Technology

NSL ANALYTICAL SERVICES, INC.
QUALITY AND RELIABILITY IN MATERIALS TESTING SINCE 1945

(FRI) OCT 1 2004 13:19/ST. 13:18/NO. 6309524306 P 1

TEST REPORT

7650 HUB PARKWAY, CLEVELAND, OHIO 44125
PHONE: (216) 447-1550 FAX: (216) 447-0716
(800) 497-6752
www.nslanalytical.com • E-MAIL: nsl@nslanalytical.com

NADCAP

THE REPORTED TEST RESULTS RELATE ONLY TO THE ITEM(S) TESTED

Rhenium Alloy Inc.
1329 Taylor Street
Elyria OH 44035-6249

Attn: Cliff Guthman

Revised Report: Mg removed

Client Description: Re Rod

Date: 9/30/04

Report No.: 121006

PO No.: 10974

NSL Lab No: 0417310 Sample ID: R-1455

Tests	Results/Units	Methods
O	<10ppm	Leco Furnace
C	<20ppm	Leco Furnace
Mo	<10ppm	ICP/MS
Fe	<10ppm	ICP/MS
Ni	<10ppm	ICP/MS
N	<10ppm	Leco Furnace
Si	<10ppm	ICP/MS
K	<10ppm	DC ARC
H	3ppm	Leco Furnace
Na	<10ppm	DC ARC
P	<10ppm	ICP/MS
W	<10ppm	ICP/MS
Zn	<5ppm	ICP/MS
TAO	<100ppm	ICP/MS

Reporting Officer: Carm D'Agostino , Wet Chem Supervisor

PR 4a

To: PITTSBURGH MATERIALS TECHNOLOGY INC
Address: 1801 Route 51
Bldg 9
Jefferson Hills, PA 15025
Attention Of: Accounts Payable

ATI Wah Chang
Allegheny Technologies
P.O. Box 460
Albany, Oregon 97321-0135
(541) 926-4211 FAX (541) 967-6948

PRODUCT CERTIFICATION

IN REGARD TO YOUR
Purchase Order No.: M04-379
Sales Order No.: 124524
Item No.: 1
Description: Hafnium Strip
Dimensions: 0.071" Thk x 0.75" W x 30" L
Specifications: ASTM B776-01, Ingot Chem Only and P.O.
Date: October 28, 2004
Quantity: 7 pcs.
Weight: 5 lbs.
Heat No.: 431728 Hf
SFC No.: 1281326

INGOT CHEMISTRY IN PERCENT

Element	Alpha Spec.	Spec. Max.	TOP	MIDDLE	BOTTOM
Al		0.010	0.004	0.004	0.005
C		0.015	0.006	0.007	0.006
Cr		0.010	<0.0020	<0.0020	<0.0020
Cu		0.010	<0.0025	<0.0025	<0.0025
Fe		0.050	0.022	0.022	0.021
H		0.0025	<0.0003		<0.0003
Mo		0.0020	<0.0010	<0.0010	<0.0010
N		0.010	<0.0020		<0.0020
Nb		0.010	<0.0050	<0.0050	<0.0050
Ni		0.0050	<0.0025	<0.0025	<0.0025
O		0.040	0.029		0.028
Si		0.010	<0.0025	<0.0025	<0.0025
Sn		0.0050	<0.0010	<0.0010	<0.0010
Ta		0.020	<0.0100	<0.0100	<0.0100
Ti		0.010	0.003	0.004	0.004
U		0.0010	<0.00010		
V		0.0050	<0.0010	<0.0010	<0.0010
W		0.0150	<0.0010	<0.0010	<0.0010
Zr			2.40	2.35	2.42
Hf	BALANCE				

Certified By: R Louie, QA Supervisor \es 10/28/04

Wah Chang Is A Registered / Certified ISO 9001:2000 Company.

To: PITTSBURGH MATERIALS TECHNOLOGY INC
Address: 1801 Route 51
Bldg 9
Jefferson Hills, PA 15025
Attention Of: Accounts Payable

ATI Wah Chang
Allegheny Technologies
P.O. Box 460
Albany, Oregon 97321-0138
(541) 926-4211 FAX (541) 967-6948

PRODUCT CERTIFICATION

IN REGARD TO YOUR

Purchase Order No.:	M04-359
Sales Order No.:	124318
Item No.:	1
Description:	Tantalum Sheet
Dimensions:	0.100" Nom. Thk x 0.75" Nom. W x 30" Nom. L
Specifications:	ASTM B364-96 (Gr R05200) Ingot Chem Only and P.O.
Date:	October 26, 2004
Quantity:	68 pcs.
Weight:	129 lbs.
Heat No.:	7-51-3
SFC No.:	1279703

RECEIVED

INGOT CHEMISTRY IN PPM

Element	Alpha Spec.	Spec. Max.	TOP	MIDDLE	BOTTOM
C		100	<20	<20	<20
Fe		100	<0.005	0.010	0.110
H		15	<3	<3	<3
Mo		200	0.110	0.130	0.160
N		100	<20	23	26
Nb		1000	15.00	17.00	78.00
Ni		100	<0.005	<0.005	0.006
O		150	<50	<50	<50
Si		50	0.005	0.001	0.010
Ti		100	<0.001	<0.001	<0.001
W		500	4.900	0.390	0.510
Ta	BALANCE				

Metallics were analyzed by outside vendor Shiva.

Certified By: R Louie, QA Supervisor \es 10/26/04

Wah Chang is A Registered / Certified ISO 9001:2000 Company.

To: PITTSBURGH MATERIALS TECHNOLOGY INC
Address: 1801 Route 51
Bldg 9
Jefferson Hills, PA 15025
Attention Of: Accounts Payable

ATI Wah Chang
Allegheny Technologies
P.O. Box 460
Albany, Oregon 97321-0136
(541) 926-4211 FAX (541) 967-6948

PRODUCT CERTIFICATION

IN REGARD TO YOUR

Purchase Order No.:	M04-358
Sales Order No.:	124277
Item No.:	1
Description:	Niobium Grade 1 Sheet
Dimensions:	0.080" Thk x 1.2" W x 30" L
Specifications:	Ingot Chem Only and Purchase Order
Date Issued:	September 24, 2004
Quantity Shipped Pcs.:	136
Weight Shipped lbs.:	138
Heat No.:	504868
SFC No.:	1279428

INGOT CHEMISTRY RESULTS ON PAGE 2

Certified By: R Louie, QA Supervisor \es 09/24/04

Wah Chang Is A Registered / Certified ISO 9001:2000 Company.

ATI Wah Chang
Allegheny Technologies
P.O. Box 460
Albany, Oregon 97321-0138
(541) 926-4211 FAX (541) 967-6948

Purchase Order No.: M04-358
Sales Order No.: 124277
Item No.: 1
Heat No.: 504868
SFC No.: 1279428

THE TEST REPORT FOLLOWS:

INGOT CHEMISTRY IN PPM

Element	Alpha Spec.	1	2	3	4	5
Al		<20	<20	<20	<20	<20
B		<5	<5	<5	<5	<5
Be		<5	<5	<5	<5	<5
C		<20	<20	<20	<20	21
Cd		<10	<10	<10	<10	<10
Co		<50	<50	<50	<50	<50
Cr		<20	<20	<20	<20	<20
Cu		26	<10	<10	<10	<10
Fe		<35	<35	<35	<35	<35
H		<3				<3
Hf		<50	<50	<50	<50	<50
Mg		<10	<10	<10	<10	<10
Mn		<20	<20	<20	<20	<20
Mo		<30	<30	<30	<30	<30
N		52				46
Ni		<20	<20	<20	<20	<20
O		60				<50
P		<30	<30	<30	<30	<30
Si		<50	<50	<50	<50	<50
Sn		<40	<40	<40	<40	<40
Ta		170	140	150	130	160
Ti		<40	<40	<40	<40	<40
V		<20	<20	<20	<20	<20
W		<30	<30	<30	<30	<30
Zr		<50	<50	<50	<50	<50
Nb	BALANCE					

(This Page Intentionally Blank)

FORM 76082
4/1999

CONCURRENCE RECORD SHEET

- DOCUMENT NUMBER: B-MT(SRME)-51
- THIS DOCUMENT CONTAINS INFORMATION WHICH SHOULD BE CONSIDERED FOR PATENT DISCLOSURES ☐ YES ☒ NO
- THIS DOCUMENT CONTAINS INFORMATION WHICH MEETS BETTIS WORK CATEGORIES [A,B,C,D or (N/A)] N/A

CONCURRENCE SIGNATURES (Activity must be included) - RESOLVE COMMENTS BEFORE SIGNING

SIGNATURE/ACTIVITY	DATE	TYPE	DETAILS OF REVIEW REQUESTED (if necessary)

TYPE OF REVIEWS (to be determined by author) [See table at end of instructions for definitions.]

1-Peer:Summary 2-Peer:Intermediate 3-Peer:Detail 4-Independent 5-Informal Committee 6-Formal Committee 7-Specialist 8-Interface

NAME TYPED AND SIGNATURE OF NEXT HIGHER MANAGER NOT SIGNING ON LETTER DATE

John E. Hack

J. E. Hack, Manager, Advanced Materials Technology

- CONTRIBUTORS AND IMPACTED PARTIES NOT REQUESTED TO CONCUR AND WHY:

DISTRIBUTION

Bettis
M. N. Smith 02B/GM
M. J. Zika, 01C/SE
S. D. Harkness, 01Q/MT
R. C. Jewart, 01C/SE
J. E. Hack, 05R/MT
R. Baranwal, 05P/MT
M. E. Petrichek, 05P/MT
R. F. Luther, 05P/MT _(3)
B. T. Randall, COB1
R. W. Buckman, 05R/MT
A. J. Mueller, 05R/MT

PNR
J. Andes
JF Koury

SNR
D. Clapper, 065
GM Millis, 065

NR
DI Curtis(3), 08S **(INFO)**
JD Yoxtheimer, 08S/8034
ST Bell, 08I/8024
DE Dei, 08A/8011
WE Evers, 08E/8019
TJ Mueller, 08R/8033
JP Mosquera, 08C/8017
MD Natale, 08I/8024
TN Rodeheaver, 08I/8024
SJ Rodgers, 08E/8019
CH Oosterman, 08C/8017
SJ Trautman, 08V/8037

KAPL
MJ Wollman, 111
SA Simonson, 081
Y Ballout, 92
CF Dempsey, 111
T. Angeliu

BPMI-P
SD Gazarik
RF Hanson